

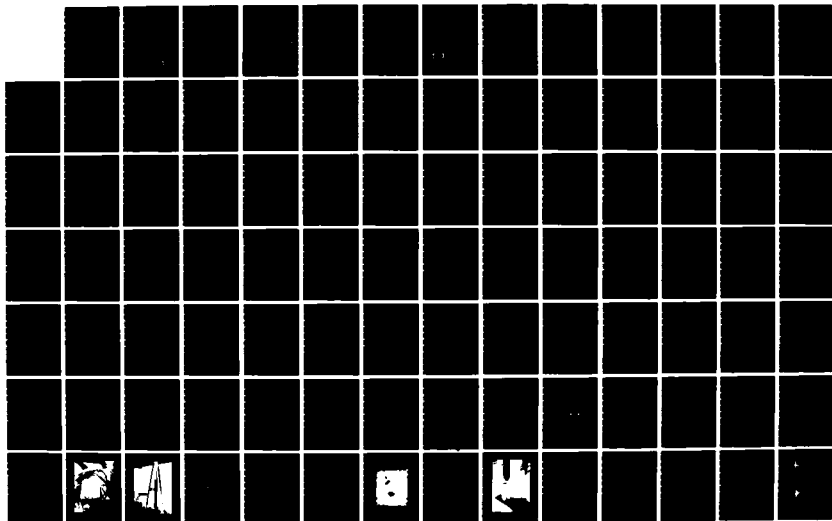
AD-A141 258

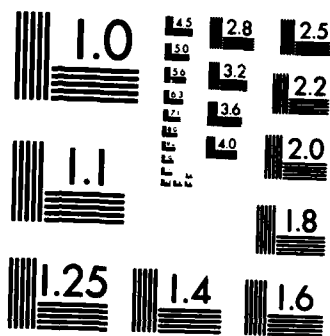
BOREHOLE TILT MEASUREMENTS AT THE CHARLEVOIX  
OBSERVATORY QUEBEC(U) DALHOUSIE UNIV HALIFAX (NOVA  
SCOTIA) DEPT OF OCEANOGRPPHY J PETERS ET AL. 31 JAN 83  
AFGL-TR-83-0027 F19628-80-C-0032 F/G 8/11

1/2

UNCLASSIFIED

NL





MICROCOPY RESOLUTION TEST CHART  
 NATIONAL BUREAU OF STANDARDS-1963-A

12

AFGL-TR-83-0027

BOREHOLE TILT MEASUREMENTS AT THE CHARLEVOIX  
OBSERVATORY, QUEBEC

John Peters  
Christopher Beaumont  
Ross Boutilier

Dept. of Oceanography  
Dalhousie University  
Halifax, N.S Canada B3H 4J1

Final Report  
12 September 1979 - 31 December 1982

31 January 1983

Approved for public release; distribution unlimited

DTIC FILE COPY

AIR FORCE GEOPHYSICS LABORATORY  
AIR FORCE SYSTEMS COMMAND  
UNITED STATES AIR FORCE  
HANSCOM AFB, MASSACHUSETTS 01731

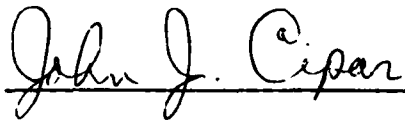
DTIC  
ELECTE  
MAY 21 1984  
S D  
B

84 05 21 002

AD-A141 258

This report has been reviewed by the ESD Public Affairs Office (PA) and is releasable to the National Technical Information Service (NTIS).

This technical report has been reviewed and is approved for publication.



JOHN J. CIPAR  
Contract Manager



HENRY A. OSSING, Chief  
Applied Crustal Physics Branch

FOR THE COMMANDER



DONALD H. ECKHARDT, Director  
Terrestrial Sciences Division

Qualified requestors may obtain additional copies from the Defense Technical Information Center. All others should apply to the National Technical Information Service.

If your address has changed, or if you wish to be removed from the mailing list, or if the addressee is no longer employed by your organization, please notify AFGL/DAA, Hanscom AFB, MA 01731. This will assist us in maintaining a current mailing list.

Do not return copies of this report unless contractual obligations or notices on a specific document requires that it be returned.

Unclassified

SECURITY CLASSIFICATION OF THIS PAGE (When Data Entered)

REPORT DOCUMENTATION PAGE		READ INSTRUCTIONS BEFORE COMPLETING FORM
1. REPORT NUMBER AFGL-TR-83-0027	2. GOVT ACCESSION NO. AD-A141258	3. RECIPIENT'S CATALOG NUMBER
4. TITLE (and Subtitle) Borehole Tilt Measurements at the Charlevoix Observatory, Quebec		5. TYPE OF REPORT & PERIOD COVERED Final Report 12 Sep 79 - 31 Dec 82
7. AUTHOR(s) John Peters Christopher Beaumont Ross Boutilier		6. PERFORMING ORG. REPORT NUMBER
9. PERFORMING ORGANIZATION NAME AND ADDRESS Dept. of Oceanography, Dalhousie University, Halifax, N.S Canada B3H 4J1		8. CONTRACT OR GRANT NUMBER(s) F19628-80-C-0032
11. CONTROLLING OFFICE NAME AND ADDRESS Air Force Geophysics Laboratory Hanscom A.F.B. Massachusetts 01731 Monitor/John J.Cipar/LWH		10. PROGRAM ELEMENT, PROJECT, TASK AREA & WORK UNIT NUMBERS 61102F 2309G2AE
14. MONITORING AGENCY NAME & ADDRESS (if different from Controlling Office)		12. REPORT DATE Jan. 31, 1983
		13. NUMBER OF PAGES 134
		15. SECURITY CLASS. (of this report) Unclassified
		15a. DECLASSIFICATION DOWNGRADING SCHEDULE
16. DISTRIBUTION STATEMENT (of this Report) <p><del>Approved for public release</del> distribution unlimited</p> <div style="border: 1px solid black; padding: 5px; display: inline-block;"><b>DISTRIBUTION STATEMENT A</b> Approved for public release Distribution Unlimited</div>		
17. DISTRIBUTION STATEMENT (of the abstract entered in Block 20, if different from Report)		
18. SUPPLEMENTARY NOTES		
19. KEY WORDS (Continue on reverse side if necessary and identify by block number) Borehole tiltmeter Earthquakes Tidal, secular and transient tilts		
20. ABSTRACT (Continue on reverse side if necessary and identify by block number) <p>An array of three Bodenseewerk Gbp borehole tiltmeters has been established to measure tidal, transient and secular tilting of the Earth's surface in the Charlevoix region of Quebec. Two of the tiltmeters operate at a depth of 47m and the third at 110m.</p>		

They are placed at the corners of a roughly equilateral triangle with side lengths of 70-90m. The Charlevoix region is an area of high intraplate seismic activity and the location of the tiltmeter array is primarily designed to investigate the relationship between earthquake activity, the tectonic stress that induces it, and the tilting of the Earth's surface.

The seismicity and geodynamics of the region are outlined within the context of other geophysical and geodetic observations that have been and are being made in the region. The drilling and casing of the boreholes, the installation of tiltmeters and their orientation, problems with lightning induced electrical currents and methods used to avoid them, the data acquisition system, and water wells used to monitor hydrological conditions are discussed.

Tilt observations for approximately one year from each of the 47m boreholes have been analyzed. The results show that: 1) the long period (secular) tilt is strongly correlated with the piezometric pressure measured in the nearby water wells; 2) there are tilt step offsets at the time of local earthquakes but these are probably a site effect; 3) the mean M<sub>2</sub> and O<sub>1</sub> load tide admittances are in reasonably good agreement with the predictions of a model of loading by the marine tides in the nearby St. Lawrence estuary; and 4) the observations show significant variations in tidal admittance with time but it is not known whether these merely reflect time changes in the marine tide admittance or whether the solid earth response to tidal forces is changing.

## Contents

Abstract

Statement of Project

Geophysical Observations in the Charlevoix Seismic Region

Scientific Basis for the Tilt Project

- (i) Linear and Nonlinear Tidal Tilt Anomalies
- (ii) The Coherency of Tilt Observations
- (iii) Transient Tilts
- (iv) Comparison of Borehole and Surface Tilt Observations
- (v) Tidal Loading

The Charlevoix Borehole Tiltmeter Array

- (i) The Earth Physics Branch Observatory
- (ii) Borehole and Tiltmeter Installation, Holes 1 and 2
- (iii) Tiltmeter Operation for 1980 and 1981
- (iv) Lightning Damage and Protection
- (v) The Automatic Geophysical Observatory System (AGOS)
- (vi) Optical Data Links from Borehole Tiltmeters to AGOS
- (vii) Borehole and Tiltmeter Installation; Hole 3
- (viii) Water Wells
- (ix) Tilt Observations in the Shallow Vault

Results

- (i) Data Characteristics
- (ii) Data Reduction and Analysis
- (iii) Variability of Tidal Estimates for Gbp105 in Borehole 1

- (iv) Variability of Tidal Estimates for Gbpl06 in Borehole 2
- (v) Variability of Tidal Estimates for Gbpl07 in Borehole 1
- (vi) Power Spectra of Borehole Tilt Data
- (vii) Comparison of the Mean  $M_2$  Admittance of the Borehole Tiltmeters with those of the ANAC Tiltmeters.

Tidal Loading

Discussion and Conclusions

Acknowledgements

References

Tables

Figure Captions

Figures

**S** DTIC ELECTE **D**  
 MAY 21 1984  
 - B

Accession For		✓
DTIC TAG		
Unnumbered		
Justified		
<b>PER CALL JC</b>		
By		
Distribution/		
Available City Codes		
Dist	Avail and/or	Special
<b>A-1</b>		

DTIC  
 ELECTE  
 MAY 21 1984

## Abstract

An array of three Bodenseewerk Gbp10 borehole tiltmeters ~~has been~~ established to measure tidal, transient and secular tilting of the Earth's surface in the Charlevoix region of Quebec. Two of the tiltmeters operate at a depth of 47m and the third at 110m. They are placed at the corners of a roughly equilateral triangle with side lengths of 70-90m. The Charlevoix region is an area of high intraplate seismic activity and the location of the tiltmeter array is primarily designed to investigate the relationship between earthquake activity, the tectonic stress that induces it, and the tilting of the Earth's surface.)

The seismicity and geodynamics of the region are outlined within the context of other geophysical and geodetic observations that have been and are being made in the region. The drilling and casing of the boreholes, the installation of tiltmeters and their orientation, problems with lightning induced electrical currents and methods used to avoid them, the data acquisition system, and water wells used to monitor hydrological conditions are discussed.

Tilt observations for <sup>about 1</sup> ~~approximately~~ one year from each of the 47m boreholes <sup>were</sup> ~~have been~~ analyzed. The results show that: 1) the long period (secular) tilt is strongly correlated with the piezometric pressure measured in the nearby water wells; (2) there are tilt step offsets at the time of local earthquakes but these are probably a site effect; (3) the mean M<sub>2</sub> and O<sub>1</sub> load tide admittances are in reasonably good agreement with the predictions of a model of loading by the marine tides in the nearby St.

Lawrence estuary; and 4) the observations show significant variations in tidal admittance with time but it is not known whether these merely reflect time changes in the marine tide admittance or whether the solid earth response to tidal forces is changing.

### Statement of Project

The purpose of the borehole tiltmeter array at the Charlevoix Observatory is fivefold:

- (i) To analyze the records for both linear and nonlinear tidal tilt anomalies that are predicted for dilatant crustal rocks.
- (ii) To examine the coherence, as a function of frequency, among the borehole tiltmeters and to establish either a deterministic or statistical model for this coherence or lack of it.
- (iii) To look for evidence of earthquake precursors in the form of transient tilts.
- (iv) To compare the borehole tilt observations with those from an existing array of near surface short baselength A.N.A.C. tiltmeters, and with other geophysical observations that are presently being made in this seismically active region.
- (v) To measure crustal deformation associated with loading by the tides in the St. Lawrence estuary.

## Geophysical Observations in the Charlevoix Seismic Region

Attention has been directed in recent years on an area 150 km northeast of Quebec City (Figure 1), where there is a concentration of microseismic activity (Leblanc et al., 1973, Leblanc and Buchbinder, 1977) and a history of large earthquakes occurring roughly every 60 to 90 years (there was a magnitude 7 earthquake in 1925). Since 1972 various kinds of geophysical control have been established by the Earth Physics Branch to supplement the existing vertical and horizontal control provided by the Geodetic Survey of Canada. Thus, at the present time the geophysical control in the area consists of the following (Figure 2): 1) first order levelling along the north and south shores of the St. Lawrence River (levelled 1926 and 1965), 2) a precise gravity network consisting of fifteen stations and twenty-two connections (established 1974), 3) a triangulation network consisting of twelve points and twenty-six connections spanning the St. Lawrence River (established 1965), 4) two permanent tide gauges at St. Joseph de la Rive and St. Jean Port Joli, 5) a permanent seismic observatory at La Pocatiere on the south shore, and 6) a tilt, strain, seismic and magnetotelluric observatory located on the north shore near La Malbaie.

Precise gravity control was introduced so that the levelling and gravity together would allow any crustal deformations associated with seismic events to be properly modelled. The combination of gravity and levelling is necessary because a deformation of the crust is likely to distort both the

surface of the ground and the reference geoidal surface. The Geodetic Survey relevelled a 40 km coastal first order line along the north shore of the river in 1977, 1978 and 1980 to provide additional control over most of the gravity network. The triangulation network established in 1965/66 was observed using Wild T3 theodolites and MRA3 tellurometers. The gravity network has been resurveyed to a precision of about 4  $\mu$ gal (1 $\sigma$ ) every six months since 1976. Significant variations of >10 $\mu$ gal have occurred between the average residuals in two zones adjacent to the levelling line (Buchbinder et al., in press). The two zones, chosen on the basis of the results from the levelling, approximately divide the Baie St. Paul to La Malbaie coastal strip in half. The longer term variations appear to correlate with a ground moisture-recharge model.

An underground observatory vault was constructed by the Earth Physics Branch during the summer of 1974 for the purpose of continuously monitoring crustal strain and tilt in this seismically active area. The installation consists of a vault housing two concrete piers 10 meters apart, poured directly on the bedrock, 2 meters below ground level. The entire vault is buried beneath a 5 meter high mound of earth to provide thermal insulation. Access to one end of the vault is through a vertical pipe connecting the vault to the recorder building at the surface. The vault, which is orientated perpendicular to the St. Lawrence River, originally housed: a vertical short period seismometer, two strainmeters in parallel (a Benioff-type quartz rod instrument and

a Cambridge University wire strainmeter), and three ANAC mercury level tiltmeters oriented to measure tilt parallel and perpendicular to the axis of the vault. The strainmeter and tiltmeters were operated at high sensitivity and good earth tide records were obtained (Peters et al., in press; Lambert and Labrecque, 1979). In 1981 the Earth Physics Branch reduced the vault instrumentation to the seismometer and three ANAC tiltmeters.

In addition to the instruments in the vault a magnetotelluric station is operated on the surface and a special order levelling range and four wells for monitoring water levels have also been installed at the observatory.

Seismicity surveys in 1968 (Milne et al., 1970), 1970 (Leblanc et al., 1973), and 1974 (Leblanc and Buchbinder, 1977) have established that the centre of the earthquake zone covers a 70 x 40 km region centred on the St. Lawrence River. During the two month period of the 1974 survey 33 events were located by at least 4 stations from a network of up to 19 stations (Figure 3). All of the hypocenters were in the Precambrian rocks of the Grenville Province, with an average depth of 11 km (Figure 3); none occurred in the Ordovician overthrusts to the southeast of Logan's line, the surface expression of the contact. On the basis of this distribution (Figure 3) both Leblanc et al., (1973) and Leblanc and Buchbinder (1977) suggest that the length of the seismic zone parallel to the St. Lawrence River is related to the ~350Ma old Charlevoix impact crater (Robertson, 1968; 1975) and

that the conjunction of Logan's line and the crater could influence the distribution. Presumably, the structures either represent a zone of weakness in which tectonic stress is released by earthquakes, or the structures focus the tectonic stress in some way causing a higher rate of seismicity in an otherwise normal crust.

The nodal plane solutions are compatible with pure thrusting, the planes dipping on average  $40^\circ$  to the west and  $50^\circ$  to the south (Leblanc and Buchbinder, 1977), with the direction of the pressure axis not in disagreement with what Sbar and Sykes (1973) found in other parts of eastern North America.

Results from more recent continuous monitoring of seismicity (Anglin and Buchbinder, 1981) suggest that the seismic zone when viewed in cross section lies between depths of 5 and 25 km and is bounded by faults dipping about  $75^\circ$  to the southeast.

Relocation studies of the instrumentally recorded earthquakes of magnitude 4.5 or greater (Stevens, 1980) have indicated that the larger earthquakes fall in two groups near the intersection of the perimeter of the Charlevoix crater and the St. Lawrence river. These positions (Figure 4) roughly beneath Ile aux Lievres and Ile aux Coudres correspond to the ends of the zone of microseismic activity. The concentration may be the result of the focusing of stress by the crust within the Charlevoix crater, which acts as a weak planar inclusion, into its immediate surroundings (Campbell, 1978).

The cumulative magnitude-recurrence relationship for the

Charlevoix region Basham (1976) (as reported by Leblanc and Buchbinder, 1977) demonstrates that magnitude 3 earthquakes occur about once per year and magnitude 5 earthquakes approximately once every 12 years. This repetition rate is suitable for an experiment which intends measurement of the relationship between the tidal response of the crust and tectonic stress.

Seismic crustal studies (Lyons et al, 1980) reinforce the interpretation that Ordovician overthrusts dip beneath the river south east of Logan's line at an average angle of  $\sim 20^\circ$  (Figure 5). Their results also indicate that the upper crustal seismic P-velocity in a belt extending along the northshore of the river is 0.2-0.3 km/sec lower than the average of 6.4-6.5 km/sec for the Grenville Province. They suggest that this is related to structural deformation, caused by the Charlevoix meteorite impact, which extends well beyond the boundaries of the crater itself. The near surface P-velocity within the crater is 6.08 km/sec suggestive of a zone weakened by fracturing during impact.

Buchbinder and Keith (1979) have analyzed seismic velocities from local explosions at La Pocatiere and St. Jerome as they cross the array of seismometers in the La Malbaie region. (Figure 6). They identified an apparently real increase in the average P wave travel-time delay over the period 1974 to 1977 of  $\sim 30$  msec with estimated errors of  $\pm 16$  msec for most station pairs. Such an increase would correspond to a velocity change of 10 percent over 1.5 km of ray path or a corresponding smaller velocity change over a larger zone. During the 1977-1980 period

the P travel times decreased by an average of a few tens of milliseconds. The timing of this decrease varies among the stations in the network but is most evident at the end of 1977 and/or at the beginning of 1980 (Buchbinder, 1981) (Figure 6).

## Scientific Basis for the Tilt Project

### (i) Linear and Nonlinear Tidal Tilt Anomalies

Beaumont and Berger (1974) suggested that if  $V_p/V_s$  seismic velocity anomalies are characteristic earthquake precursors, and they also measure changes in the elastic properties of a zone in the crust containing the focal region of an upcoming earthquake, then anomalous changes in earth tide amplitudes should also accompany the  $V_p/V_s$  anomalies. Simple elastic inclusion models (Figure 7), suggested that these tidal anomalies would be predominantly a change in amplitude, the magnitude of which would depend on the distance from tiltmeter or strainmeter to the anomalous inclusion. Extension of this theoretical work (Beaumont, 1979) demonstrates that the elastic inclusion model is valid only under rather restrictive circumstances. A more general model in which the anomalous inclusion is undergoing dilatant opening of micro-cracks (as observed in laboratory experiments on intact samples) suggests much more interesting results. Dilatant expansion involving microcracks is essentially a plastic process and exhibits hysteresis. As such, the process is nonlinear with respect to stress increments and decrements (Figure 8). Depending on the rate of tectonic stress increase, the response to superimposed tidal stresses will be linear or nonlinear. Even nonlinearities of 10 percent will be easily recognizable (by bispectral analysis) if recorded by a tiltmeter that is itself linear. We therefore have a possible tool with which to recognize

hysteretic micro-crack dilatancy in crustal rocks as opposed to elastic changes which remain linear, although almost certainly anisotropic, in their response to tidal forcing. The earth tide in this context acts as a spatially and temporally known probe of the stress state and continuum properties of the crust. These interesting properties occur only at deviatoric stress states in excess of  $\sim 0.6$  of the failure strength of rocks.

More recently Agnew (1981) has extended the theoretical analysis to consider various types of nonlinearity and has searched tidal strain observations for their signature without success. However, there was no independent evidence to suggest that the region sampled by the strain observations at Pinon Flat was either dilatant or subject to stresses that were sufficiently large to induce other geophysical anomalies during the interval analyzed. It is believed that the existence of such nonlinearities and their amplitude remains an open question that will best be resolved by observations in a seismically active area.

(ii) The Coherency of Tilt Observations

There are three basic types of geophysical tiltmeters, short baselength (for near surface and mine observations), borehole, and long baselength 'liquid in tube' (for surface or near surface observations). To date most observations have been made with short baselength tiltmeters. The results from short baselength instruments may be summarized in the following way.

Semi-diurnal and diurnal tidal tilt observations are now reasonably well understood. If it were not for hydrological, cavity, geologic, and topographic effects (some of which are complex), tiltmeters would provide tidal tilts that are spatially and temporally coherent at approximately the 90-95% level. This is not to say that the perturbations just listed render all short baselength tilt observations useless (see Beaumont and Boutilier 1978, and Peters *et al.*, in press, for example). Nevertheless, a broad brush picture is that we understand the elastic response of the Earth to tidal forces and that departures from theoretical predictions are not manifestations of geophysically interesting processes, but largely just a failure on the part of the tiltmeter to 'sample' tilt that is representative of a spatial average.

The development of borehole and long baselength tiltmeters is based on the idea that these will provide a more representative sampling of regional tilt and that the observations will be less contaminated by random or coherent (thermoelastic, hydrologic, or cavity, for example) ground noise than the existing observations. This expectation has been confirmed for at least one site, Pinon Flat California, where a comparison of observations from shallowly buried (4.5 m) short baselength tiltmeters (Delta and Beta, Figure 9), a borehole tiltmeter (ADL), and a long baselength surface instrument (LFT), shows much greater long term stability and tidal signal to noise ratios for ADL and LFT than for the near surface instruments. (Wyatt *et al.*, 1982), (Figure 9).

Coherence among tilt observations for timescales

significantly longer than tidal periods has not been established on any spatial scale. Tiltmeters sited within a few meters of each other may not exhibit the same secular tilt. There are two explanations. The tiltmeter or its connection with the surrounding rock is unstable, or the rock surrounding the tiltmeter deforms in a way that is not representative of the secular tilting of the crust in that region. Problems of the first type (see for example, Wyatt and Berger, 1980) must be solved by better tiltmeter and interface design. Problems of the second kind (see for example Kumpel, 1982) may be approached in two ways; larger spatial integration (for example, re-leveling over long distances apparently produces coherent results), and through a better understanding of the behaviour of rock and rock-groundwater interactions on a small scale.

The Charlevoix tiltmeter array is designed to examine the coherency of tilt observed by three borehole tiltmeters with a spatial separation of  $\sim 100$  m. This is to be done for all frequencies by standard statistical techniques. In particular, the relationship between the tidal and secular coherency will be examined to determine whether a transfer function,  $H_T(f)$ , defined in the following way,

$$O_T(f) = H_T(f)T_T(f)$$

may be used to 'correct' secular tilts in the manner,

$$T_S(f) = H_T^{-1}(f)O_S(f),$$

where  $O_T(f)$  and  $T_T(f)$  are the observed and theoretical tidal tilts and  $O_S(f)$  are the observed tilts.  $T_S(f)$  may be regarded as the secular tilt 'corrected' for local effects. How closely does  $H_T(f)$  correspond to the unknown  $H_S(f)$ ?

(iii) Transient Tilts

Evidence exists for transient tilts at the Charlevoix site. However, it is important to note that transient tilts induced by rainfall have a similar signature in the near surface A.N.A.C. tiltmeters to those tentatively associated with earthquake activity. It is important to determine whether any of these transients are more than local effects monitored by the shallow tiltmeters. In particular, a study of the relationship among the observations from the borehole tiltmeters, their relationship to the surface tilt observations, and in turn, their relationship to the earthquakes is necessary. A critical question to be answered is whether the surface and/or borehole tiltmeters measure transient signals that are recognizably characteristic of known processes, for example pre-earthquake creep. Alternatively, the signal may be so distorted by inhomogeneities in the crust between its source and the tiltmeters, or very local inhomogeneities around the tiltmeter, that it can only be recognized as being 'anomalous'. This question must be answered before model studies can be considered. Only by comparing surface and borehole observations will we be able to estimate the fidelity of the recorded signal and to determine whether the signal is

representative of the source process filtered by a simple transfer function.

Two extreme models may be useful in illustrating this point. The first idealization is that the transients correspond to the propagation of a dislocation within a perfectly homogeneous elastic crust. In this case the source to receiver transfer function is that of a unit dislocation in an elastic half-space and passes our criterion of a 'simple' transfer function. The second, and probably worst of all 'pathologies', is that the transients correspond to the propagation of a dislocation within the crust that looks like a 'heap of rubble'. In this case there is no common transfer function. The best that can be expected is that the same movement at the same place at different times will give the same characteristic signal at each of the tiltmeters. With sufficient events a statistical relationship between source position and transient signal could be established.

In reality, the crust may behave like rubble at the surface and like a continuum at depth, with some gradational region between them. A tiltmeter buried in the continuum would record transients having simple transfer functions. The surface tiltmeter would just record an anomalous tilt. We have no idea whether this model of the crust is correct, or even if it is correct, the size of the skin depth of the rubble layer. This is not a problem particularly amenable to theoretical analysis. A comparison of the transients from the borehole and near-surface tiltmeters should, however, indicate whether this model has any

validity and whether the skin depth is  $\sim 100$  m, or is in excess of 1 km.

(iv) Comparison of Borehole and Surface Tilt Observations

Most aspects of a comparison of near surface and borehole tilt observations have already been mentioned but in the context of the physical processes occurring in the crust. A comparison of the two sets of observations is also valid purely from the aspect of measurement science. The intent of borehole tiltmeters is that they should provide better measurements of tilt. The main aim of the intercomparison is to determine noise level spectra that are typical of borehole installations at 110 m and 50 m depths and near surface observations. These are useful in designing future experiments and placing bounds on noise attenuation with depth and its relationship to hydrological conditions.

(v) Tidal Loading

Observations made during the last ten years have established that the tilting of the Earth's surface under the weight of the ocean tides is sensitive to the elastic properties of the crust and upper mantle (see for example, Beaumont and Lambert, 1972; Beaumont, 1978; Beaumont and Boutilier, 1978; Zschau, 1976; and Baker, 1980). The tides in the St. Lawrence estuary are sufficiently large that load induced tilts in the Charlevoix region will provide evidence on the structure of the

crust in this region. In particular, any large scale anomalies in crustal properties that may be related to the seismicity should be detectable.

## The Charlevoix Borehole Tiltmeter Array

### (i) The Earth Physics Branch Observatory

The borehole tiltmeters are installed at a field station operated by the Gravity, Geothermics, and Geodynamics division of the Earth Physics Branch of the Federal Department of Energy, Mines and Resources. The Charlevoix Observatory (Figure 1) is located near the centre of the Charlevoix impact crater 8km northwest of the north shore of the St. Lawrence estuary between La Malbaie and Baie St. Paul some 150 km north-east of Quebec City. The plan (Figure 10) shows the site to be located on the flanks of a small hill at a height of  $\sim 420\text{m}$  in a region of moderate relief.

The Precambrian Grenville bedrock of the area is a charnockitic gneiss which suffered shock metamorphism and exhumation during the meteorite impact. It is competent though large scale fractures probably exist in the nearsurface. The intrinsic porosity and permeability of the bedrock are both very low and the hydrology of the site is dominated by fracture porosity and permeability. The bedrock is overlain by up to 4m of glacial till.

Earth Physics Branch experiments at the site include: the near surface ANAC tilt measurements in the vault; a short period vertical seismometer for monitoring local earthquakes; the levelling array; a magnetotelluric experiment; and a series of boreholes for monitoring groundwater piezometric pressure. Two

trailers house the main source of uninterrupted power and the central data acquisition system (AGOS).

The borehole tiltmeter array forms a roughly equilateral triangle with sides of from 70 to 90 m. Holes 1 and 2 are 47 m deep, and hole 3 extends to a depth of 110 m.

(ii) Borehole and Tiltmeter Installation; Holes 1 and 2

Boreholes 1 and 2 were drilled under subcontract during October to November of 1979 by Bisson-Maple Leaf using a hammer-rotary technique powered by compressed air. The specifications for the 12 inch diameter 50 m deep holes were that they be sufficiently straight that more than one half of the bottom should be visible from the surface and that the inclination should not exceed  $\pm 2^\circ$ . The specifications were checked during drilling by plumb bob, inclination of the drill stem, and by sighting on an 11.5 inch diameter dummy ring of lights which was lowered to the bottom of the hole. The holes were cased using 8 inch internal diameter 24 feet long standard steel pipe sections which were welded together during installation (Figure 11). The first section of this casing was welded to the top of each of the stainless steel tiltmeter pods, described below, before final installation. Settling of drilling spoil had by this time reduced the hole depths to 47 m.

The holes were sealed with Masterflow 713 non-shrink thixotropic grout which was pumped from the bottom upwards through a 1.25 inch grout pipe to ensure complete filling and the best

seal to the surrounding bedrock. After settling the borehole was again tested for verticality and straightness and an attempt was made to pressure test the pipe. Despite penetrating 30 m below the water table, the holes have proven to be water tight and dry.

The tiltmeter pods (Figure 11) were designed to provide maximum stability of the tiltmeter mount. Their 6m length effectively increases the baselength of the tiltmeter to this length. They are constructed of 316L stainless steel to minimize corrosion induced instabilities at the contact points with the tiltmeters. The tiltmeter is positioned centrally along the length of the pod for symmetry and rests on a support pin (Figure 11) designed to accommodate the Bodenseewerk instrument.

It is not known whether any settling of the pods or casing occurred in the nearly one year interval between borehole completion and the installation of the first tiltmeter in September 1980. It seems that settling would be short term and no movements have subsequently been recorded by the tiltmeters.

Bodenseewerk Gbpl0 tiltmeters 105 and 106 were installed in boreholes 1 and 2 respectively in September 1980. They were aligned with the north-south direction within an accuracy of  $\sim 3^\circ$  using an optical plummet to compare the directions of the light source slits on the top of the tiltmeters with that of a thin reference thread stretched across the top of the borehole. Standard surveying techniques were used to position the reference thread with respect to a north-south line through the Earth Physics Branch levelling array (Figure 10) which had already been

established. The orientation of the tiltmeters by this method is imprecise because the light slits appear as very small images when viewed at a distance of 50 m. The effect of other inaccuracies is much smaller.

We have devised a much more accurate photographic orientation technique in which a double exposure of the illuminated slits with a telephoto lens is made after first photographing the reference thread with a normal lens (Figure 12). By using fine grained film and printing enlargements of the negatives a precision of  $\sim 0.1^\circ$  can be achieved (Figure 13).

The Bodenseewerk Gbpl0 tiltmeter comprises a 60 cm long simple pendulum with biaxial capacitive detection of position and electromagnetic proportional feedback (Figures 14 and 15). The complete tiltmeter is constructed of three pieces. The outer sensor casing sits on a location pin in the tiltmeter pod and is supported concentrically within the pod by three spring loaded studs or pins that project from the casing near its top. The pendulum carrier, itself a pendulum, is mounted on gimbals within the sensor casing. It can be driven electrically by cross-slide motors at its base to an inclination up to  $\pm 3^\circ$  with respect to the axis of the sensor casing. In this way it can be set vertical despite small deviations from the vertical of the borehole. Once set vertical the pendulum carrier is clamped and the measuring pendulum, the third component, unclamped. The measuring range of the tiltmeter is  $\sim 2.5 \times 10^{-5}$  radians but this can be stepped across the entire  $\pm 3^\circ$  by tilting the pendulum carrier. The

resolution of the transducer is claimed to be  $\sim 0.15 \times 10^{-9}$  radians although this depends on the background noise level in which the instrument operates. The main advantages of the Bodenseewerk Gbp10 is that it can be accurately calibrated to  $\pm 0.3$  percent by moving a small ball between two cups on the measuring pendulum. This ball displacement tilts the pendulum by a known amount in virtue of having moved its centre of mass. With repeated ball movements a calibration accuracy of  $\pm 0.1$  percent can be achieved. A linearity of 0.1 percent is also claimed for the instrument (Bodenseewerk Tech. Bull. 19, 1979). The output from the feedback loop is amplified, low pass filtered to remove microseismic noise (Figure 16), and then recorded on dual Watanabe SR61/02 two channel chart recorders. This provides redundancy in recording in case either one of the chart recorders fails.

The tiltmeters were modified by Bodenseewerk in two small ways prior to delivery. As originally designed the tiltmeter should be installed in a 6 inch borehole; therefore, it was necessary to increase the length of the spring loaded studs, which hold the upper end of the tiltmeter, for operation in our larger diameter pods. A guard ring for the studs was also provided. The control electronics were also modified to include a 20 times automatic repeat of the ball calibration once the calibration cycle has been triggered. The original recording configuration for Gbp 105 and 106 placed the control electronics, chart recorders, and Q-tech digital magnetic tape recorder in the trailers some 50 m from the boreholes. This was later modified,

partly as a result of the installation of AGOS, and more importantly as part of the improvements necessary to overcome failures which occurred during electrical storms. The present recording configuration is shown in Figure 17.

(iii) Tiltmeter Operation for 1980 and 1981

The first series of observations in the results section of this report and in Peters and Beaumont (in press) are from Gbpl05 operating in borehole 1 during the interval September 27, 1980 to March 25, 1981 (181 days). During this period considerable difficulties were experienced in operating Gbpl06 in borehole 2. Despite the replacement of the support pins the tiltmeter appeared unstable when operated at tidal sensitivity and the problem was attributed to the failure of the support pin release mechanism. The pins are designed to retract when the pendulum is hanging from a cable and extend as the tension is removed when the tiltmeter comes to rest on the support pin in the pod. When tested at the surface the pins intermittently became jammed in a semi-retracted position as the cable tension was released. For this reason Gbpl06 was returned to Bodenseewerk in December 1980 for testing.

A dummy tiltmeter, made from mild steel pipe to the same dimensions as the Gbpl0's and also having a guard ring, was constructed to test installation procedures. On April 21 it was found that the dummy tiltmeter without guard ring came to rest some 2 m deeper in borehole 2 than did Gbpl06. Photographs taken with a camera and flashlight assembly lowered down the borehole

showed that protruding beads of weldment around part of the joint between the pod and the first section of casing probably formed an obstruction beyond which the guard ring for Gbp106 would not pass (Figure 18). Once segments of the guard ring had been cut back somewhat Gbp106 passed the obstruction and entered the pod. The observed instability probably resulted from operating the tiltmeter while suspended by the guard ring on the weldment. Nevertheless, sticking of the support pins has been noted on subsequent installations of this tiltmeter. Gbp106 was finally installed and oriented in borehole 2 on April 23, 1981 where it operated until damaged by lightning on May 24, 1981.

(iv) Lightning Damage and Protection

During the summer of 1981 tiltmeters Gbp 105, 106 and 107 were plagued by problems due to electrical storms which are common in the St. Lawrence valley between June and September. Gbp106 was the first to be disabled followed by Gbp107, which was used to replace it. Gbp105 was less seriously affected, the damage being confined to the above ground control electronics. Following repair in July the equipment was again damaged and the experiment was discontinued until the end of the thunder storm season. The source of the problems appears to have been twofold: powerline voltage surges that entered the electronics through the uninterruptable power supply causing damage in the power supplies of the tiltmeters; and induced currents in the signal lines from the tiltmeters to the recording equipment and in the feedback

loop.

We believe that this problem has now been partly overcome by the protection system shown in Figure 19. The first step was to relocate the control electronics at the well head. Varistors and/or transzorb were then used to protect the AC-DC converters within the transducers and the feedback loop at the transducer end of the circuit. The same technique was used to protect the connections between tiltmeters and recorders. Powerline surges are minimized by isolating each borehole station from all other grounds and by using a local ground to the borehole casing. This is accomplished using isolation transformers which are themselves, protected on the primary and secondary windings by heavy duty Varistors. Each wellhead system is powered by an independent uninterruptable power supply consisting of a precision regulated battery charger backed up by batteries capable of operating the system for at least 24 hours in the event of power failure. The uninterruptable power supply drives a DC-AC inverter which powers the tiltmeters and analogue chart recorders.

The protection system appears to have been successful, the system having weathered major electrical storms during the summer of 1982. Its major weakness remains the signal cables from the well heads to AGOS. A prototype of an optical data link, which will make the wellheads secure from surges passing through AGOS or induced currents in the signal cables, has been constructed and tested. This link is described below.

(v) The Automatic Geophysical Observatory System (AGOS)

The Earth Physics Branch AGOS is the central data acquisition system at the Charlevoix Observatory. It is designed to receive, process, store, and retransmit data. The system is constructed around the Digital LS111/23 microcomputer and uses the Digital communications software package DECnet to transmit data over telephone lines to the Earth Physics Branch in Ottawa. Future development will upgrade AGOS to include control of some aspects of the experiments at the Charlevoix Observatory. The Charlevoix node of AGOS presently consists of a processor, non-volatile storage and a modem. The system samples analogue or digital input channels at 60 Hz, computes one minute averages, and applies a Kalman filter to either the 60 Hz data or its decimated equivalent. 1 or 10 minute samples which have been smoothed and edited for spurious points, steps, and anomalously high variances are stored on the system magnetic cassette and are available for transmission at 300 baud.

AGOS has had some teething troubles since it was installed in 1981. These have largely been corrected. However, its major limitation from the point of view of the borehole tiltmeter experiment is that A to D conversion is limited to 12 bit resolution. This presents a problem of resolution in signals that have a significant secular drift that must be accommodated within this bandwidth. Least-count noise is not a serious problem with regard to tidal tilt signals but it does limit the precision of calibration pulses and, therefore, the overall calibration of the

borehole tilt results. This problem will be eliminated by the 15 bit A to D conversion at the wellheads which will be part of the optical link systems. Until these are installed AGOS is regarded as a 'backup' data storage system for the borehole tilt observations. Our primary data source is the dual analogue chart records of each channel.

(vi) Optical Data Links from Borehole Tiltmeters to AGOS

The requirements of wide dynamic range and optimal recording resolution discussed earlier necessitate the use of digital data transmission between the borehole tiltmeters and AGOS.

A prototype digital link has been developed by Dr. Barry Paton of the Physics Department at Dalhousie. The unit consists of two Analog Devices model DAS1156 15-bit A-D converters, one each for the X and Y channels, with a least count resolution of  $60\mu\text{V}$  (0.1% of the calibration step size). The parallel output of the A-D converters is transformed to serial within an Intel 8031 microprocessor which subsequently drives a local RS232C port and an ITT model TXD004 optical transmitter.

Data will be sampled at one second intervals and will be transmitted in ASCII text at 300 baud over optical fibre to AGOS. The optical fibre link will complete the total electrical isolation of the tiltmeter installations from all other equipment at the site, and should substantially eliminate susceptibility to lightning induced surges in the signal lines.

At the AGOS location the data will be received by an ITT

model RXD007 optical receiver and output through an RS232C port. Each data record will consist of the sample time and the X and Y voltage levels.

Apart from its data acquisition task the 8031 microprocessor also performs a calibration control function. Every 107 minutes a pulse will be relayed to the tiltmeter control electronics which will initiate a calibration level change. An alternating X calibration 'on and off' and Y calibration 'on and off' sequence will be stepped through continuously; each step uniquely identified by a message in the data stream to AGOS. AGOS will then be able to identify each level change and evaluate it through the Kalman filtering routine described earlier. Further development and field installation of the data link requires the completion of an interface between the receiver RS232C port and the GPIB (general purpose instrumentation bus) of AGOS. The Earth Physics Branch is responsible for providing this component which is also in the prototype stage. Completion of the interface stage is expected early in 1983.

(vii) Borehole and Tiltmeter Installation; Hole 3

It is suspected on the basis of research elsewhere (M. Dence, pers. comm.) that hydrological conditions in hard rock terrains may stabilize at depths greater than 100 m. Our experience with tilts from borehole 1 had shown that the secular signal was strongly correlated with variations in piezometric pressure in a nearby water well, indicating a lack of hydrological

stability at a depth of 47 m. It was therefore decided to install the third tiltmeter in a 150 m deep borehole in an attempt to gain additional long term stability. The Earth Physics Branch provided the additional funds necessary to extend drilling beyond 50 m and to case the added length. The Earth Physics Branch also drilled a nearby deep water well.

The borehole was drilled by Les Puits de Quebec under subcontract during the period October 1981 to July 1982 using a hammer-rotary technique. The drillers first sank a 6 inch diameter hole which encountered a fracture at  $\approx 440$  feet that flowed water so rapidly that it was decided that this depth would be unsuitable for the tiltmeter. The hole was plugged and backfilled with concrete to 360 feet. The hole was then successively reamed to 8, 10 and 12 inch diameters to 350 feet. It was found that the hole deviated from being straight at a depth of  $\approx 220$  feet.

A second 6 inch diameter test hole apparently deviated from being straight at approximately the same depth as the first. A decision was made to accept the first hole if it met the verticality specifications at the bottom. This would mean that the tiltmeters could operate at that depth but that neither the optical nor photographic methods could be used to orient it. Verticality of the bottom section was established by operating a tiltmeter within the pod after the casing had been installed but before it had been grouted. The tiltmeter pod was modified by the Earth Physics Branch to include a muleshoe assembly (Figure 20)

into which a key or lug mounted on the outside of the tiltmeter can penetrate, and in the process cause the tiltmeter to take up a unique orientation. The pod was returned to Charlevoix, the casing reinserted into borehole 3 and grouted during May and June 1982. The final depth to the pod is 110 m.

The final orientation of the slot on the muleshoe assembly was determined by a survey during November 1982 in which a gyrocompass was attached to the top of the dummy tiltmeter. The dummy tiltmeter was installed in the hole six times and the orientation determined to a precision of  $1^\circ$ . No additional surveys of this type are necessary because the key on the outside of the tiltmeter can be rotated and fixed so that on successive installations the tiltmeter always takes up the same orientation in the north-south direction. The reproducibility of each successive orientation is determined by the play between the muleshoe slot and the key on the tiltmeter. It is judged to be no worse than  $0.5^\circ$ .

Gpb 105 was installed in borehole 3 on 13 November 1982. Repairs had previously been made for damage caused by lightning. Unfortunately one channel, north-south, is not working properly. It appears that there is an instability in the feedback loop which results from an incorrect match between the impedance of the replacement components and those already in the feedback loop. It is anticipated that this problem can be corrected without removing the tiltmeters from the borehole. The other channel is producing good tidal records, although there are occasional small steps

which may indicate an instability in the coupling between the tiltmeter and its pod.

(viii) Water Wells

The water wells at the Charlevoix site are designed to investigate the hydrological conditions both in their own right in terms of secular, transient and tidal variations and in their influence on the tilts. The wells (Figure 10) are located near the boreholes and are labelled A,B and C corresponding to tiltmeter boreholes 1, 2 and 3. The figure in brackets is the depth of the well in meters. A(70) and B(70) are both cased to a depth of 30 m and open from that depth to the bottom. They sample the piezometric pressure in deeper formations than B(30) which is only cased to 10 m. Well C(134) is yet to be cased, and therefore, presently integrates the pressure variations in any separate aquifers along its length. The water level in each of the wells is continuously monitored by the Earth Physics Branch using a capacitance probe method. Manual readings are also taken on a weekly basis to supplement and provide datum control for the continuous records which sometimes go off scale during periods of rapid transients, during the spring thaw for example.

(ix) Tilt Observations in the Shallow Vault

ANAC tiltmeter observations from the shallow vault for the interval 1976-1980 have been described by Peters et al (in press).

Three ANAC tiltmeters installed on two concrete piers 10m apart recorded tilt in azimuth N52° E (called position D) in azimuth N142E (called position A and position C). The positions A and C are at opposite ends of the vault. The data were recorded on continuous charts or cassette tape.

The time averaged results are compared with those from the borehole tiltmeters in the results section of this report. The monthly variations in tidal admittance for the M<sub>2</sub> constituent in terms of amplitude and phase are shown in Figures 21 and 22. There are apparently significant variations in both amplitude and phase over this period which are larger than the 2 σ bar associated with each result. Some variations are as large as 25 percent of the mean. Peters et al showed that the admittance variations correlated with other parameters; electric field polarization angle, tilt of the levelling array, and piezometric pressure in the A(70) and B(70) wells, (referred to, by them as 'Deep well'). They concluded that there may be a causal relationship between the tidal variation and the dynamics of the water table but that there was no evidence that the admittance is varying in response to regional elastic parameter changes associated with tectonics. The hydrological and meteorological effects on the secular signal of the ANAC tiltmeters (Lambert and Labrecque, 1980) are considerable. Large annual variations, (20-30) x 10<sup>-6</sup> radians, correlate with temperature and are probably thermoelastic in origin. The piezometric pressure also correlates with the D position tiltmeter. Aperiodic tilts with

frequencies similar to the tides occur during winter months and there are also large episodic tilts that correlate with rainfall and snow melt.

## Results

### (i) Data Characteristics

The periods for which good quality tilt data have been collected are shown in Figure 23. There are small gaps even within the larger data blocks but these have not prevented analysis of the data. The analysis techniques employed can cope with data that contain embedded gaps. The major interval of missing data is from the summer of 1981 and was the result of electrical problems induced by lightning. Borehole 3 was occupied soon after its completion in the summer of 1982.

Characteristic properties of the data can be assessed from Figures 24 to 29. Figure 24 illustrates a typical calibration sequence. A small amount of cross-talk exists between the X and Y channels but this is unimportant because calibrations of the two channels are sequential. The overshoot following the step due to the ball movement results from the analogue filtering of the output signal. Figure 25 shows the response on both X and Y channels to a typical teleseism. The offset in arrival times of the various phases results from the offset of the pens on the analogue chart recorder. The tiltmeter response to the magnitude 4.1 local earthquake of December 4 1982 is shown in Figure 26.

The drift signal from Gbpl05 operating in Borehole 1 during 1980 and 1981 (Figure 27) shows a strong correlation with the hand measurements of water level in A(70) and with rainfall. The large transient at about day 40 of 1981 corresponds to the groundwater

recharge at the time of the spring thaw of that year.

Typical unfiltered tidal data (Figure 28) from Gbpl06 west component operating in borehole 2 show that the tides are dominated by the semi-diurnal signal. These data are from the latter part of 1982.

The drift characteristics of Gbpl06 and Gbpl07 operating in boreholes 2 and 1 respectively during the latter part of 1981 and most of 1982 are illustrated in Figure 29. These are essentially raw data that have only been corrected for offsets, had calibration pulses removed, and been correctly scaled. The gaps show the intervals for which data has been lost. With the exception of Gbpl06 operating in borehole 1 (N21°E) the baseline has not been lost during the large transient caused by the spring thaw at about day 90.

Much of the data corresponding to the gaps was lost due to malfunction of the chart recorders or failure of the operator to renew the charts. However, such data can be recovered because it has been recorded by AGOS. In a final analysis the AGOS and chart data sets will be merged. Figure 29 also shows that the drift signals are closely correlated with the groundwater piezometric pressure in wells A(70) and B(70).

(ii) Data Reduction and Analysis

The analogue data from the chart records were digitized at hourly intervals using time marks on the records from a quartz clock as time base. The raw data were then edited to remove any

steps and the offsets due to calibration pulses. The calibrations were then used to scale the digital data from chart units to tilt in milliseconds of arc. The edited data were finally divided into subsets for spectral analysis.

Several analysis techniques have been used including: i) power spectral analysis; ii) Fourier scanning, which assumes the data to be continuous and computes the Fourier transform of it; iii) Least-squares analysis in which 12 sinusoids corresponding to the major tidal constituents were regressed on the data to determine their best fitting amplitudes and phases; and iv) Hybrid least-squares frequency domain convolution analysis (HYCON) Schuller (1976, 1977). HYCON is the most suited of these methods to the analysis of relatively short tidal series; therefore, the tidal analysis results given in this report are restricted to those given by this method. The accuracy of the analysis results is assessed by comparing the spectrum of the original data with the spectrum of the residual data series from which the estimated tide has been subtracted. The spectrum is most useful in calculations of the magnitude of the non-tidal background noise in the data and its variation with time.

We are most concerned with the stability of tidal estimates for sequential short, approximately one month, intervals; therefore, the results are presented in terms of these variations and the value of their mean. The starting times and number of hourly samples in each of the data sets that have been analyzed are given in Table 1. In the following sections the data are

grouped according to; the tiltmeter, the borehole in which it was recording, and its orientation.

(iii) Variability of Tidal Estimates for Gbpl05 in Borehole 1

Figure 30 illustrates the variations in the amplitudes and phase lags of the M<sub>2</sub>, S<sub>2</sub>, O<sub>1</sub> and K<sub>1</sub> constituents during 1980 and 1981. The data sets (Table 1) have an average length of about one month. Clearly, there are significant variations in the tidal admittance that are greater than the  $\pm 1\sigma$  error estimates both for the X(west) and Y(north) directions. The same M<sub>2</sub> data are presented as phasor plots in Figures 31 and 32 to demonstrate the effect of the variability on the vector character of the tilt. Our first impression of these results is that the variations in the south tilt phasor are random in character, no significant trends or excursions in any particular direction having been observed. It is not known whether the strong lineation apparent in the west tilt phasors has any significance. In neither the west nor south directions do the excursions exceed an amplitude of 1msec from the position of their mean. A more complete interpretation of the admittance variations will be possible when the variations in phasor plots and tidal tilt ellipses for a number of constituents have been compared. The approach will be to look for significant excursions from the mean that correlate between constituents. (Peters et al, in prep.).

(iv) Variability of Tidal Estimates for Gbpl06 in Borehole 2

Figures 33 and 34 illustrate the variations in  $M_2$  tidal admittance for monthly analyses for Gbpl06 operating in borehole 2 (labelled borehole 2, west and borehole 2, south) during 1982. Figure 33 shows that there are significant variations at the one standard deviation level in amplitude while Figure 34 shows the corresponding variations in phase. The vertical bars on the plot are  $\pm 1\sigma$ . The same results are presented as phasor diagrams in Figures 35 and 36. It should be remembered that during the first four months of the period Gbpl06 was operating with its sensitive axes oriented at azimuths of  $21^\circ$  and  $111^\circ$ . It was then rotated to corresponding angles of  $0^\circ$  and  $90^\circ$ . In diagrams 30 to 34 the results for the first four months have been rotated so that they can be compared with those of the last three months and with those from Gbpl07 operating in borehole 1.

Significant variability is again seen but it is not known whether this is the result of random noise or from a distinct physical process.

(v) Variability of Tidal Estimates for Gbpl07 in Borehole 1

The results from Gbpl07 in borehole 1 are probably the most interesting because the eight data sets are apparently enough to have established a pattern in the admittance behaviour. For the south tilt the phase lags first decrease, data sets 1 to 2, and then show a progressive increase, data sets 3 to 7. Alternatively, the pattern may be regarded as a cluster around results 1,5,6,7, and 8 with significant departures in phase at

data sets 2,3 and 4. This interpretation also applies to the west tilt variability, the major excursion from the clustered group having occurred for data sets 2 and 3. No physical significance should be attached to such 'excursions'. Tests must be made to determine whether they are even statistically significant. However, this is the type of pattern that would be expected were the admittance of the crust in the Charlevoix region changing with time.

(vi) Power Spectra of Borehole Tilt Data

The power spectra of the data and residuals for some representative data sets (Figures 30 to 42) show that there is a high signal to noise ratio in the tidal bands. Energy in 24, 12, 6 and 4 hour period bands can clearly be seen in the Gbp107 (West) and Gbp106 (N111°E), whereas 6 and 4 hour period energy is less evident in the other two data sets. The power spectra were calculated for sets of 2048 hourly samples that had been Hamming windowed and were then averaged among samples on the assumption that they were each realizations of stationary processes. The underlying assumption may not be strictly true, but the averaging increases the confidence levels of the spectral estimates by increasing the number of degrees of freedom associated with each. A linear trend was removed from each data set before transforming but no other filtering has been used.

Hycon estimates of the linear tidal constituents to second order were subtracted to give the residual spectra. These are normalized in the same way as the observed spectra; that is, by

the variance of the detrended tidal observations. The significant energy that remains in the higher order tidal bands for two of the residual spectra is probably a measure of the nonlinearity within this system.

The background energy in the spectra appears to decrease linearly with frequency within the tidal bands. That it does not continue this trend for even higher frequencies up to the Nyquist frequency may be a measure of least-count noise from the digitizing or true high frequency noise. It should, however, be noted that this noise is 5 orders of magnitude below the maximum tidal peak energy.

(vii) Comparison of the Mean  $M_2$  Admittance of the Borehole Tiltmeters and those of the ANAC tiltmeters

The mean admittances for  $M_2$  and  $O_1$  for the ANAC tiltmeters are given in Peters et al (in press). In Figures 43 to 47 the same results have been rotated to the west and south directions and are plotted in terms of their Greenwich phase lag. (An error in the Peters et al results has also been corrected). Two sets of results are given, those combining A and D and those combining C and D position tiltmeters (labelled A-D and C-D). There is good agreement in phase for these combinations for the  $M_2$  results but the amplitudes differ by about 10 per cent. For  $O_1$  the agreement is not so good probably because the signal to noise ratio is worse at this frequency.

A comparison of the  $M_2$  results from the ANAC and borehole tiltmeters shows that there is good agreement for the west component

with Gbpl07 in borehole 1 especially for the C-D combination. For the south direction, Gbpl07 lies between the two ANAC results. It is not known whether the differences are significant. If they are, they may arise from either a 'site' effect, or from non-stationary admittances because the data series are not concurrent.

The equivalent comparison for the  $O_1$  results shows similar difference between the means of A-D and C-D ANAC results and the borehole results. That the borehole results are a more internally consistent set leads us to believe that the ANAC's either have higher noise levels or that there are small cavity or pier tilt effects which cause the observations to deviate from the theoretical predictions and between piers.

#### Tidal Loading

Most of the tidal tilt observed at the Charlevoix site is caused by crustal deformation due to loading by the marine tides in the nearby St. Lawrence river estuary. In this section we present a comparison of observations with theoretical calculations of this effect for the  $M_2$  and  $O_1$  constituents on the assumption that the crust beneath the region is composed of uniform layers. This approach may be a poor approximation due to the lateral change in crustal structure at Logan's Line and the nature of the overthrust wedge beneath the St. Lawrence estuary (Figure 5). A method of calculating the effect of this wedge on load tilt, earth tide body tilt, and through strain-tilt coupling, at the Charlevoix Observatory is discussed at the end of this section.

The load tilt calculations were made by the same method as those of Beaumont and Lambert (1972), Beaumont (1978), and Beaumont and Boutilier (1978). Cotidal charts for the world oceans based on Hendershott's (1972) results were divided into spherical triangular regions of approximately equal amplitude and phase. The load tilt is calculated by convolving these triangular load distributions, each of which is assigned a uniform amplitude and phase, with the Green functions for tilt calculated by Farrell (1972, and pers. comm.) and by finite element calculations (Beaumont, 1973). Hendershott's numerical results for the North Atlantic ocean have been modified in an empirical way to agree with both coastal and offshore tide gauge measurements (Beaumont and Boutilier, 1978). A more detailed representation of the tides in the St. Lawrence estuary and Saguenay river (Figures 47 and 48) is used in this work. The cotidal charts for this region are empirical but are based on observations from the coastal sites shown (Figures 49 and 50) and numerical calculations of the  $M_2$  and  $O_1$  constituents (El-Sabh et al., 1979). We suspect that the largest errors in the marine tidal model arise from areas that 'dry' during the tidal cycle, and from the nonstationarity and nonlinearity of the tides. Because the marine tide at each of the gauges and the tilt tide observations were made over largely non-overlapping time intervals the results we present must be regarded as an average loading model. The site is remote from the major oceans and we are modelling tilt; therefore, errors arising from Hendershott's numerical model should be negligible in the

same way that those from the more recent calculations would be, and we judged it unnecessary to include these models in this calculation.

The results, Figures 51 to 62 are presented in the normal way as phasor plots with phase lag referenced to the transit of the moon at Greenwich, the Greenwich equilibrium potential, measured anticlockwise from  $0^\circ$ . The lengths of the vectors are proportional to the amplitudes of the observed and theoretical load tilts. The body tilt multiplied by a diminishing factor of 0.700 has been subtracted from the measured tilts. For  $M_2$  the resulting observed load phasor, OBS, is surrounded by a square box which is enlarged in the inset panel. Results of individual analyses and their mean are plotted in the enlargement. They are coupled by dashed lines to illustrate the time sequence of the tidal load admittance variations. No enlargement is needed for  $O_1$ .

The theoretical loads are only shown for the Gutenberg-Bullen earth model, FGB, to reduce confusion and for reasons explained below. Contributions from loads in the St. Lawrence estuary, remaining world oceans, and an upper bound estimate of the influence of local areas that 'dry' at low tide are shown by the 1, 2 and D phasors. It is estimated that: the 1 phasor is accurate to >95 percent in amplitude and  $\sim 3^\circ$  in phase; the 2 phasor is 80 percent accurate because this amount of loading comes from the well known tides in the seas adjacent to eastern North America; and that D has been grossly overestimated by

assuming that the areas which 'dry' remain permanently dry. That is, FGB for which D is ignored was calculated assuming no drying. Including D assumes that areas which dry are permanently dry. An accurate estimate of D is difficult because the clipping of each constituent varies during the lunar month. We believe that D should have an amplitude of 30-50 percent of that shown.

While large uncertainties in the 2 and D phasors remain it is not possible to use the loading results to choose among the various crustal models for this region. However, the agreement between observation and theory demonstrates that the departure of the tilt from that predicted for an oceanless earth is indeed caused by tidal loading, most of which comes from the nearby St. Lawrence estuary. The M<sub>2</sub> south component results are particularly encouraging. The three tiltmeters operating in two different boreholes are probably in agreement when phase errors, arising from uncertainties in tiltmeter orientation, and the month to month variability in the observed load admittance are taken into account. The corresponding agreement for the M<sub>2</sub> west components among the three tiltmeters and with theory is not quite so good. Gbp 106 operating in borehole 2 produces results with little variability and that are in within 2° of agreement with the theory, but both Gbp 105 and Gbp 107 operating in borehole 1 produce results with larger phase discrepancies and amplitudes that are too small. The difference cannot be attributed to marine tidal variability because there is a significant discrepancy between the 6, 7 and 8 data sets from Gbp 107 and the 1, 2 and 3

data sets of Gbp 106 which were recorded simultaneously. It therefore appears that there may be a small 'site effect' in the east-west direction.

The agreement between observed and theoretical load tilts for the O<sub>1</sub> constituent is surprisingly good. Despite the monthly variability, the means all agree with predictions to better than one millisecond and in most cases the agreement is even better. Another encouraging aspect of the results is that the three tiltmeters operating in two boreholes show remarkable internal consistency in their mean observed load tilts. It is not known whether the variability is random but the similarity in behaviour of the admittance for data sets 1, 2 and 3 for Gbp106 to that of data sets 6, 7 and 8 of Gbp107 which were recorded simultaneously leads us to suspect that it is not. The O<sub>1</sub> results suggest that the signal to noise ratio in these data is sufficiently high that other constituents of similar amplitude will yield useful results.

We have also calculated the body and 'far field' strain tensors for the Charlevoix region as a first step in assessing the effects of lateral variations in crustal structure and topography on the observed tilts. The 'far field' calculations do not include the local loading effects from the tides in the St. Lawrence estuary. These M<sub>2</sub> and O<sub>1</sub> tensors can be used to determine boundary conditions for finite element models of the Charlevoix region which include lateral changes in crustal structure. This approach assumes that the tilt anomalies arising from lateral changes in crustal structure and topography can be

calculated by representing the region as an 'inclusion' embedded in an otherwise radially symmetric earth. It is the same technique that Berger and Beaumont (1976) used to calculate the effects of topography on tidal strain at the Pinon Flat Observatory. The major difference is that in the present case most of the tidal loading occurs over the major lateral discontinuity in structure, the Ordovician overthrusts, and must therefore be included as a 'near field' effect in the finite element model. The crustal response to both surface loads and the tidal forces is believed to be elastic; therefore, the near and far field effects of inhomogeneities and topography can be calculated separately and then linearly superimposed to determine the resultant tilt perturbation. This resultant perturbation cannot be very large because the agreement between observations and theory which ignores inhomogeneities and topography is reasonably good.

## Discussion and Conclusions

Any discussion of the results obtained so far from our tiltmeter array is inevitably a preliminary one. We have established an array of three borehole tiltmeters that is apparently measuring tilt signals that can be interpreted in terms of the physical processes occurring at the site and in the Charlevoix region.

Charlevoix is particularly interesting because intraplate seismicity in this region is high. A question to be answered is whether high seismicity implies a high state of tectonic stress within the crust or whether the crust is merely weak, perhaps as a consequence of the Paleozoic impact of a meteorite. If the tectonic deviatoric stress is greater than  $\sim 0.6$  of the failure strength of intact crustal rocks within a significant volume of the crust, we expect that the crust's rheological properties will reflect this state.

Earth tide tilts would then be expected to behave anomalously. The signal characteristics might take the form of a time dependence and/or nonlinearities in the tidal admittance over an interval in which the tectonic stress changes significantly. This is why we have concentrated on the results of sequential analyses of monthly sets of data.

Unfortunately, tilts at Charlevoix are inevitably corrupted by another source of nonstationary and nonlinear signals; the marine tides in the nearby St. Lawrence river estuary. The river is shallow and there are nonlinearities in its tidal response.

There are also seasonal variations in the linear tides caused by changes in river discharge and mean wind stress.

The analysis of the tidal admittance for the  $M_2$  and  $O_1$  constituents has shown that in excess of 80 percent of the mean observed  $M_2$  tilt and a significant part of  $O_1$  arises from tidal loading from the tides in the St. Lawrence estuary. Small nonlinearities and time variations in this signal could explain the variability of the monthly  $M_2$  and  $O_1$  tilts. Alternatively, the variability of approximately 1msec in an approximately 16msec signal (6 percent) for  $M_2$ , for example, may be a random effect caused by the background noise in the tilt signal. Similar reasoning can be applied to the  $O_1$  signal. A third possibility is that the crustal admittance is really varying with time.

Several approaches are necessary to determine which of these explanations is correct. Longer concurrent data series from all three tiltmeters will determine the characteristics of the variability. Are the changes coherent among the tiltmeter array and from constituent to constituent? Does the removal of the incoherent part of the signal reduce the variability significantly? It appears that the signal to noise ratio of the data is high; therefore several constituents can be used in this comparison. High coherence among the variations would indicate that the effect is not due to random noise, or if it is due to random noise, that the noise is coherent over the tiltmeter array. The signal to noise ratio of the power spectra also provides a bound on the variations expected from background noise. This

approach is based on the notion that noise levels within and adjacent to the tidal bands are equal, a result that is not well established, but commonly used in practice. Cross-spectral analysis of the tilts with an 'areally integrated measure' of the marine tides would be the ideal way to determine whether it is the input signal (marine tides) or the filter (the Earth's crust) that exhibits time varying properties. In practice point observations will have to be substituted for the 'areally integrated measure' of the marine tides. We will analyze tide data from several locations to determine its variability and the character of the nonlinearities. The data that are available are not concurrent with the tilt data; therefore we will try to arrange a cooperative project with the Canadian Hydrographic Service in which a long series of bottom pressure measurements are made in the centre of the river to the south and east of the Charlevoix Observatory.

The reasonably good agreement among the time averaged observed load tilts from the two boreholes and with theory gives us confidence that at tidal periods the tiltmeters are measuring a signal that is representative of 'regional structure'. That is, structure of the crust averaged over spatial scales equal to the distance from the tiltmeters to the centre of the St. Lawrence estuary,  $\sim 20\text{km}$ . These are the spatial scales that must be sampled if we are to look for time dependent properties of the crust.

The more than 1msec disagreement between the mean  $M_2$  west load tilts for Gbpl05 and 107 operating in borehole 1 must, however, be explained. It cannot be caused by uncertainties in

the orientation of the tiltmeters, nor can large errors in absolute calibration be invoked without destroying the significantly better agreement in the corresponding results for the south components. A possible but highly speculative cause is a significant change in the tidal admittance in the west direction in the interval from 1980/81 to 1982. The disagreement is not peculiar to the  $M_2$ , a similar decrease having, occurred in  $O_1$ . In this case, however, the change is less certain because the variability of the two phasor sets causes them to overlap somewhat.

Although we have not addressed the problem of higher order tides and nonlinearities in this report, it can be seen from the power spectra that there is significant energy in the six and four hour period ranges for Gbp106 ( $111^\circ$  azimuth) and Gbp107 ( $90^\circ$  azimuth). The more southerly directed components Gbp106 ( $201^\circ$  azimuth) and Gbp107 ( $180^\circ$  azimuth), however, exhibit very little energy in this period range even though the signal to noise ratios are similar. Given that the most probable source of this energy is the marine tide loading and that the water is equidistant in both the east and south directions from the site, this imbalance is unexpected. It may be that there is an amphidrome for all short period tidal constituents in that part of the river to the south of the site, but this seems unlikely. Before this interesting result is attributed to anomalous properties of the Earth a more careful analysis of the tilt and marine tides for these short periods must be made. Nevertheless, this is the type

of behaviour that we are seeking.

The longer term drift tilts are consistently correlated with the piezometric pressure measured in the deeper water wells A(70) and B(70) at the site. Therefore, we do not want to ascribe any regional significance to the first order part of this drift. A statistical or preferably physical model must be found to account for and predict the vector tilt that results from groundwater fluctuations. Once that part of the tilt which is coherent with water levels has been removed, the residual can be assessed for its tectonic significance.

Progressively more evidence is accumulating that hydrologic variations are the major source of long term, and in some cases transient, tilts measured by near surface and borehole tiltmeters. It is important to note that the levelling array at the Charlevoix site is even more strongly affected by groundwater variations. Lambert (pers. comm). The implication of this is that a long baselength tiltmeter operating at the surface or shallowly buried would be similarly affected. If we are to make progress on measuring regionally meaningful secular tilts with borehole tiltmeters, the direction will inevitably be toward deeper boreholes. In this regard the drift signal from Gbp105 in borehole 3 will help to establish how significantly hydrological contamination of tilt decreases with depth.

Aperiodic and transient tilts certainly occur on the borehole tiltmeter records. Most appear to be correlated with rainfall or snowmelt and, more directly, with recharge of the

aquifers at the site. The mechanism may be as simple as the response of the tiltmeter pod to external pressure changes that are not entirely symmetrical. It will be necessary to compare the vector transients among the tiltmeters in the array to investigate their coherence. A predictive model can then be developed that relates groundwater recharge to induced tilt. Only when these transients have been removed will it be possible to analyze the residual for any tectonically induced transients that may be related to the earthquake cycle.

### Acknowledgements

This project was supported by the Air Force Geophysics Laboratory, Hanscom AFB, (under the terms of this contract F19628-80-C-0032), the Natural Sciences and Engineering Research Council, and the Gravity, Geothermics and Geodynamics Division of the Earth Physics Branch. We would like to thank Earth Physics Branch personnel, in particular Jacques Labrecque, for assistance in operations at the Charleviox Observatory, Daniel Lemieux and Benoit Dostaler, who maintained the tiltmeter array on a day-to-day basis, Jim Covill who assisted with data reduction and analysis, Georg Lohr, who showed us how to revive dead tiltmeters, and Kathleen Sawler, who ably manipulated the manuscript on the word processor.

We would also like to thank Gerry Cabaniss for support and advice during the period of this contract.

## References

- Agnew, D.C., 1981. Nonlinearity in rock: evidence from earth tides, *J.G.R.*, 86, 3969-3978.
- Anglin, F., and G. Buchbinder, 1981. Micro-seismicity in the mid-St. Lawrence Valley Charlevoix zone, Quebec, *Bull. Seism. Soc. Am.*, 71, 1553-1560.
- Baker, T.F., 1980. Tidal tilt at Llanrwst, N. Wales: tidal loading and Earth structure, *Geophys. J.R. astr. Soc.*, 62, 269-290.
- Beaumont, C., 1979. Linear and nonlinear interactions between the earth tide and a tectonically stressed earth, in: Applications of Geodesy to Geodynamics, I. Mueller, ed., Ohio State University Press, 313-318.
- Beaumont, C., 1978. Tidal loading: crustal structure of Nova Scotia and the M<sub>2</sub> tide in the northwest Atlantic from tilt and gravity observations, *Geophys. J. R. astr. Soc.*, 53, 27-53.
- Beaumont, C., and R. Boutilier, 1978. Tidal loading in Nova Scotia: results from improved ocean tide models, *Can. J. Earth Sci.*, 15, 981-993.
- Beaumont, C., and J. Berger, 1974. Earthquake prediction: modification of the earth tide tilts and strains by dilatancy, *Geophys. J. R. astr. Soc.*, 39, 111-121.
- Beaumont, C., 1973. Tilts and tides: a study of the deformation of the Earth by ocean tide loading. unpubl. Ph.D. thesis Dalhousie University, Halifax, Nova Scotia, Canada.
- Beaumont, C., and A. Lambert, 1972. Crustal structure from surface load tilts, using a finite element model, *Geophys. J.R. astr. Soc.*, 29, 203-226.
- Berger, J., and C. Beaumont, 1976. An analysis of tidal strain observations from the United States of America: II. The inhomogeneous tide, *Bull. Seism. Soc. Am.*, 66, 1821-1846.
- Bodenseewerk, 1979. Technical Bulletin No. 19, Borehole Tiltmeter Gbp10.
- Buchbinder, G., R. Kurtz, and A. Lambert, in press. A review of time-dependent geophysical parameters in the Charlevoix Region, Quebec, in, *Earthquake Prediction Research*, 2,
- Buchbinder, G., 1981. Velocity changes in the Charlevoix Region, Quebec, in: Earthquake Prediction, an International Review,

- D.W. Simpson and P.G. Richards eds., A.G.U. Maurice Ewing Series 4, 367-376.
- Buchbinder, G., and C.M. Keith, 1979. Stability of P travel times in the region of La Malbaie, Quebec, Bull. Seism. Soc. Am., 69, 463-481.
- Campbell, D.L., 1978. Investigation of the stress-concentration mechanism for intraplate earthquakes, Geophys. Res. Letters, 5, 477-479.
- El-Sabh, M.I., T.S. Murty, et L. Levesque, 1979, Mouvements des eaux induits par la maree et le vent dans l'estuaire du Saint-Laurent, Le Naturaliste Canadien, 106, 89-104.
- Farrell, W.E., 1972. Deformation of the Earth by surface loads, Rev. Geophys. and Space Phys., 10, 761-797.
- Hendershott, M., 1972. The effects of solid earth deformation on global ocean tides, Geophys. J.R. astr. Soc., 29, 389-403.
- Kumpel, H-J, in press. The influence of variations of the groundwater table on borehole tiltmeters, in: Proceedings of the 9th International Symposium on Earth Tides, ed., J.T. Kuo.
- Lambert, A., and Labrecque, J.J., 1980. Meteorological and hydrological effects on near surface bedrock tilt measurements, E.O.S. Trans. Am. Geophys. Un., 61, 367.
- Lambert, A., 1970. The response of the Earth to ocean tides around Nova Scotia, Geophys. J.R. astr. Soc., 19, 449-477.
- Leblanc, G., and G. Buchbinder, 1977. Second microearthquake survey of the St. Lawrence valley near La Malbaie, Quebec, Can. J. Earth Sci., 14, 2278-2789.
- Leblanc, G., A.E. Stevens, R.J. Wetmiller, and R. DuBerger, 1973. A microearthquake survey of the St. Lawrence valley near La Malbaie, Quebec, Can. J. Earth Sci., 10, 42-53.
- Lyons, J.A., D.A. Forsyth, and J.A. Mair, 1980. Crustal studies in the La Malbaie region, Quebec, Can. J. Earth Sci., 17, 478-490.
- Milne, W.G., W.E.T. Smith, and G.C. Rogers, 1970. Canadian seismicity and microearthquake research in Canada, Can. J. Earth Sci., 7, 591-601.
- Peters, J.A., and C. Beaumont, in press. Preliminary results from a new borehole tiltmeter array, Charlevoix, Quebec, in: Proceedings of the 9th International Symposium on Earth

Tides, ed., J.T. Kuo.

Peters, J.A., D.R. Bower, and A. Lambert, in press. Tidal tilt response at Charlevoix, Quebec, in: Proceedings of the 9th International Symposium on Earth Tides, ed., J.T. Kuo.

Robertson, P.B., 1975. Zones of shock metamorphism at the Charlevoix impact structure, Quebec, Geol. Soc. Am. Bull., 86, 1630-1638.

Robertson, P.B., 1968. La Malbaie structure, Quebec - a Paleozoic meteorite impact site. Meteoritics, 4, 89-112.

Sbar, M.L., and R.L. Sykes, 1973. Contemporary compressive stress and seismicity in Eastern North America: An example of intra-plate tectonics. Geol. Soc. Am. Bull., 84, 1861-1881.

Schuller, K., 1977. Tidal analysis by the Hybrid Least Squares Frequency Domain Convolution Method, in: Proceedings of the 8th International Symposium on Earth Tides, eds., M. Bonatz and P. Melchior.

Schuller, K., 1976. Ein Beitrag zur Auswertung von Erdzeitenregistrierungen Veroffl. Deutsche Geod. Komm., Reiche, C., Nr. 227, Munchen.

Stevens, A.E., 1980. Reexamination of some larger La Malbaie, Quebec Earthquakes (1924-1978), Bull. Seism. Soc. Am., 70, 529-557.

Wyatt, F., G. Cabaniss and D.C. Agnew, 1982. A comparison of tiltmeters at tidal frequencies, Geophys. Res. Letters, 9, 743-746.

Wyatt, F., and J. Berger, 1980. Investigations of tilt measurements using shallow borehole tiltmeters, J.G.R., 85, 4351-4362.

Zschau, J., 1976. Tidal sea load tilt of the crust, and its application to the study of crustal and upper mantle structures, Geophys. J.R. astr. Soc., 44, 577-593.

TABLE 1

Gbp 105 Hole 1

X component Az 270°(West)		Y component Az 0°(North)			
Data Set	Start	Length(H)	Data Set	Start	Length(H)
1	27/9/80	696	1	27/9/80	696
2	26/10/80	696	2	26/10/80	696
3	24/11/80	696	3	24/11/80	696
4	23/12/80	792	4	23/12/80	792
5	25/1/81	768	5	25/1/81	768
6	26/2/81	696	6	26/2/81	696

TABLE 2

Gbp 107 Hole 1

X component Az 270°(West)		Y component Az 0°(North)			
Data Set	Start	Length(H)	Data Set	Start	Length(H)
1	24/11/81	1424	1	24/11/81	1424
2	6/2/82	670	2	6/2/82	670
3	11/3/82	826	3	11/3/82	826
4	21/4/82	682	4	21/4/82	682
5	26/5/82	706	5	26/5/82	706
6	7/7/82	742	6	7/7/82	742
7	14/8/82	586	7	13/8/82	610
8	14/9/82	1056	8	16/9/82	1104

TABLE 3

Gbp 106 Hole 2

X component Az 21°			Y component Az 111°		
Data Set	Start	Length(H)	Data Set	Start	Length(H)
1	8/12/81	1018	1	8/12/81	1018
2	3/2/82	718	2	3/2/82	718
3	11/3/82	598	3	25/2/82	718
4	19/4/82	802	4	21/4/82	766
5	26/5/82	754	5	26/5/82	754

X component Az 180°(South)			Y component Az 270°(West)		
Data Set	Start	Length(H)	Data Set	Start	Length(H)
1	9/7/82	706	1	9/7/82	706
2	14/8/82	766	2	14/8/82	766
3	18/9/82	874	3	18/9/82	874

## Figure Captions

- Figure 1: Topographic map of the Charlevoix region of Quebec.
- Figure 2: Geodynamic surveys in the Charlevoix region (courtesy of A. Lambert).
- Figure 3: Stations and epicentral locations of the 1974 microearthquakes survey (from Stevens, 1980).
- Figure 4: Results of the relocation study of major recorded earthquakes (from Stevens, 1980).
- Figure 5: Results of a seismic survey of the relationship between the Ordovician overthrusts and the Grenville Province's basement (from Lyons et al, 1980).
- Figure 6: Location of shotpoints and recording stations for the P-wave velocity studies and variations in the P-wave station residuals over the period 1974 to 1980. (from Buchbinder and Keith, 1979 and Buchbinder et al, in press).
- Figure 7: Tilt anomalies predicted for simple inclusion models (from Beaumont and Berger, 1974).
- Figure 8: Interaction between the earth tide and an idealized stress hysteresis loop for three tectonic stress rates, A, B and C (from Beaumont, 1979).
- Figure 9: Tiltmeter configuration and results from the Pinon Flat Observatory, California (from Wyatt et al, 1982).
- Figure 10: Plan of the Charlevoix Observatory. The tiltmeter boreholes are labelled Hole 1, 2 and 3.
- Figure 11: Schematic diagram of a borehole and tiltmeter pod showing the basal support pin.
- Figure 12: The photographic method for determining the orientation of tiltmeters.
- Figure 13: Down borehole photograph showing the alignment thread and one light source at the base of the borehole. (The light is the short line parallel to the thread and to the left of it.)
- Figure 14: The Gbp10 borehole tiltmeter (from Bodenseewerk manual).
- Figure 15: Schematic diagram showing the major components of the sensor of the borehole tiltmeter (from Bodenseewerk manual).
- Figure 16: Block diagram of the electronics for the Bodenseewerk

Gbpl0 tiltmeter.

Figure 17: Recording configuration for the borehole tiltmeters and water wells at the Charlevoix Observatory.

Figure 18: Photograph taken by a camera and flashlight assembly lowered down borehole 2. Lumps of weldment can clearly be seen as an arc in the upper part of the picture.

Figure 19: Wiring diagram for a borehole tiltmeter showing components at the wellhead, AGOS, and the lightning protection system.

Figure 20: The muleshoe assembly used to orient tiltmeters in borehole 3. The 'key', which fits inside the muleshoe slot, can clearly be seen projecting from the base of the tiltmeter suspended above the muleshoe. The muleshoe is normally inserted inside the tiltmeter pod.

Figure 21: Time variations in the amplitude part of the  $M_2$  admittance of the ANAC tiltmeters installed in positions C, D, and A of the shallow vault at the Charlevoix Observatory (from Peters et al, in press).

Figure 22: Time variations in the phase part of the admittance corresponding to figure 21. (from Peters et al, in press).

Figure 23: Major intervals of time for which borehole tilt data have been recorded at the Charlevoix site.

Figure 24: A typical calibration sequence of a Bodenseewerk tiltmeter showing the response of both the X and Y channels.

Figure 25: Typical response of a Bodenseewerk tiltmeter to a teleseism.

Figure 26: Response of Gbpl06 in borehole 2 to a local earthquake on Dec. 4, 1982.

Figure 27: Plot against time of: groundwater level; borehole tiltmeter 105 secular tilt in X(east) and Y(north) directions; and rainfall for the period September 27, 1980 to April 10, 1981 (from Peters and Beaumont, in press).

Figure 28: Typical tilt records. These are unfiltered but have had calibration pulses and steps removed.

Figure 29: Plot against time of: groundwater level from the A(70) and B(70) wells; tilt of Gbpl06 in borehole 2 (labelled bh2) with sensitive axes oriented at  $N111^\circ E$  and  $N21^\circ E$ ; and tilt of Gbpl07 in borehole 1 (labelled bh1) with sensitive axes oriented north and west, for 1981 and

1982.

Figure 30: Consecutive monthly amplitude and relative phase lag results for Gbp105 in borehole 1 in the X(west) and Y(north) directions. Amplitude and phase lag curves are plotted for the  $M_2$ ,  $S_2$ ,  $O_1$  and  $K_1$  constituents. X results are on the left, Y on the right.

Figure 31: Variability of the  $M_2$  west(X) tilt phasor for Gbp105 operating in borehole 1. The inset shows an enlargement of the box surrounding the mean phasor. Greenwich phase lags behind the equilibrium potential (G) are measured anticlockwise.

Figure 32: Variability of the  $M_2$  south(Y) tilt phasor for Gbp105 operating in borehole 1. Format is like that of Figure 31.

Figure 33: Consecutive monthly amplitude parts of the  $M_2$  admittance for Gbp107 operating in borehole 1 (bh1) and Gbp106 operating in borehole 2 (bh2) during 1982.

Figure 34: Phase parts of the  $M_2$  admittance corresponding to Figure 33.

Figure 35: Variability of the  $M_2$  west tilt phasor for Gbp106 in borehole 2 during 1982. Format is like that of Figure 31.

Figure 36: Variability of the  $M_2$  south tilt phasor for Gbp106 operating in borehole 2 during 1982. Format is like that of Figure 31.

Figure 37: Variability of the  $M_2$  west tilt phasor for Gbp107 operating in borehole 1 during 1982. Format is like that of Figure 31.

Figure 38: Variability of the  $M_2$  south tilt phasor for Gbp107 operating in borehole 1 during 1982. Format is like that of Figure 31.

Figure 39: Power spectrum of Gbp106 X (N21°E) tilt data.

Figure 40: Power spectrum of Gbp106 Y (N111°E) tilt data.

Figure 41: Power spectrum of Gbp107 south tilt data.

Figure 42: Power spectrum of Gbp107 west tilt data.

Figure 43: Phasor plot of the ANAC tiltmeter results for  $M_2$  in the west direction.

Figure 44: Phasor plot of the ANAC tiltmeter results for  $M_2$  in the south direction.

- Figure 45: Phasor plot of the ANAC tiltmeter results for  $O_1$  in the west direction.
- Figure 46: Phasor plot of the ANAC tiltmeter results for  $O_1$  in the south direction.
- Figure 47: Triangular division of the area of the St. Lawrence estuary adjacent to the Charlevoix site for  $M_2$  load calculations.
- Figure 48: Triangular division of the whole of the St. Lawrence River estuary for  $M_2$  load calculations. It is the loading from the tides in this area that contributes the local, 'l', part of the phasors to  $O_1$  and  $M_2$  load tilts.
- Figure 49: Empirical  $M_2$  cotidal chart for the St. Lawrence estuary. Amplitudes are in feet and phases are Greenwich phase lags.
- Figure 50: Empirical  $O_1$  cotidal chart for the St. Lawrence estuary. Amplitudes are in feet and phases are Greenwich phase lags.
- Figure 51: Comparison of observed and theoretical  $M_2$  west load tilt phasors for Gbpl05 in borehole 1. The theoretical prediction 'FGB' is for the Gutenberg-Bullen earth model using Green functions calculated by Farrell (1972). Vector '1' is due to loading in the St. Lawrence estuary. Vector '2' is a measure of the load tilt from the remaining seas and oceans. 'D', as is explained in the text, provides a measure of the maximum effect of local areas that 'dry' at low water. The mean observation result 'OBS' is surrounded by a 2msec box which is enlarged in the inset. The variability of monthly analyses is shown in this box. The phase lags, measured anticlockwise, are Greenwich equilibrium potential phase lags.
- Figure 52: Comparison of observed and theoretical  $M_2$  west load tilt phasors for Gbpl06 operating in borehole 2. The style of the figure is the same as Figure 51.
- Figure 53: Comparison of observed and theoretical  $M_2$  west load tilt phasors for Gbpl07 operating in borehole 1. The style of the figure is the same as Figure 51.
- Figure 54: Comparison of observed and theoretical  $M_2$  south load tilt phasors for Gbpl05 operating in borehole 1. The style of the figure is the same as Figure 51.
- Figure 55: Comparison of observed and theoretical  $M_2$  south load tilt phasors for Gbpl06 operating in borehole 2. The style of the figure is the same as Figure 51.

- Figure 56: Comparison of observed and theoretical M<sub>2</sub> south load tilt phasors for Gbpl07 operating in borehole 1. The style of the figure is the same as Figure 51.
- Figure 57: Comparison of observed and theoretical O<sub>1</sub> west load tilt phasors for Gbpl05 operating in borehole 1. The model result is again FCB and the mean observation result is marked 'OBS'. Variability of the monthly analyses is plotted directly on the main diagram. The '1', '2' and 'D' vectors have the same meaning as they had in the M<sub>2</sub> load phasor plots. Phase lags are measured anticlockwise and are Greenwich equilibrium potential phase lags.
- Figure 58: Comparison of observed and theoretical O<sub>1</sub> west load tilt phasors for Gbpl06 operating in borehole 2. The style of the figure is the same as Figure 57.
- Figure 59: Comparison of observed and theoretical O<sub>1</sub> west load tilt phasors for Gbpl07 operating in borehole 1. The style of the figure is the same as Figure 57.
- Figure 60: Comparison of observed and theoretical O<sub>1</sub> south load tilt phasors for Gbpl05 operating in borehole 1. The style of the figure is the same as Figure 57.
- Figure 61: Comparison of observed and theoretical O<sub>1</sub> south load tilt phasors for Gbpl06 operating in borehole 2. The style of the figure is the same as Figure 57.
- Figure 62: Comparison of observed and theoretical O<sub>1</sub> south load tilt phasors for Gbpl07 operating in borehole 1. The style of the figure is the same as Figure 57.

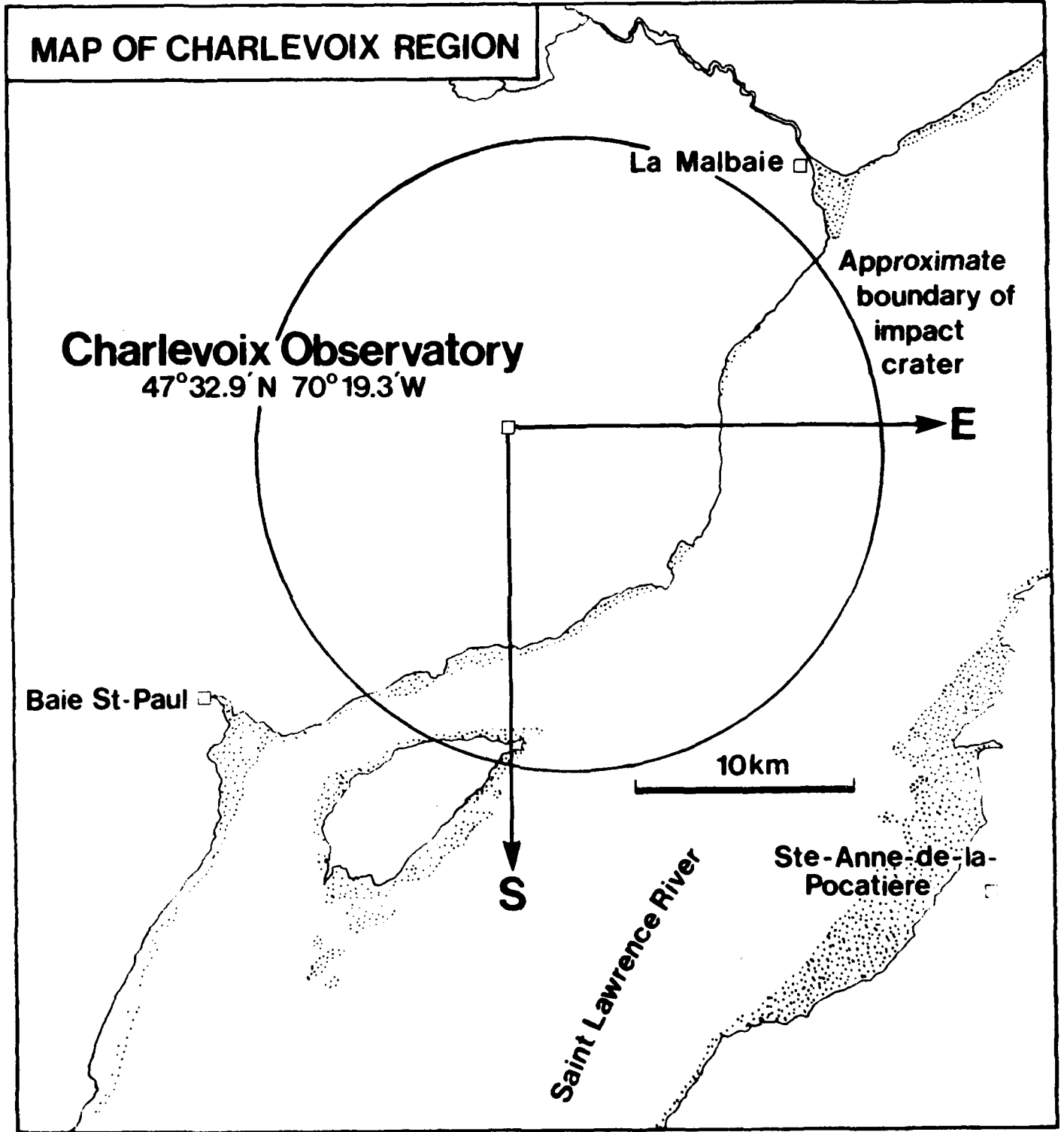


Figure 1

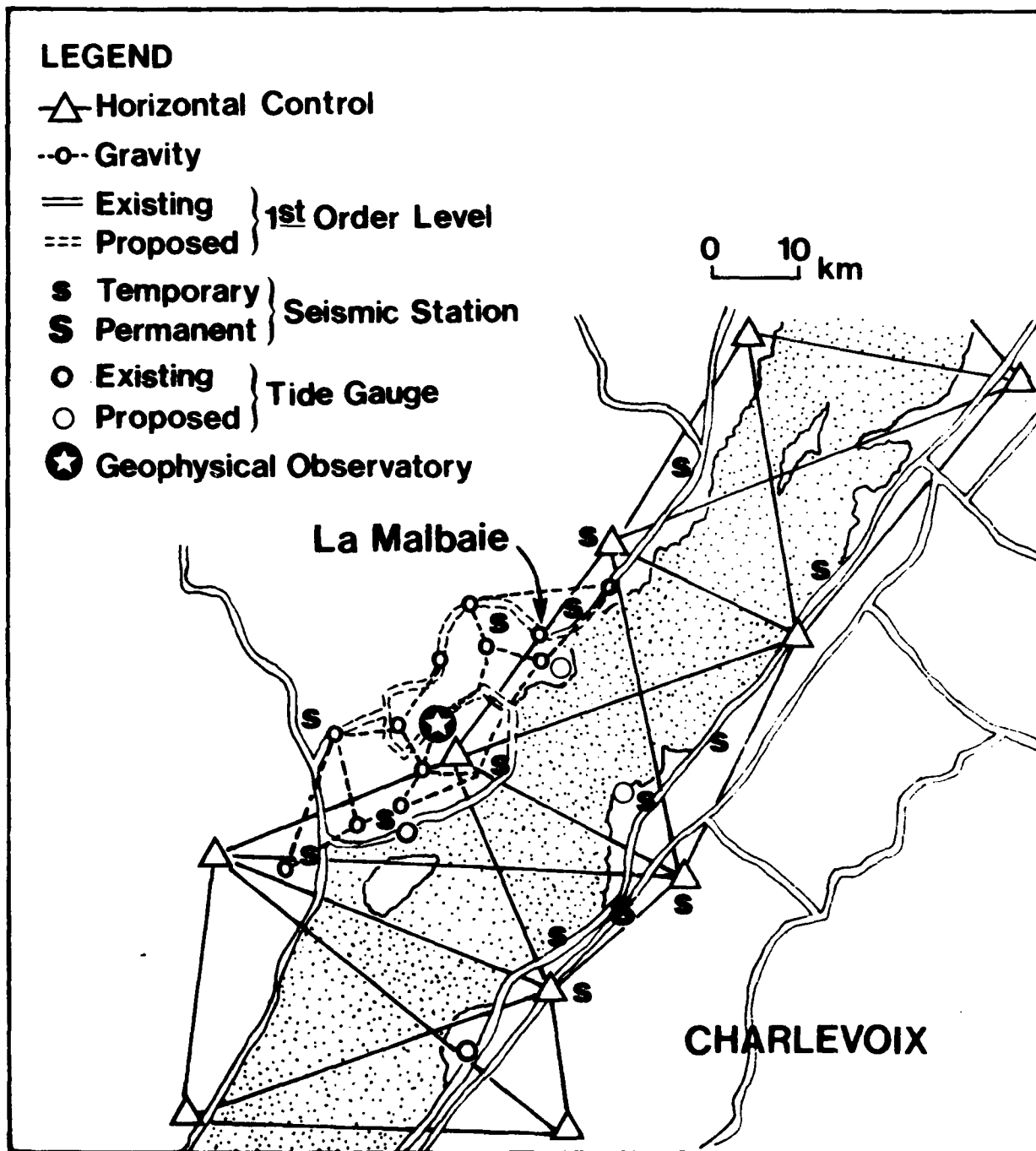
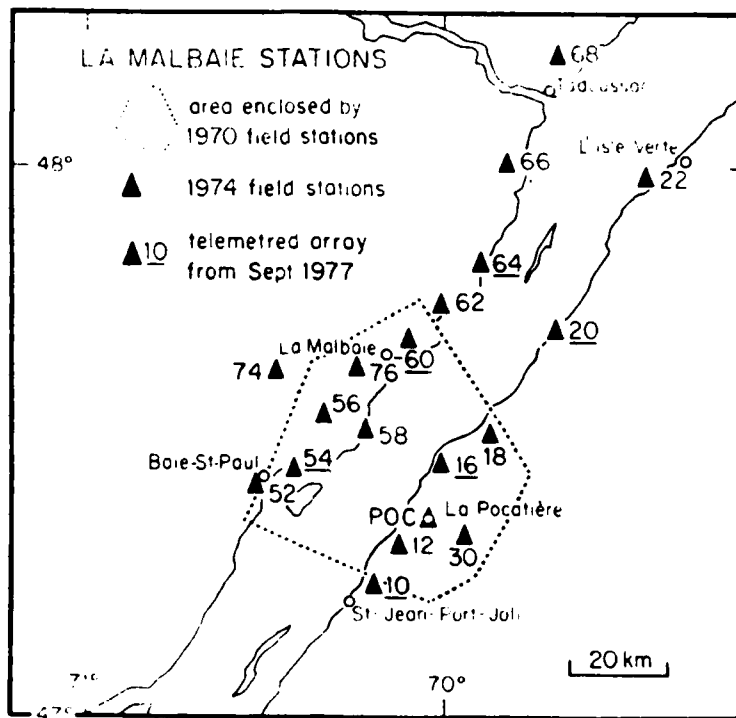
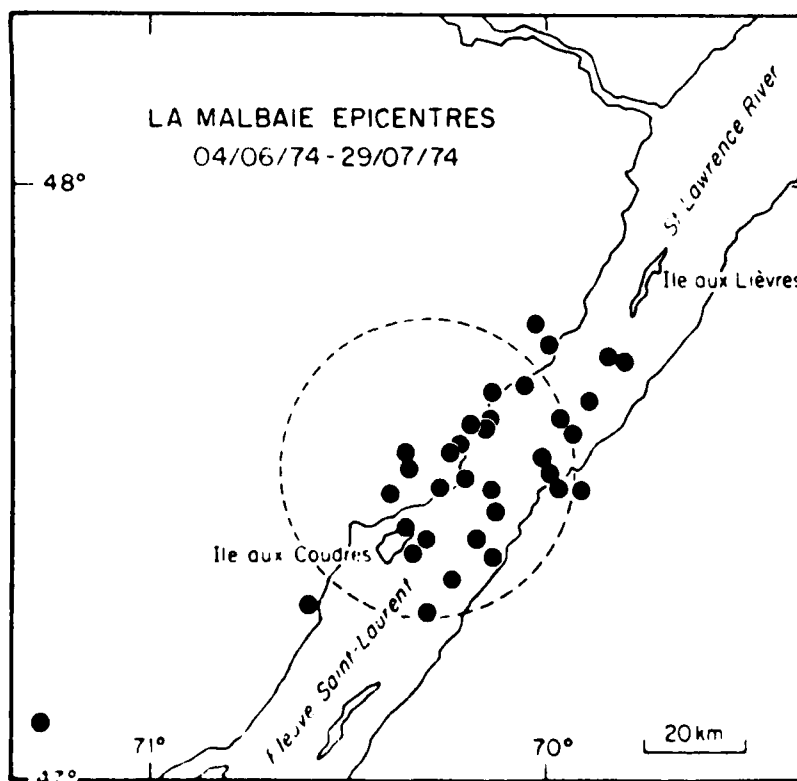


Figure 2

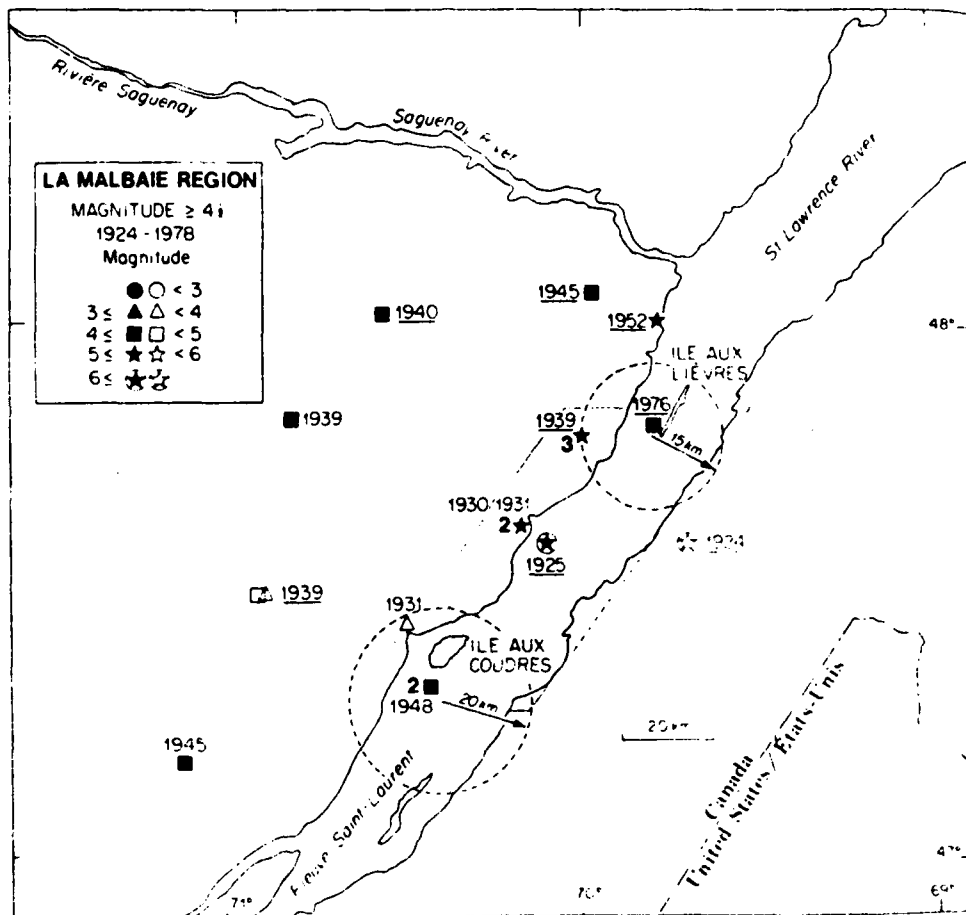


Recording sites occupied during the microearthquake survey of 1974 (after Leblanc and Buchbinder, 1977). POC is a regional station (SPZ) established in January 1972 and upgraded (3 SPZ's) in September 1977. Regional station LMQ was installed in November 1976 at virtually the same site as field station 76.



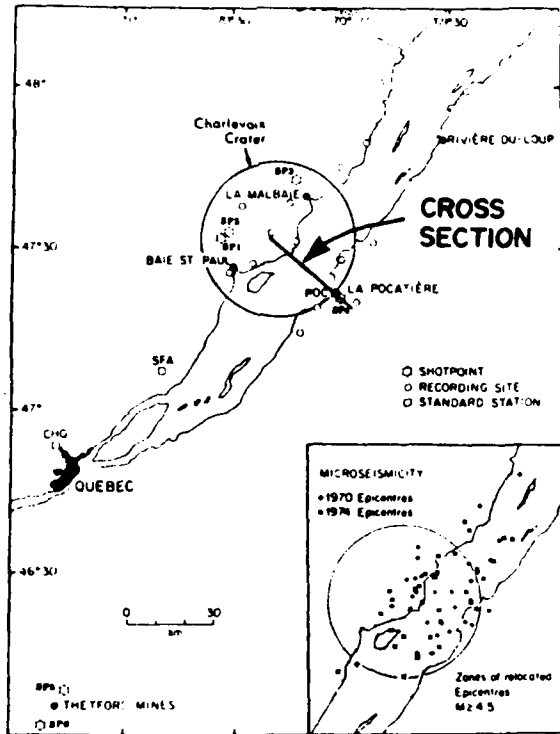
Microearthquake survey of 1974 (after Leblanc and Buchbinder, 1977). Circles denote locations of microearthquake epicenters. Recording sites are shown in Figure 1. The dashed circle marks the approximate position of the outer rim of the Charlevoix impact crater (from Rondot, 1971).

Figure 3

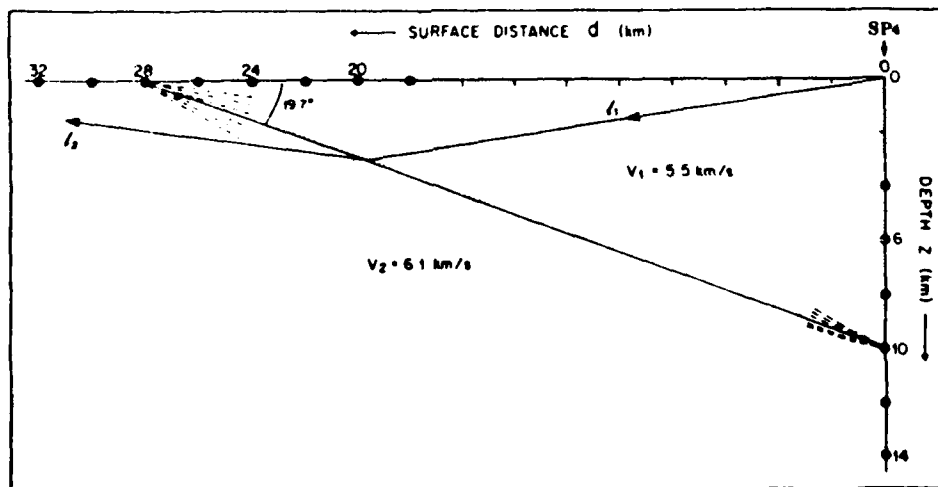


The 48 events studied for this report identified by year and magnitude range. See Table 1 for details. All known earthquakes in this region and period with magnitude  $\geq 4$  are included. A boldface digit beside an epicenter gives the number of earthquakes with the same published epicenter. A filled symbol indicates an epicentral uncertainty not more than 40 km according to the relevant catalog. An open symbol indicates greater uncertainty. An underlined date denotes the 11 earthquakes relocated near Ile aux Lievres. The remainder (except June 1945) are relocated near Ile aux Coudres. The dashed circles mark the approximate source areas of the relocated events. The shaded area is the microseismicity zone of Figures 6 and 8. For details see the Results section.

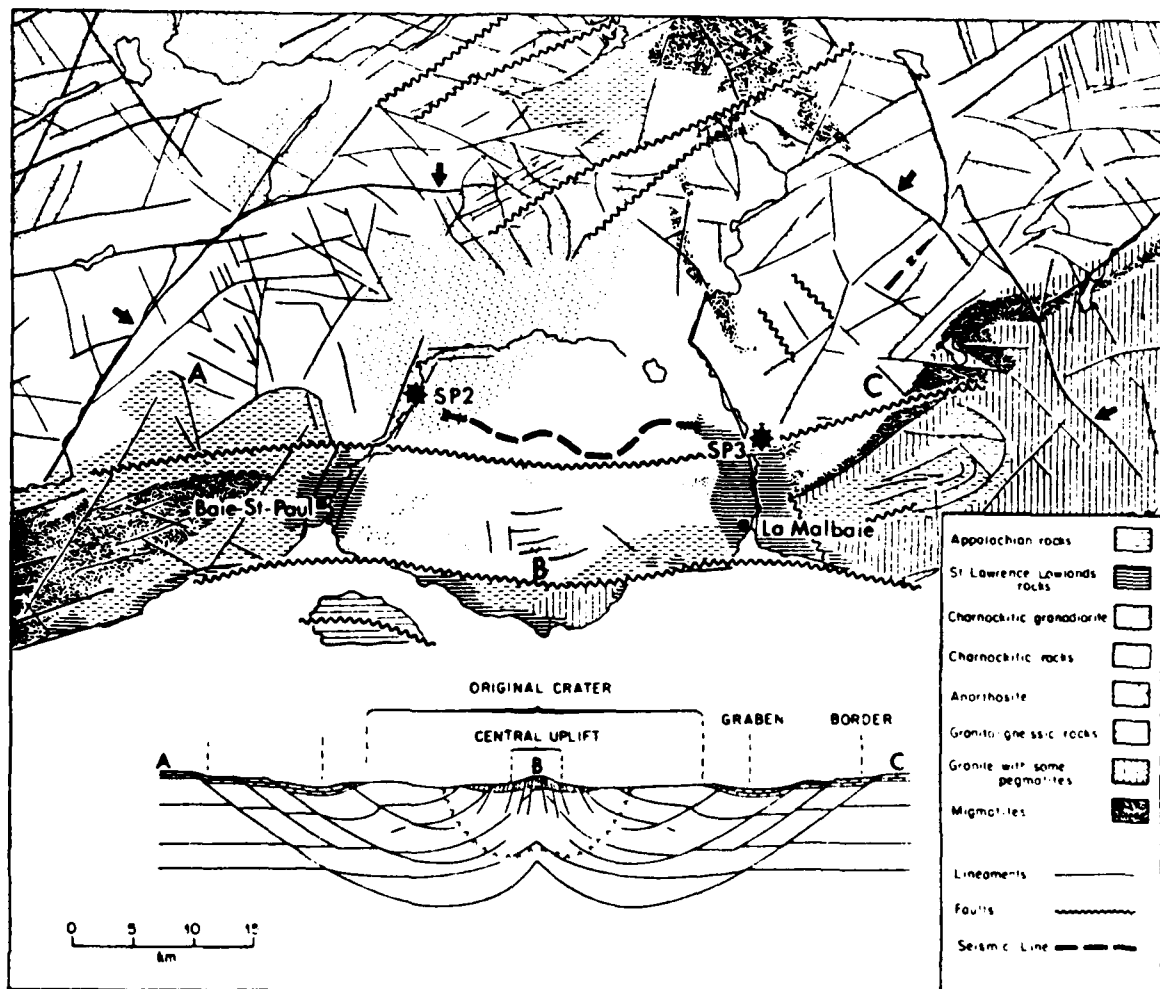
Figure 4



Location map showing the shotpoints, recording sites, and standard stations in the La Malbaie Region. Inset shows spatial relationship of seismicity to Charlevoix crater.

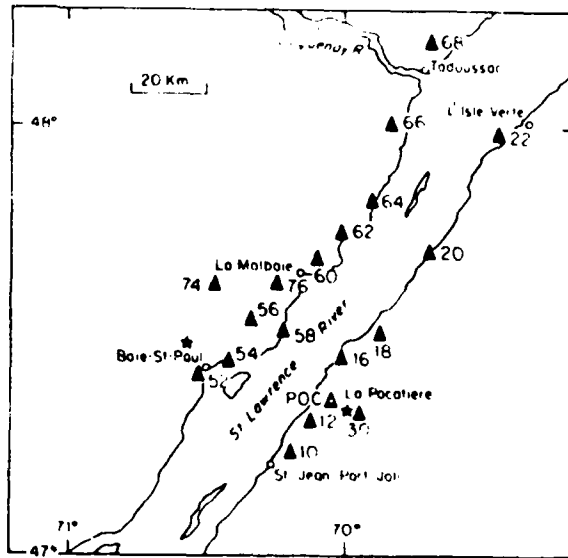


Results of numerical modelling of Logan's contact. Best-fitting model had a surface distance of 28 km, a depth beneath SP4 of 10 km, and a dip of  $19.7^\circ$ . A seismic ray traversing the sedimentary wedge and refracting into the Precambrian is denoted by the segments  $I_1$  and  $I_2$ , respectively. Solid dots along the axes denote trial values of  $d$  and  $z$ .



Location of the Charlevoix reflection-refraction survey shotpoints (SP2 and SP3) and profile (heavy dashed line) relative to the geology and structural lineaments in the vicinity of the Charlevoix crater. Arrows indicate possible extent of structural disruption due to impact, as interpreted from Landsat imagery. Lower section after Rondot (1971) shows hypothetical subsurface zones of slip due to crater formation.

Figure 5b



Seismometer stations are triangles and shot points are stars.

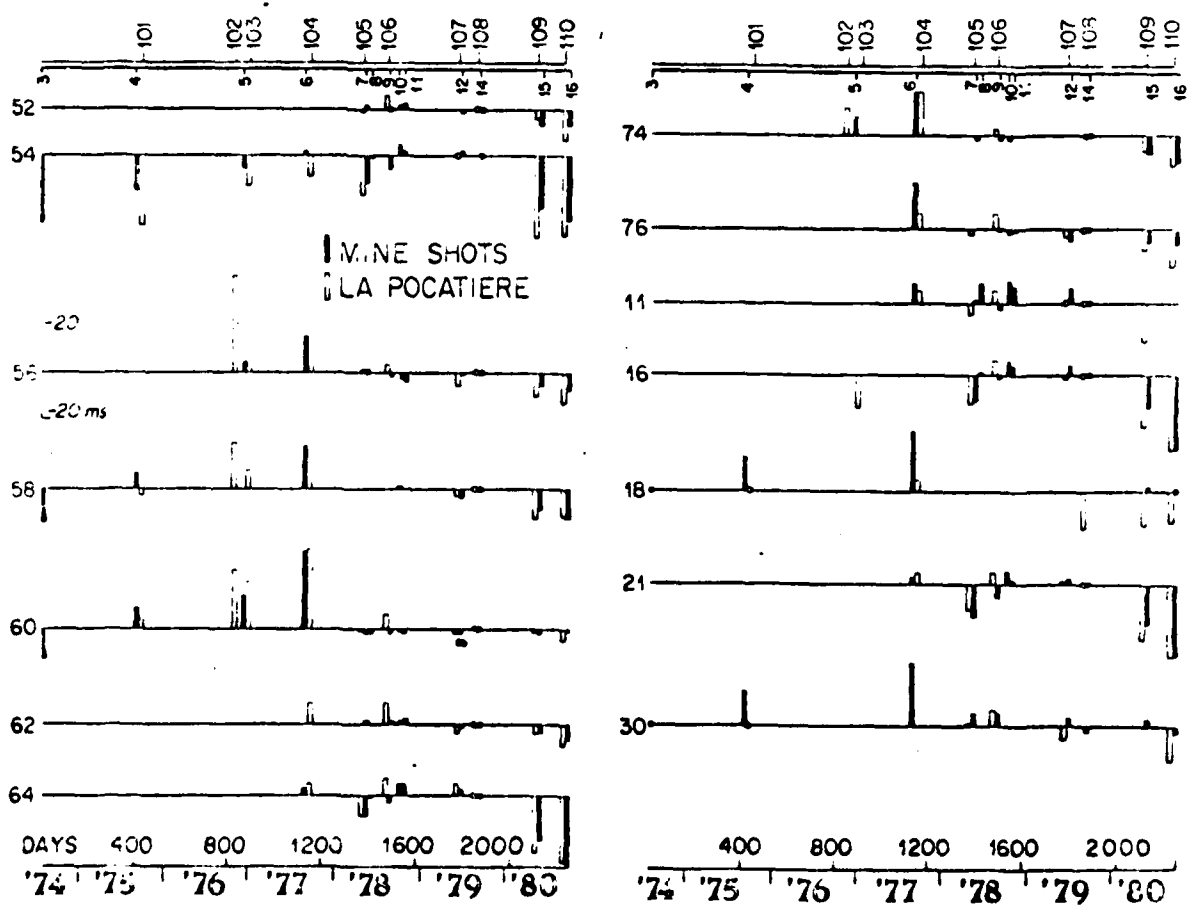
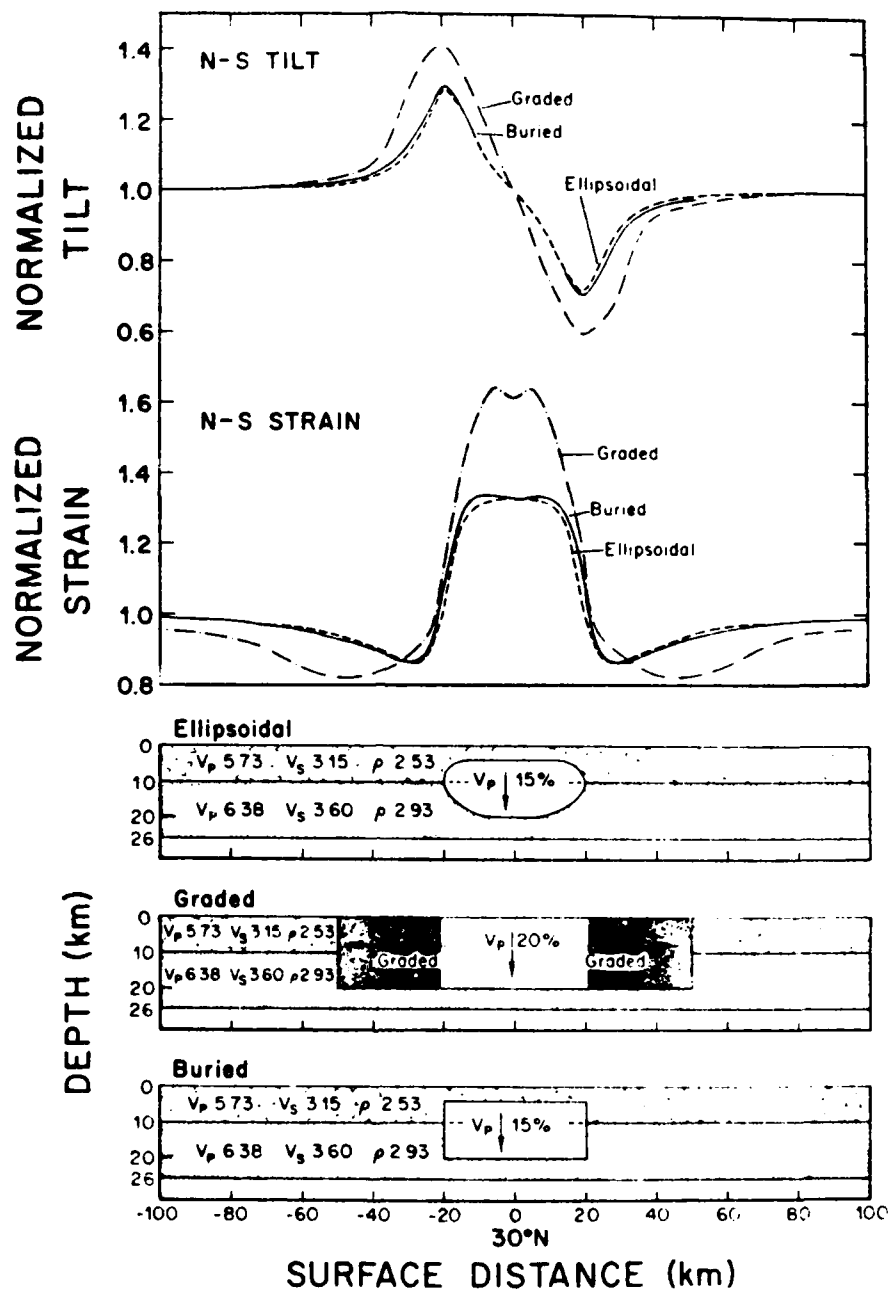


Figure 6



North-south components of the normalized tilt and strain tide amplitude for ellipsoidal, graded and buried dilatant zones. Model properties below 26 km are based on the Gutenberg-Bullen A model. The depth to the upper boundary of the ellipsoidal and buried zones is 4 km. In the graded model,  $V_p$  is reduced by 20 per cent in the central region.  $V_p$  linearly decreases outwards to the boundary with the non-dilatant zone.

Figure 7

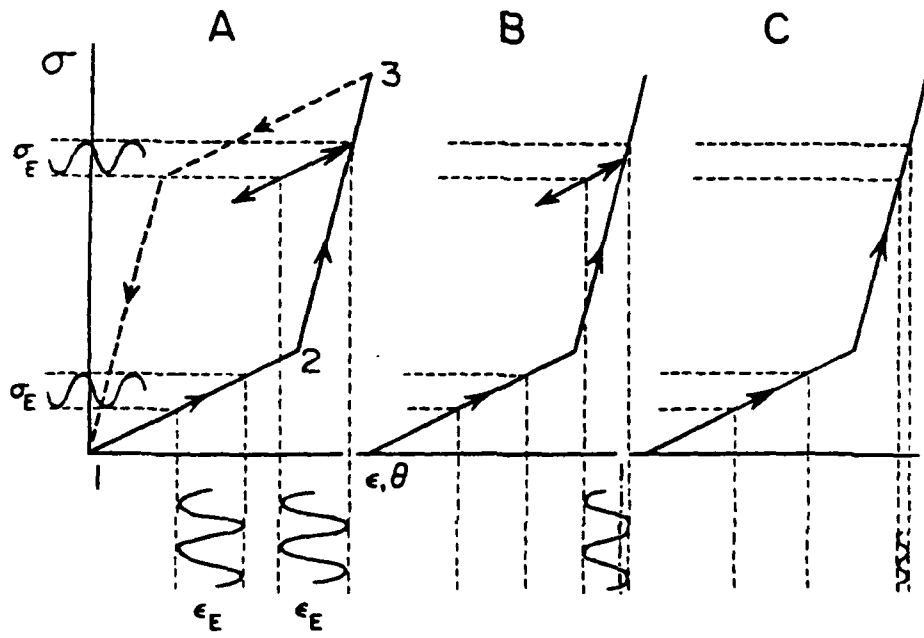


Figure 8

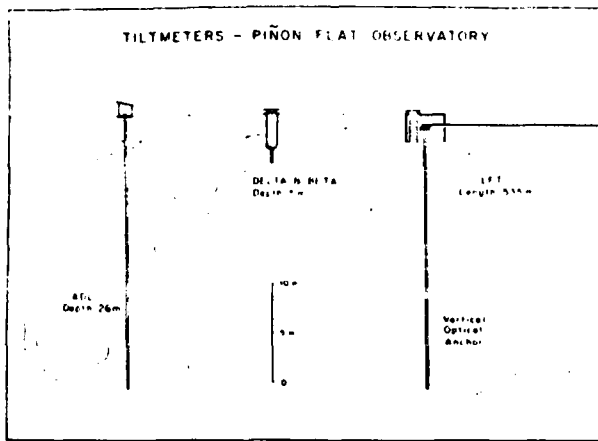


Fig. 1 Sketch showing installation of the tiltmeters. On the left is the ADL transducer, placed at a depth of 26 m, in the middle the Kinemetrics sensors at a depth of 4.5 m, and extending to the right, the 535 m long fluid tiltmeter. The vertical optical anchor is used to monitor and correct for vertical motions of the reference monument

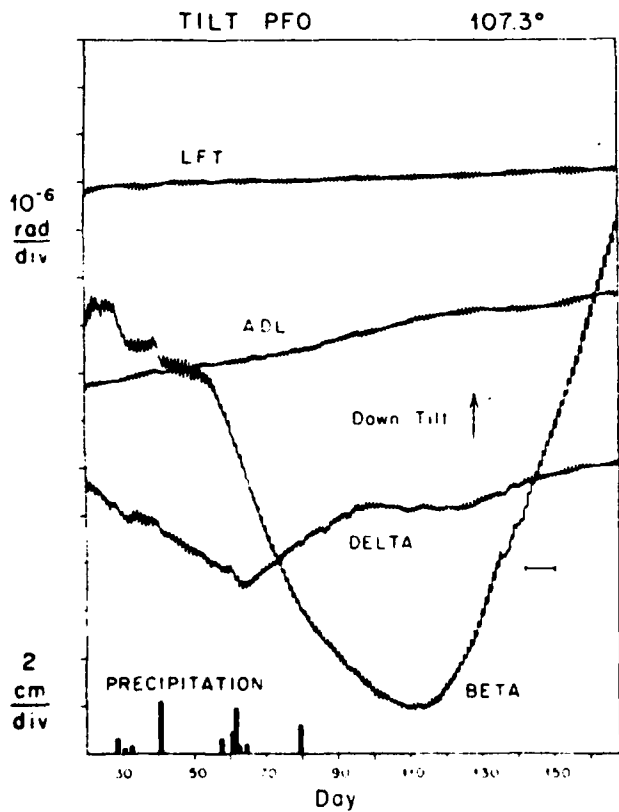


Fig 2 Edited tilt data. A 10-day gap in the original data (horizontal bar) has been filled by tidal interpolation. Positive tilt at an azimuth of  $107.3^\circ$  corresponds to a pendulum bob moving in that direction

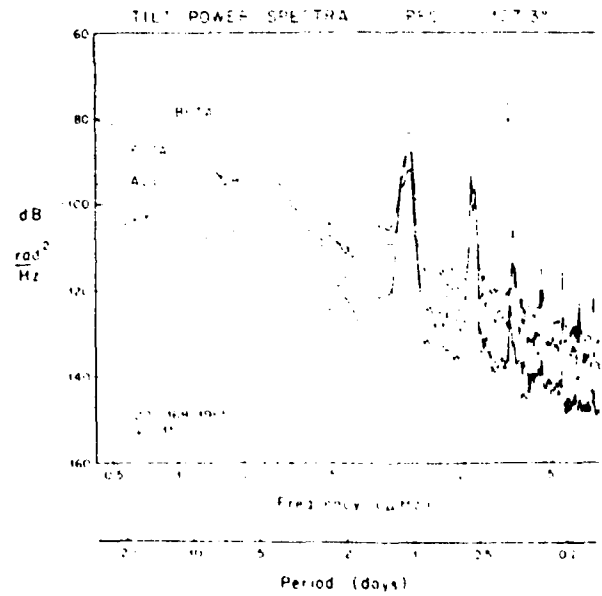


Fig 3 Power spectral density for the observations presented in Figure 2. The vertical bar shows the range of 95% confidence limits

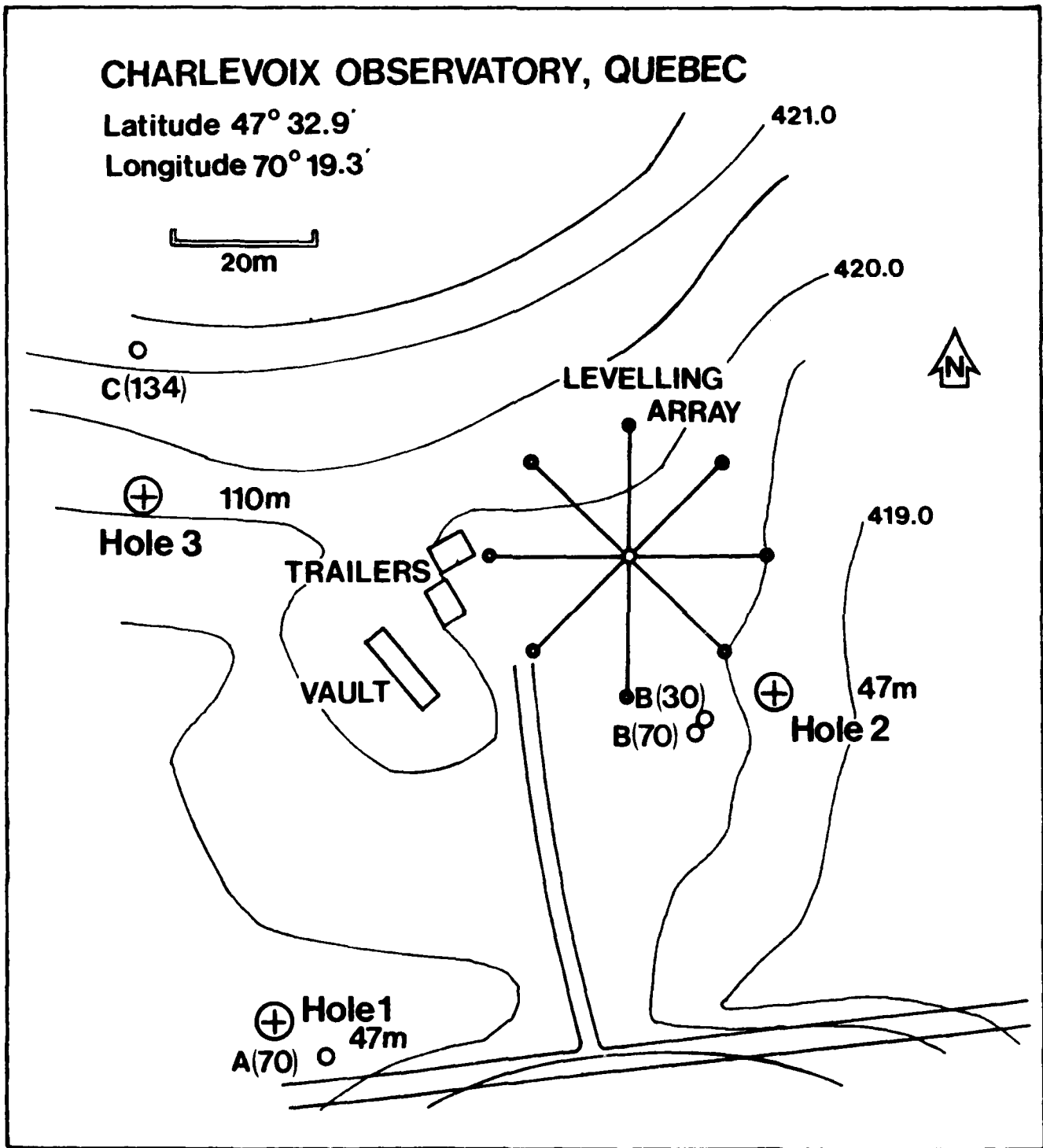


Figure 10

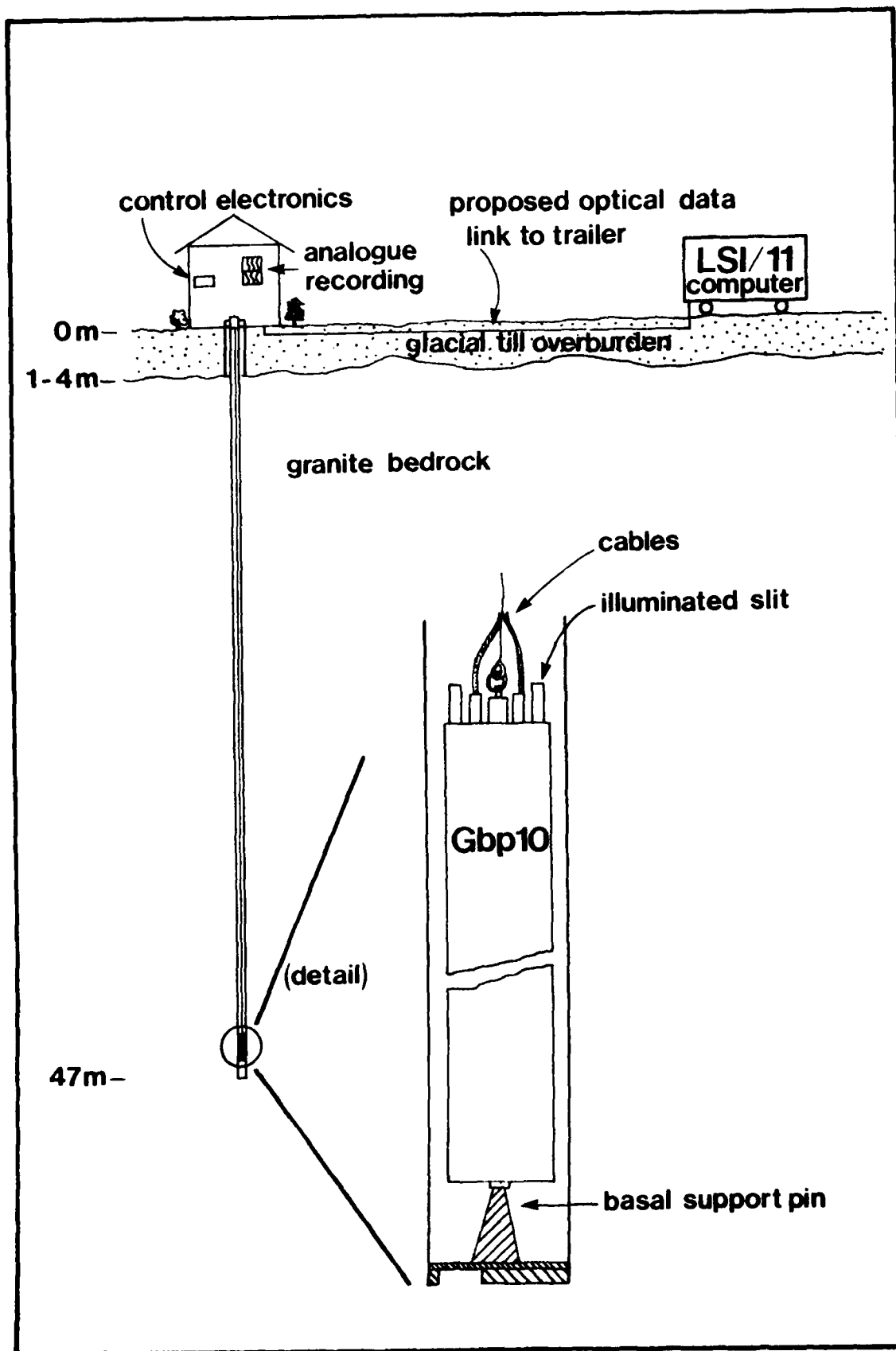


Figure 11  
79

# Photographic Azimuth Determination

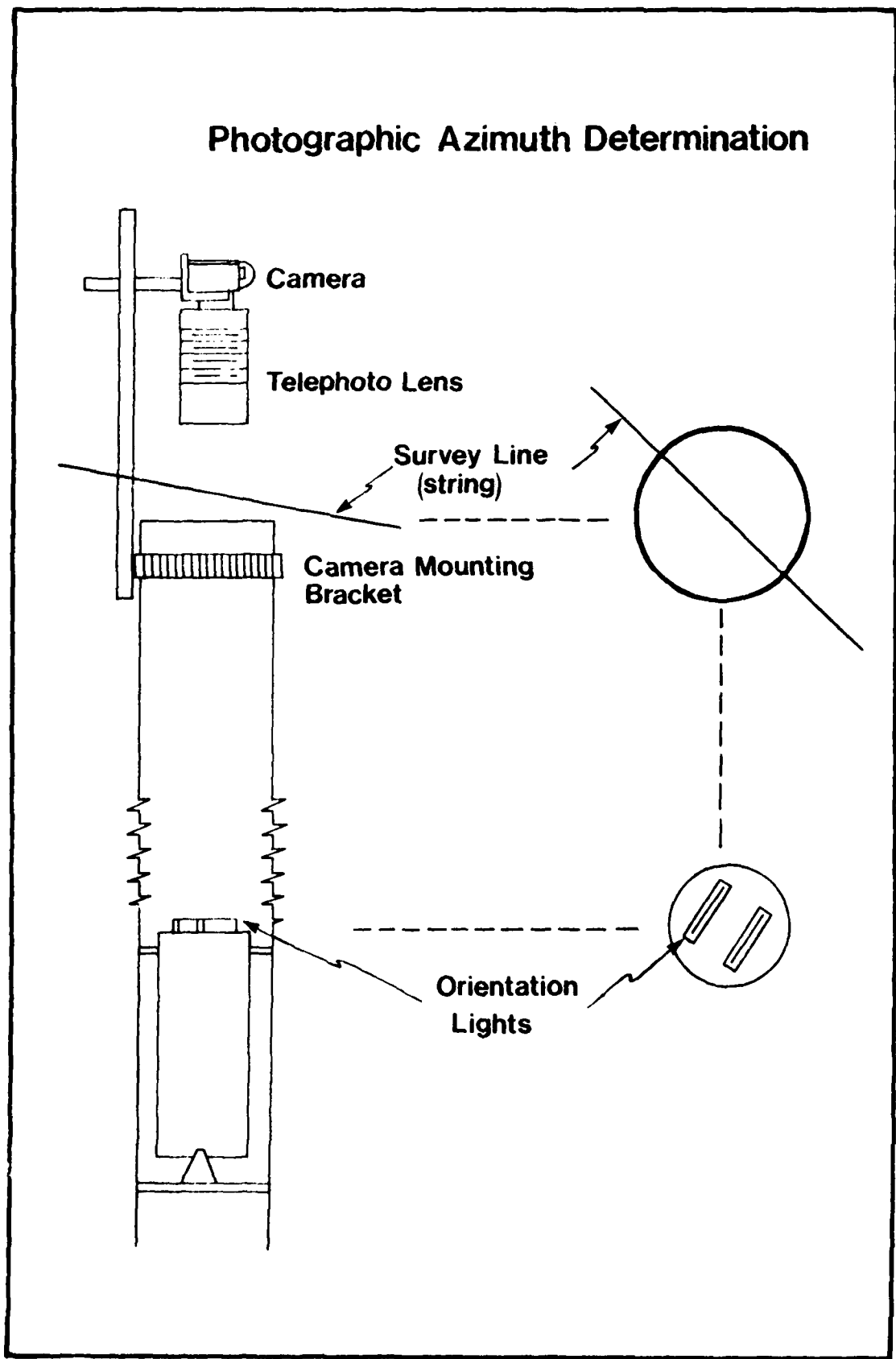


Figure 12



Figure 13  
81

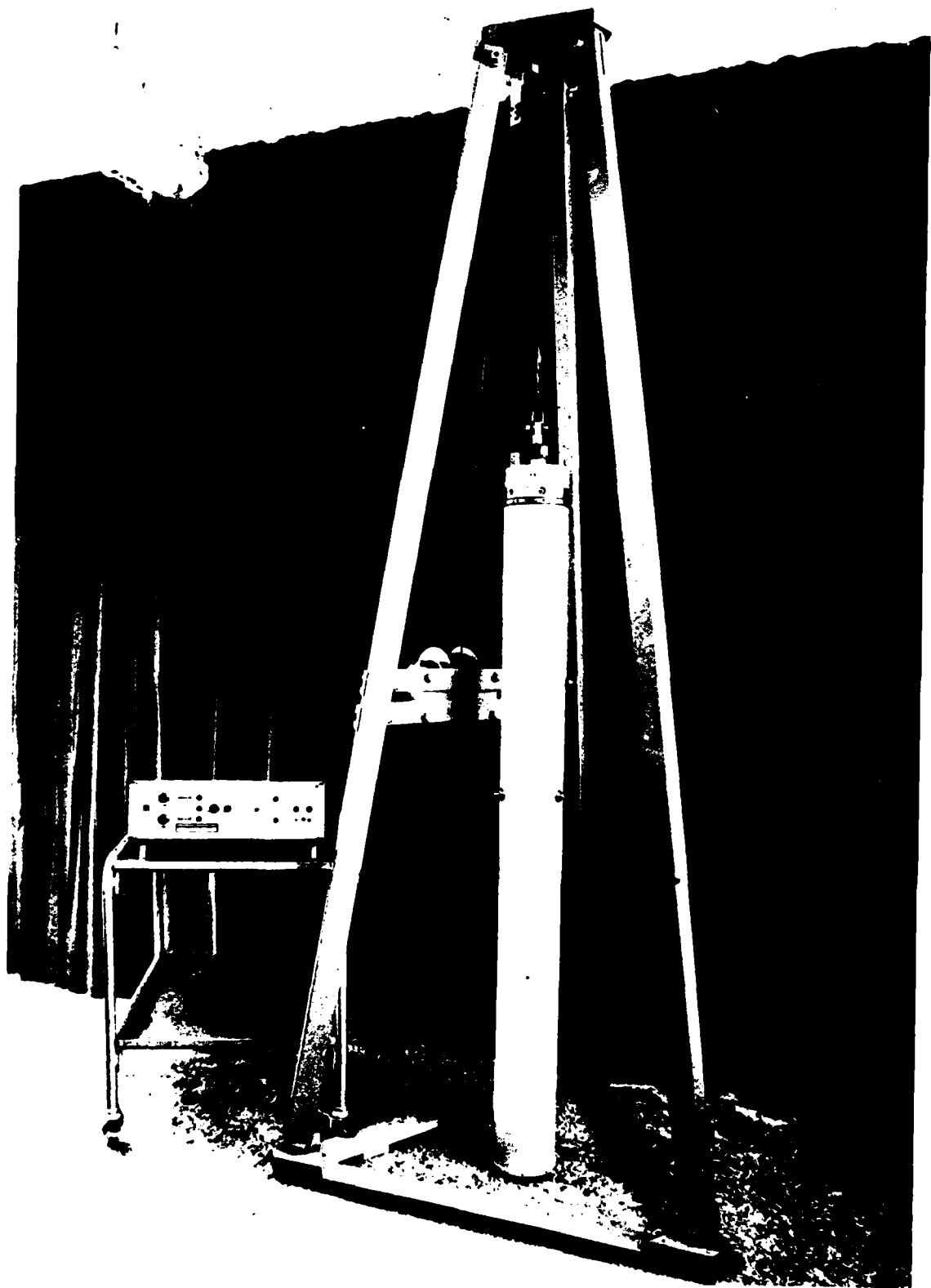
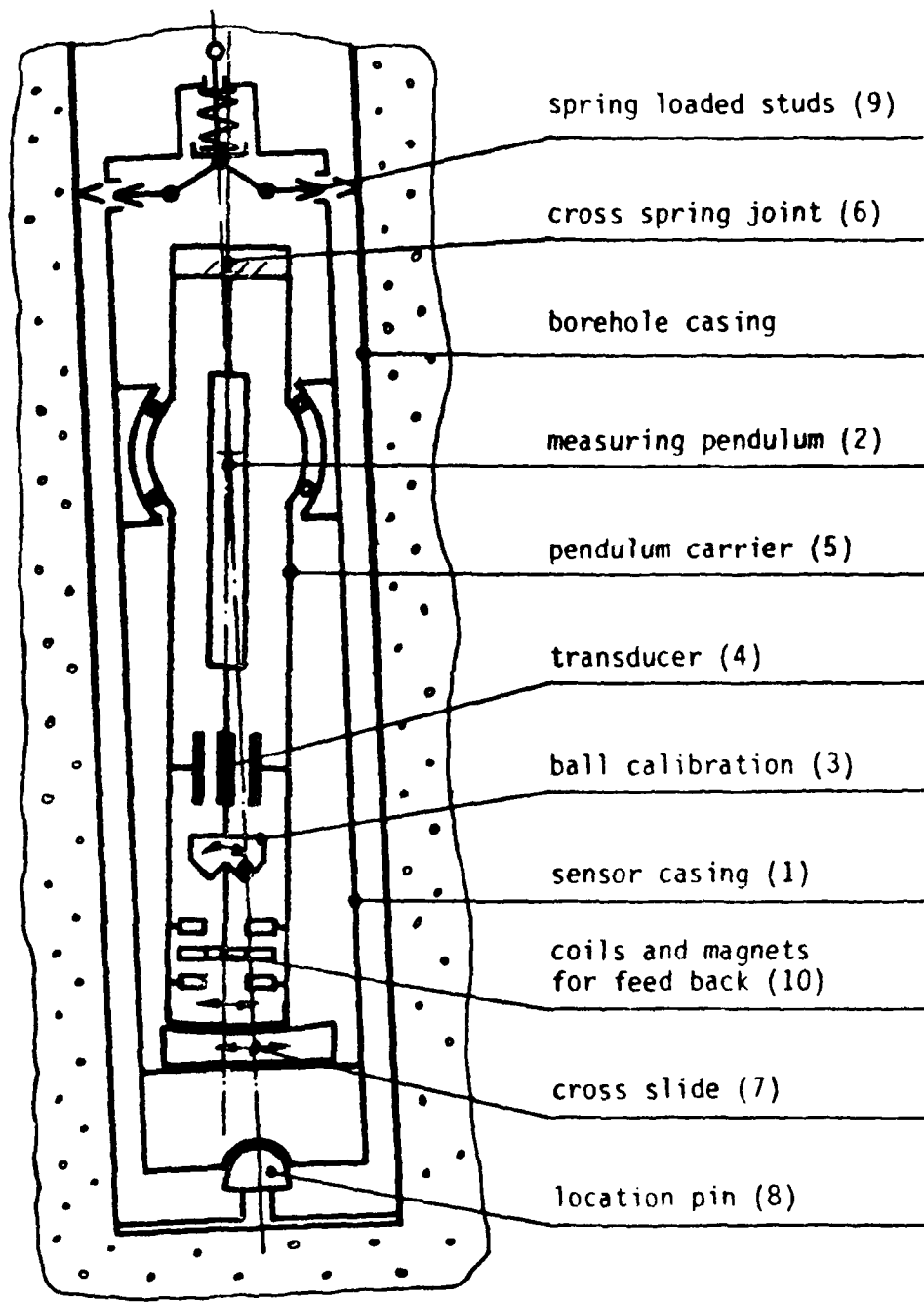


Figure 14



Schematic diagram showing major components of the Sensor of the borehole tiltmeter

Figure 15

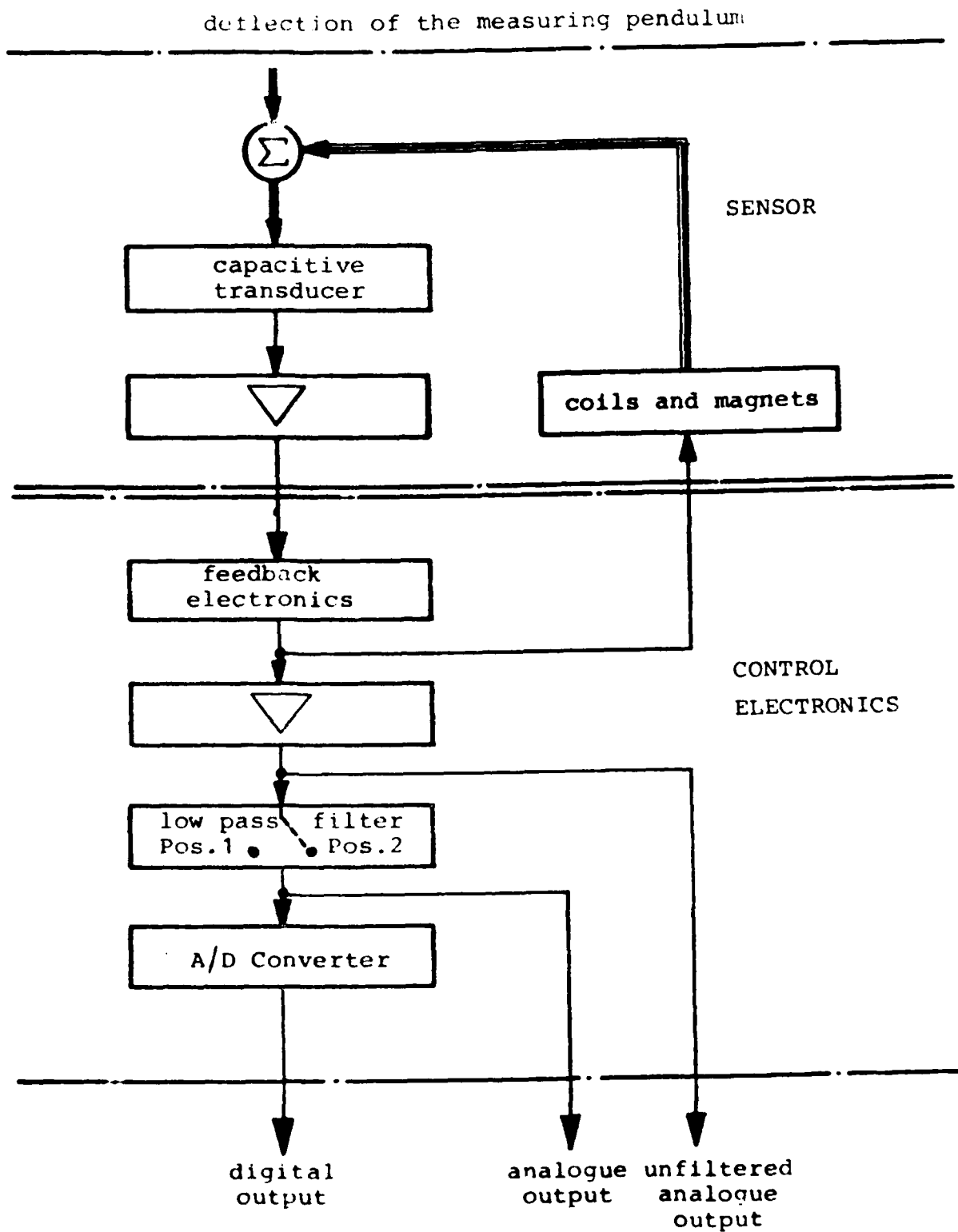
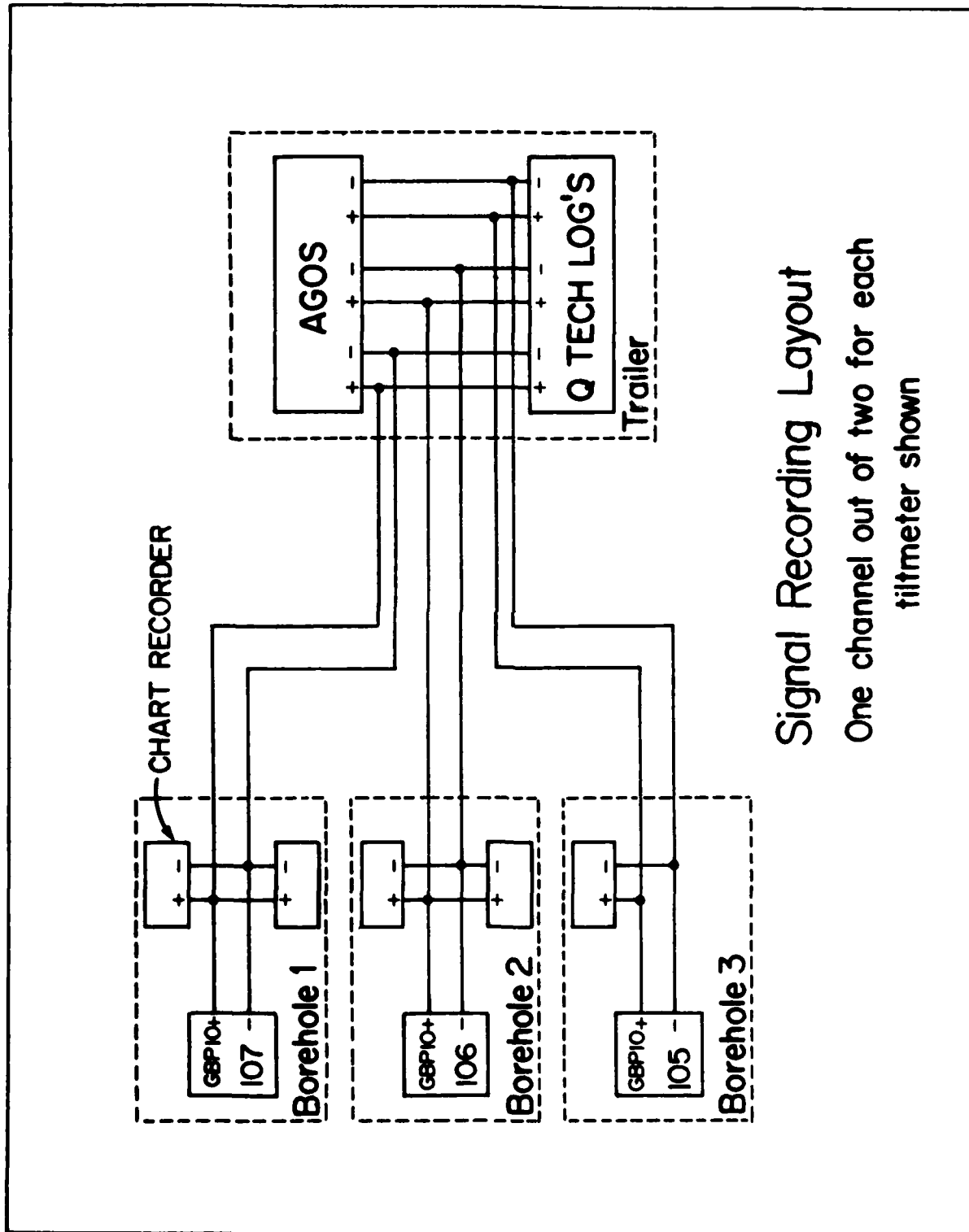


Figure 16

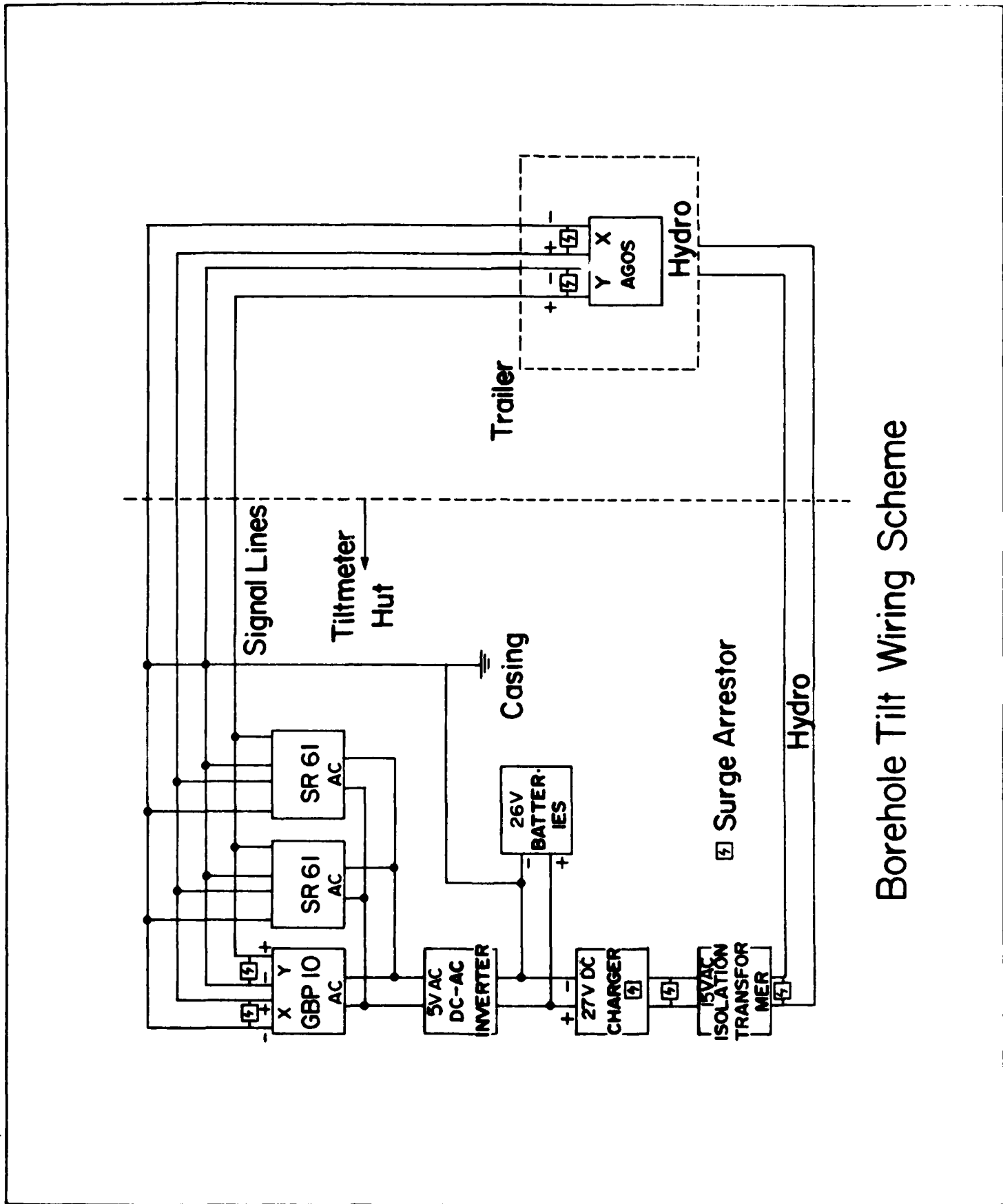


Signal Recording Layout  
 One channel out of two for each  
 tiltmeter shown

Figure 17



Figure 18



Borehole Tilt Wiring Scheme

Figure 19

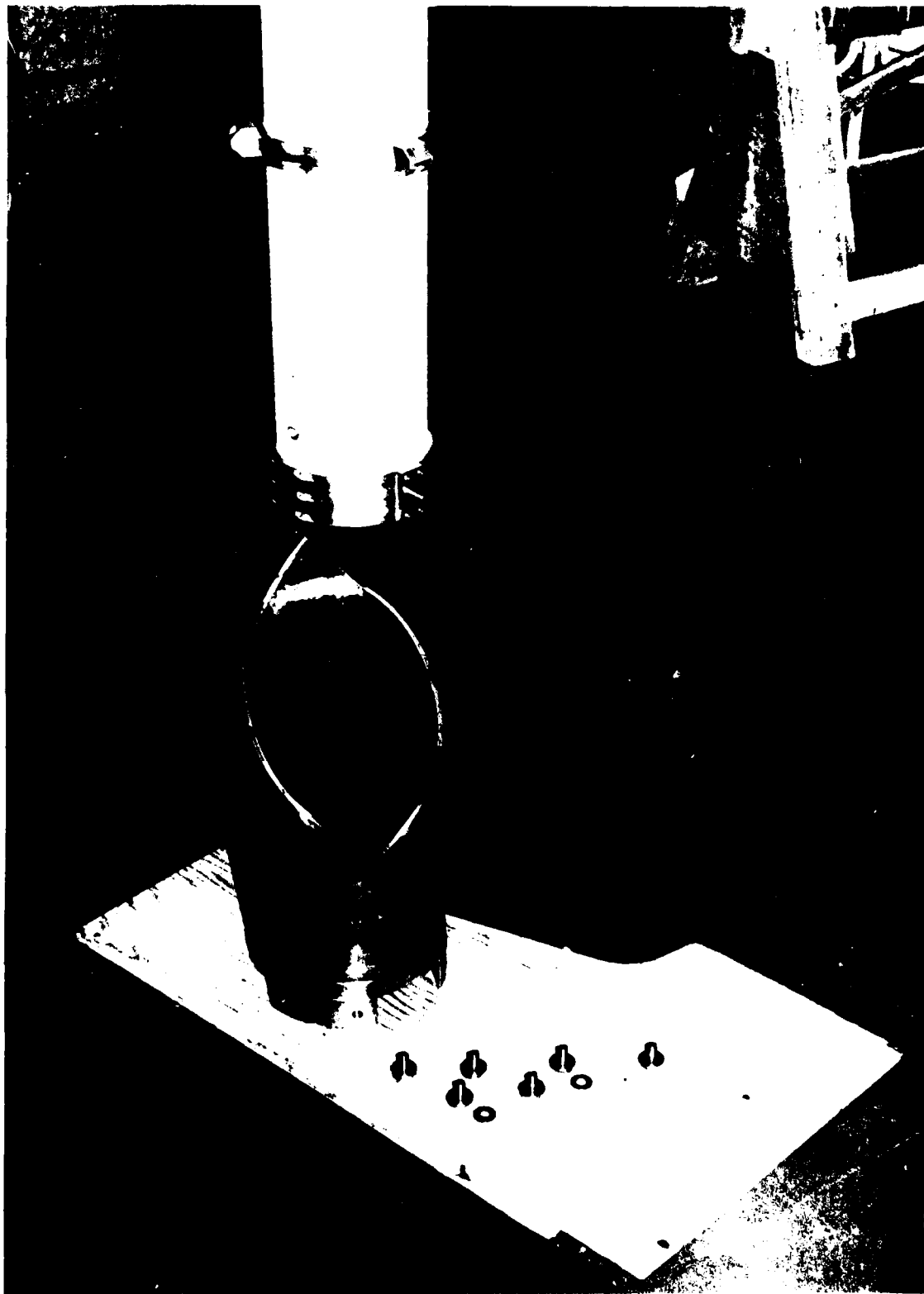


Figure 20

# Charlevoix M<sub>2</sub> Amplitudes

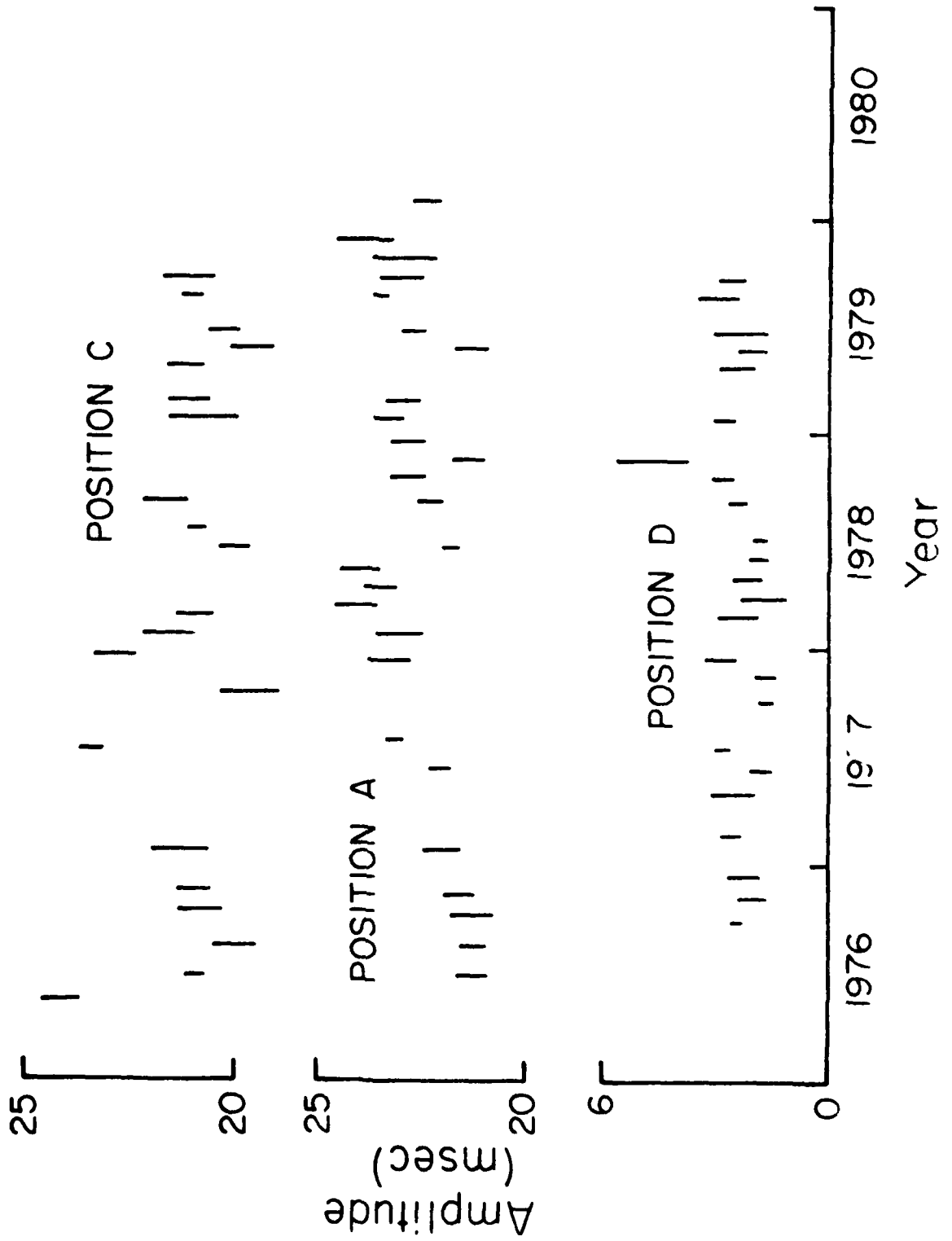


Figure 21

# Charlevoix M<sub>2</sub> Phase Lags

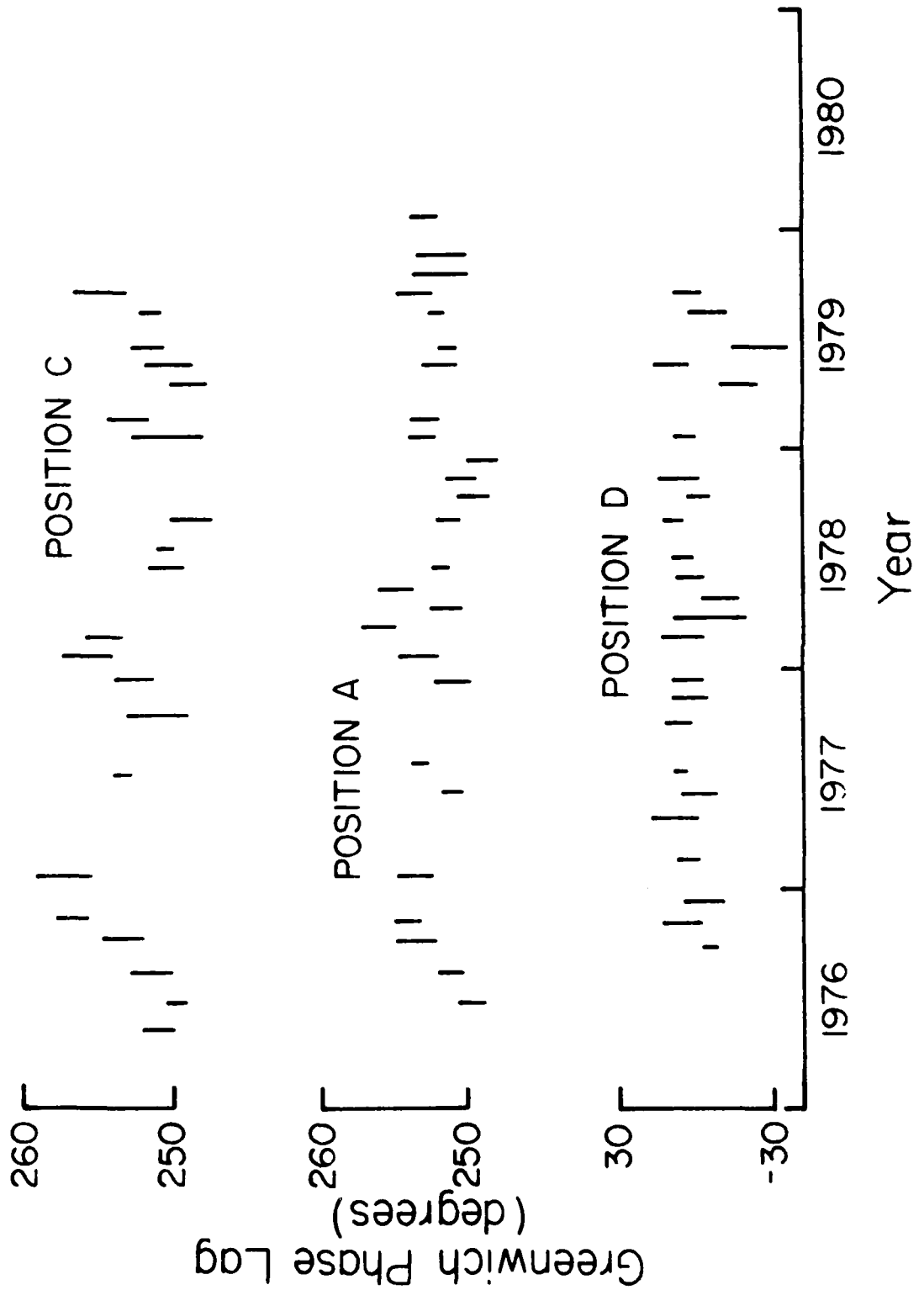


Figure 22  
90

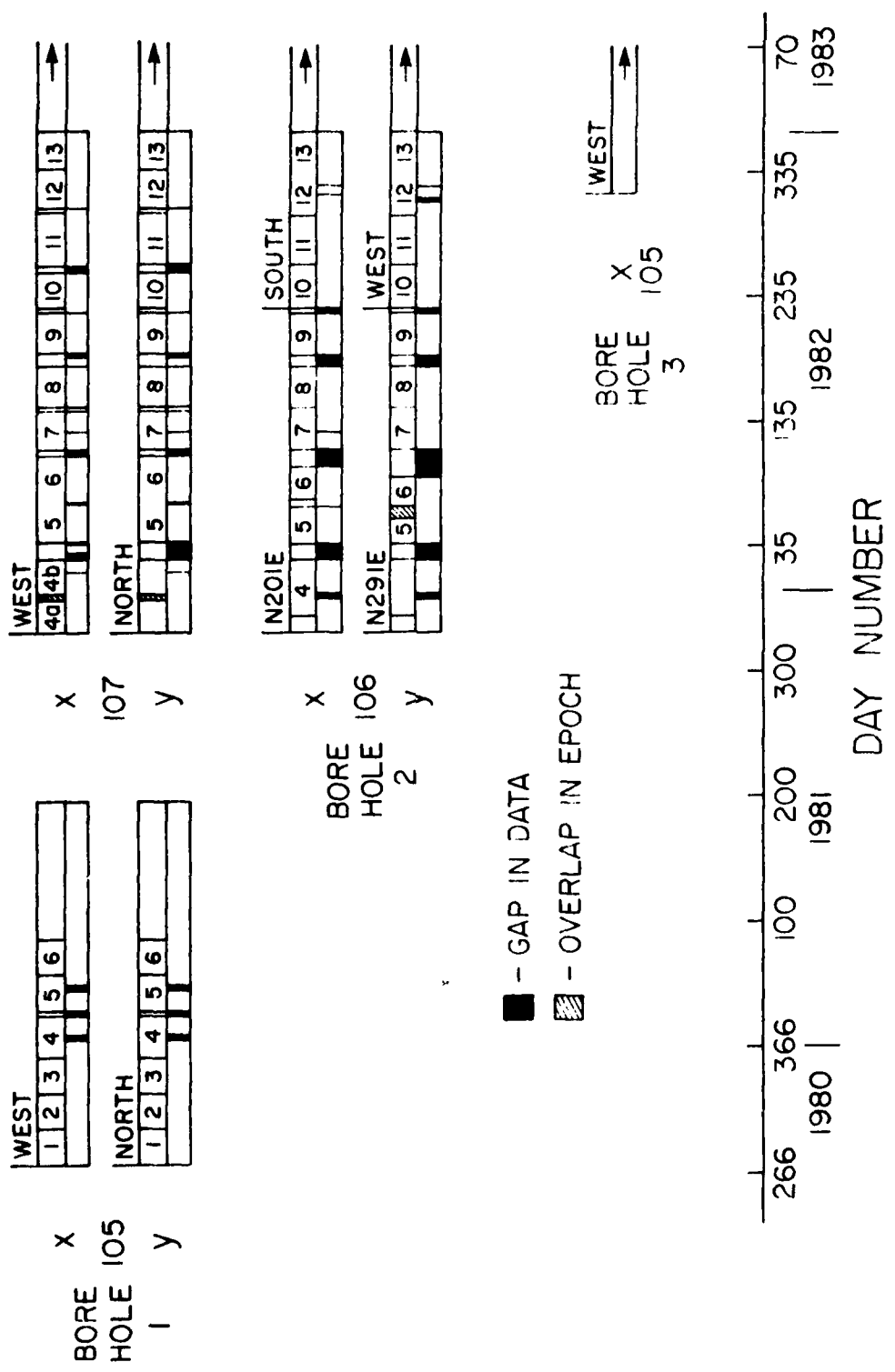


Figure 23

# Gbp 107

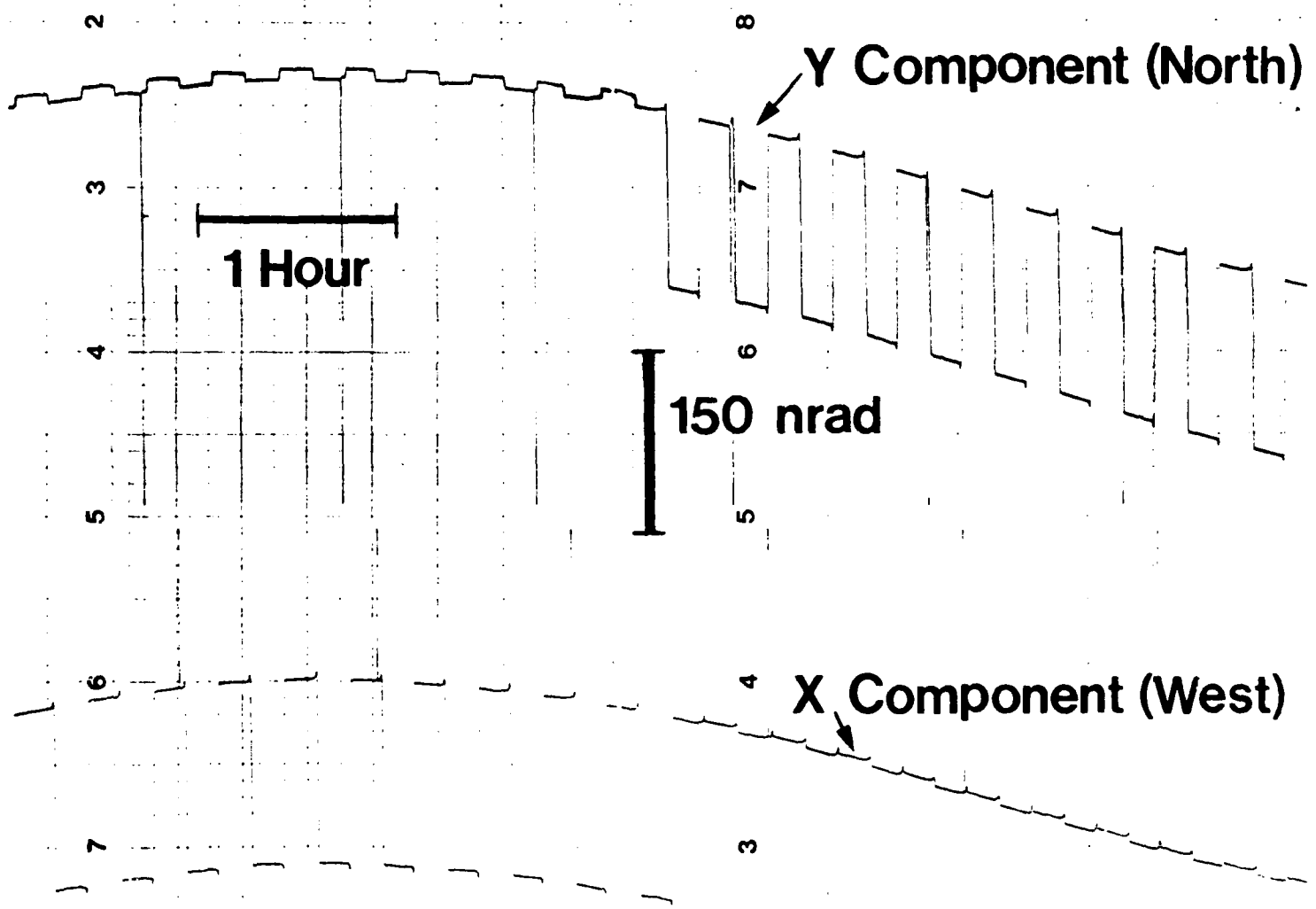


Figure 24

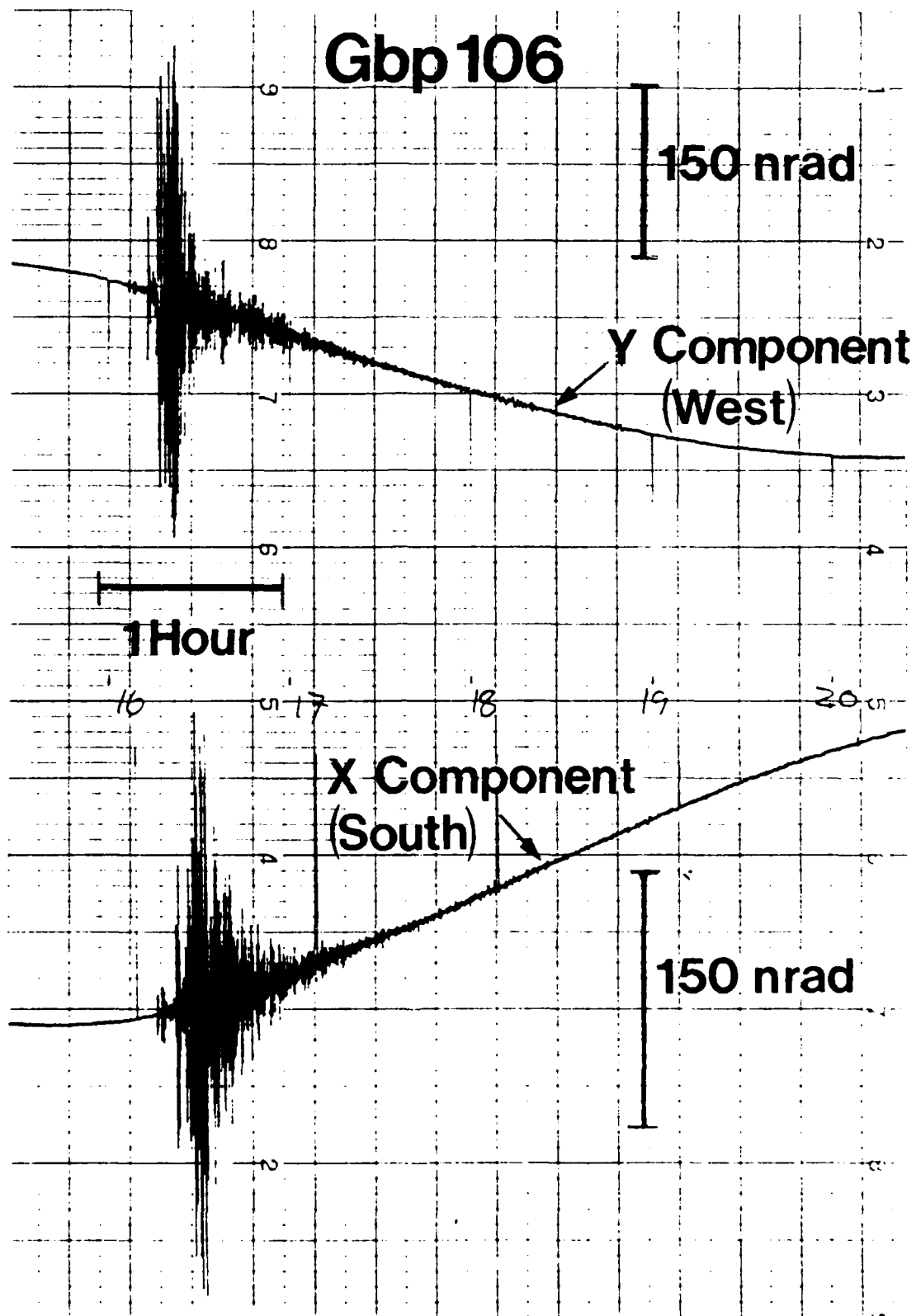
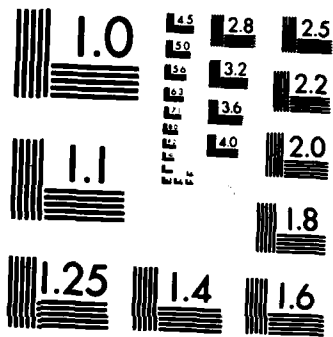


Figure 25





MICROCOPY RESOLUTION TEST CHART  
NATIONAL BUREAU OF STANDARDS-1963-A

# Gbp106

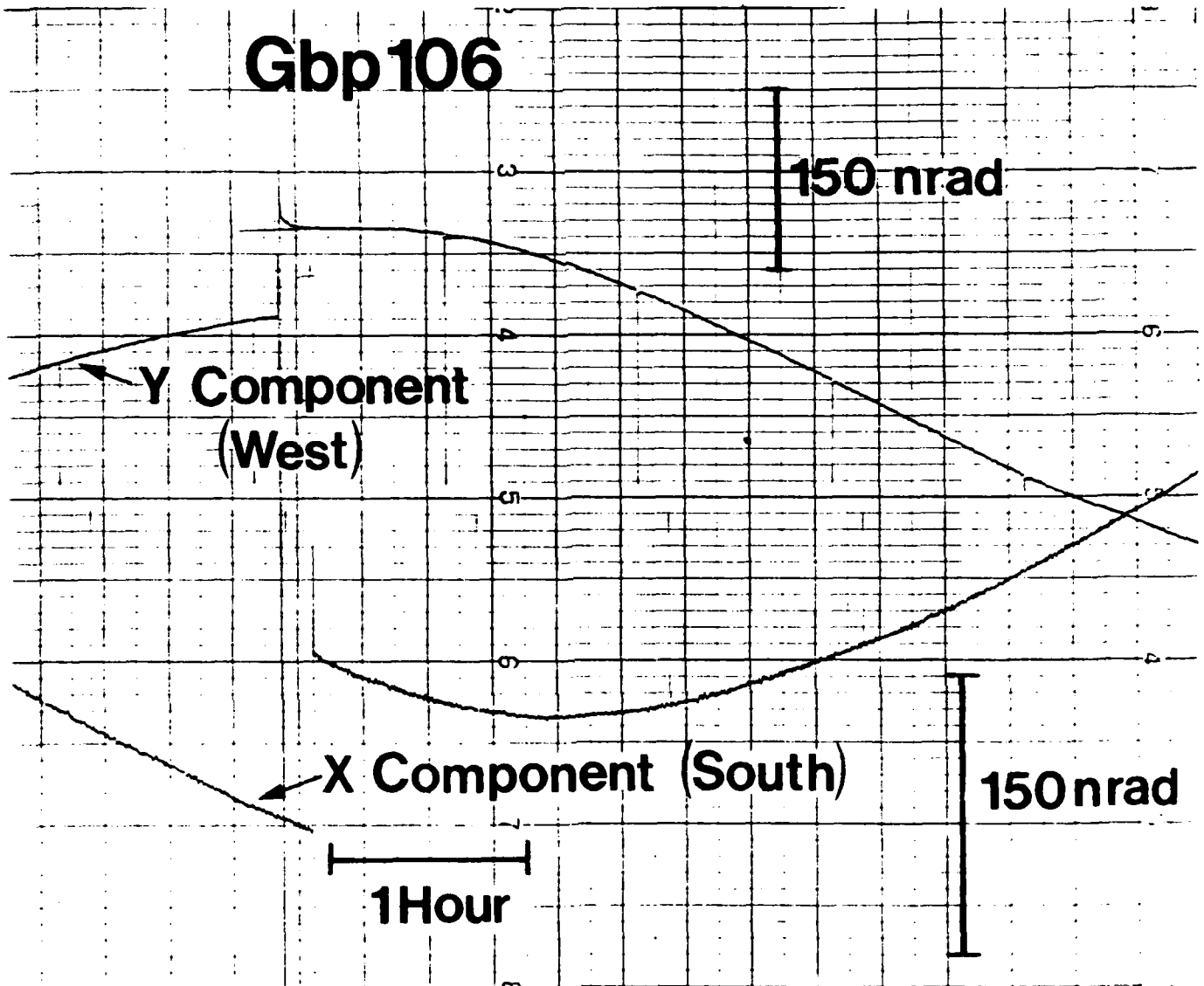


Figure 26

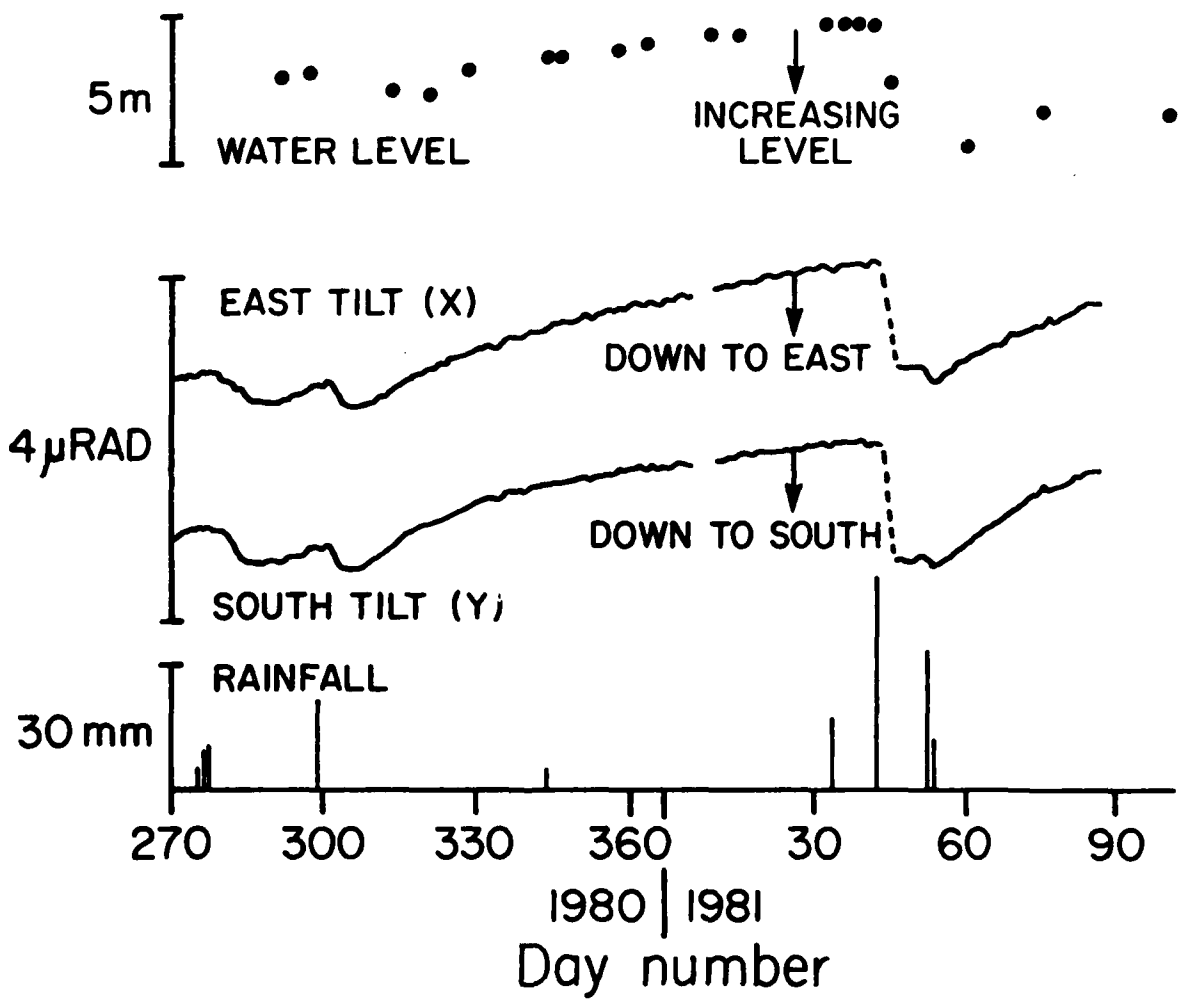


Figure 27

# GBP 106 Operating in Borehole 2

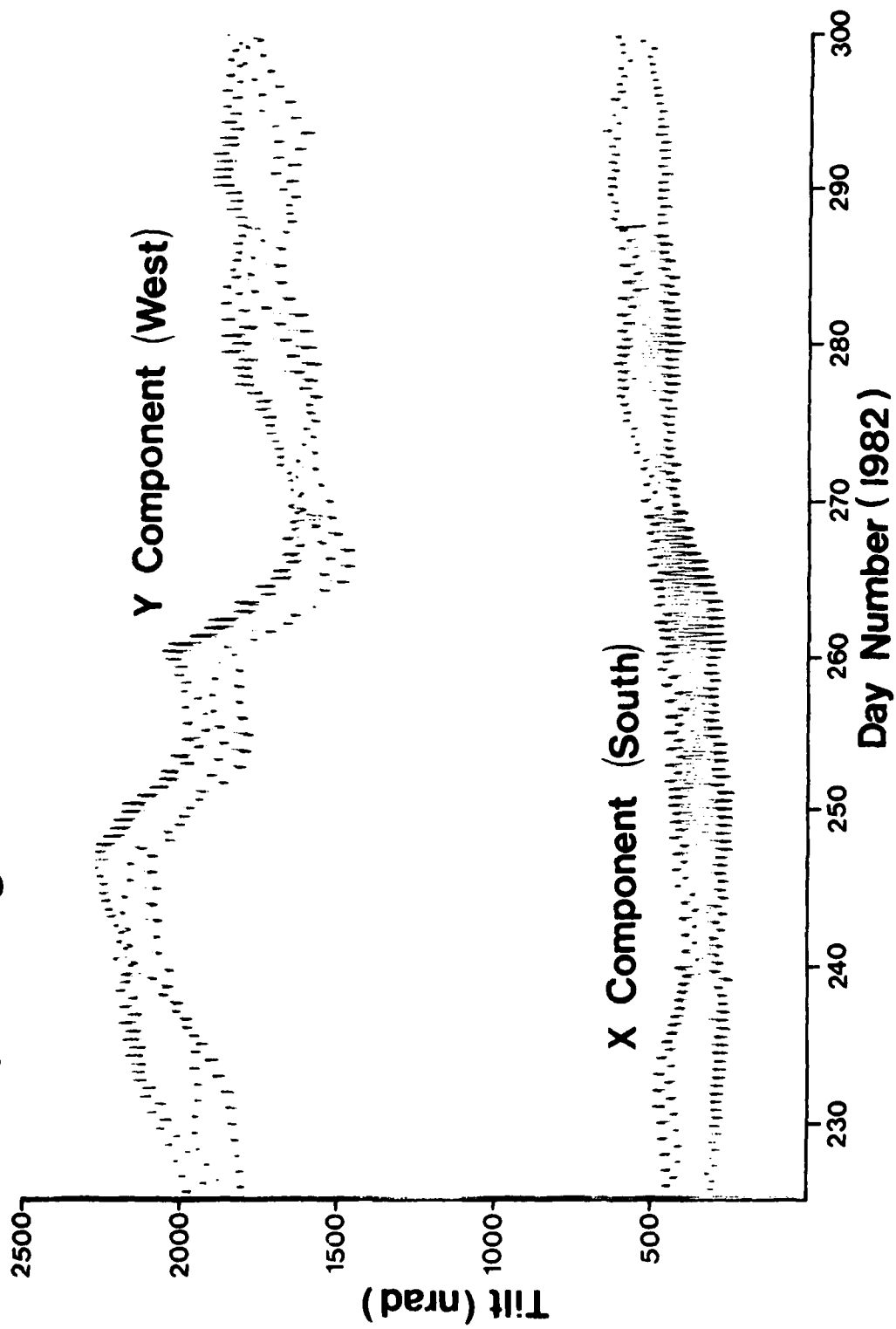


Figure 28

# BOREHOLE SECULAR TILT

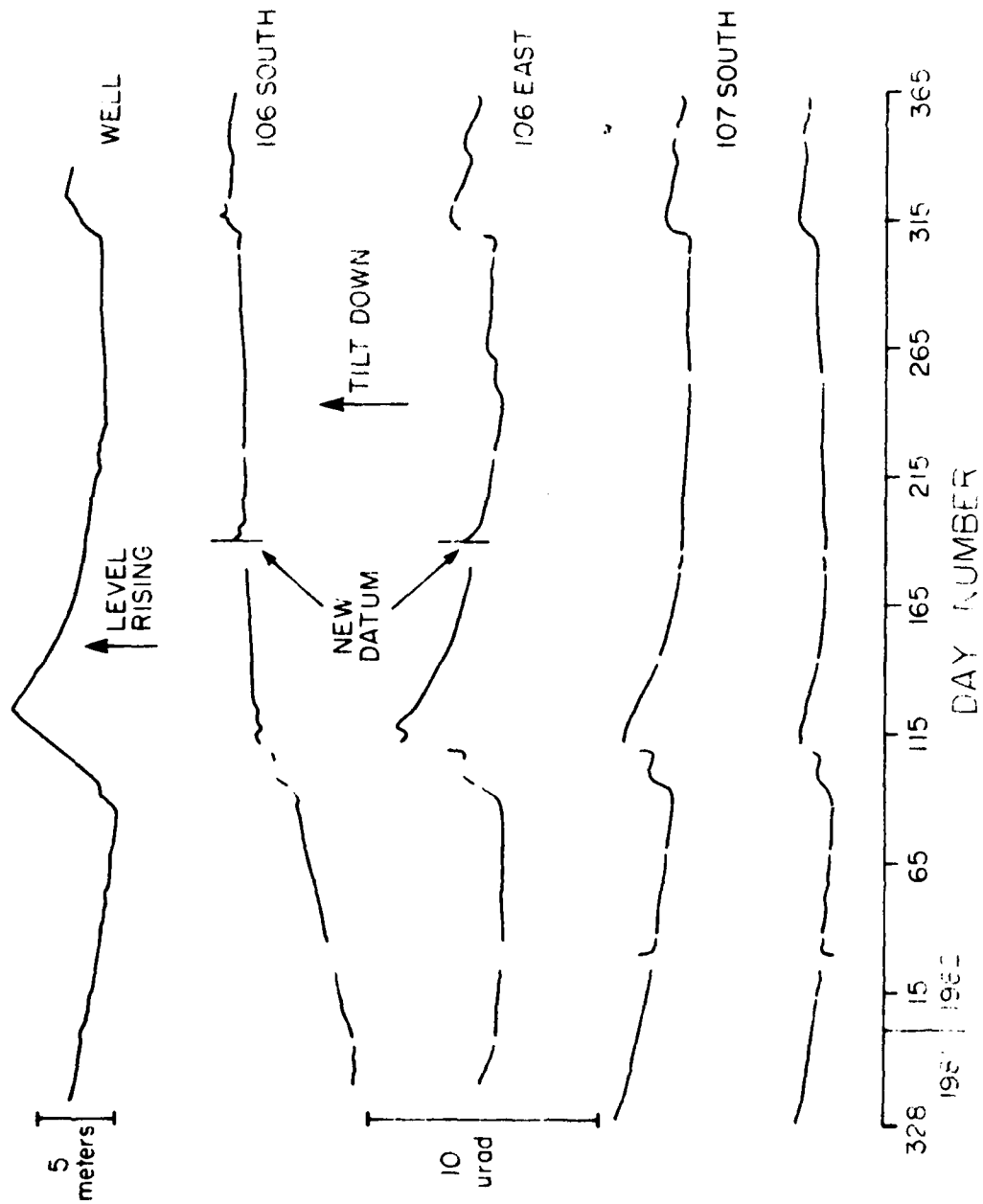
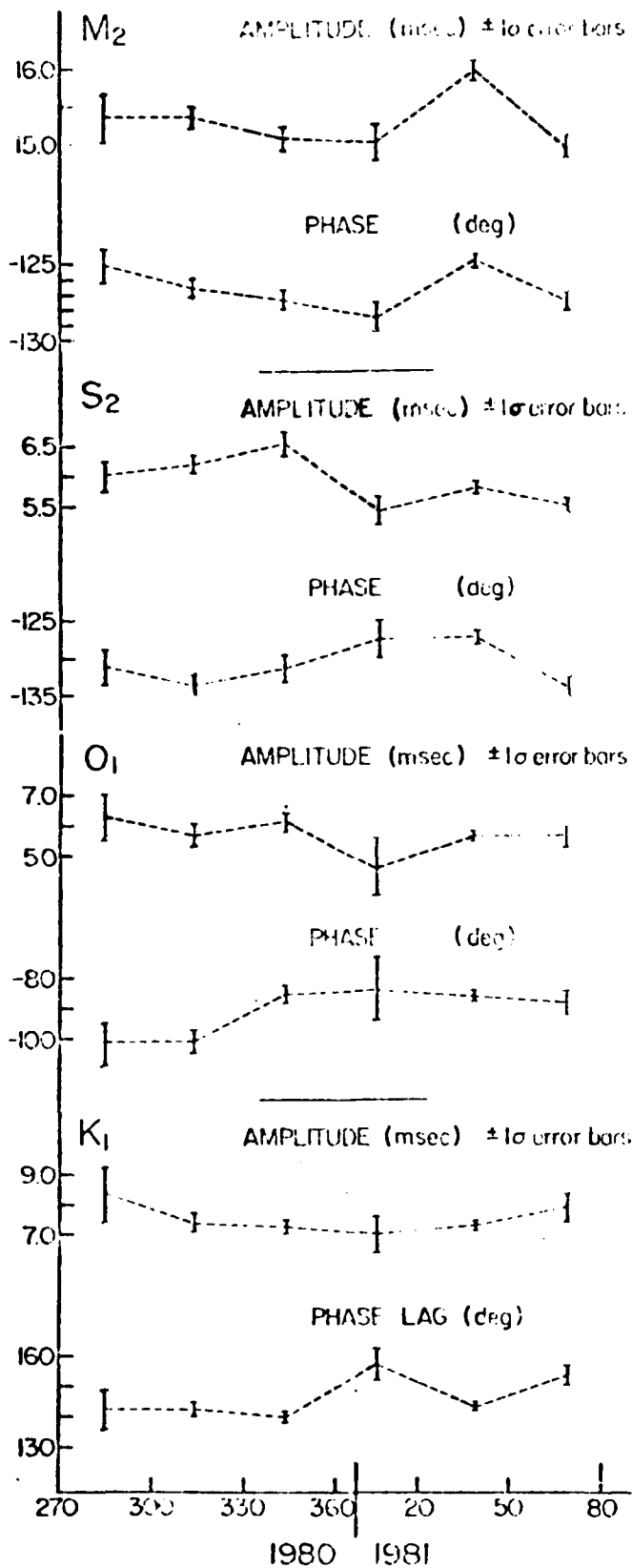


Figure 29  
97

### Gbp105 (X Component)



### Gbp105 (Y Component)

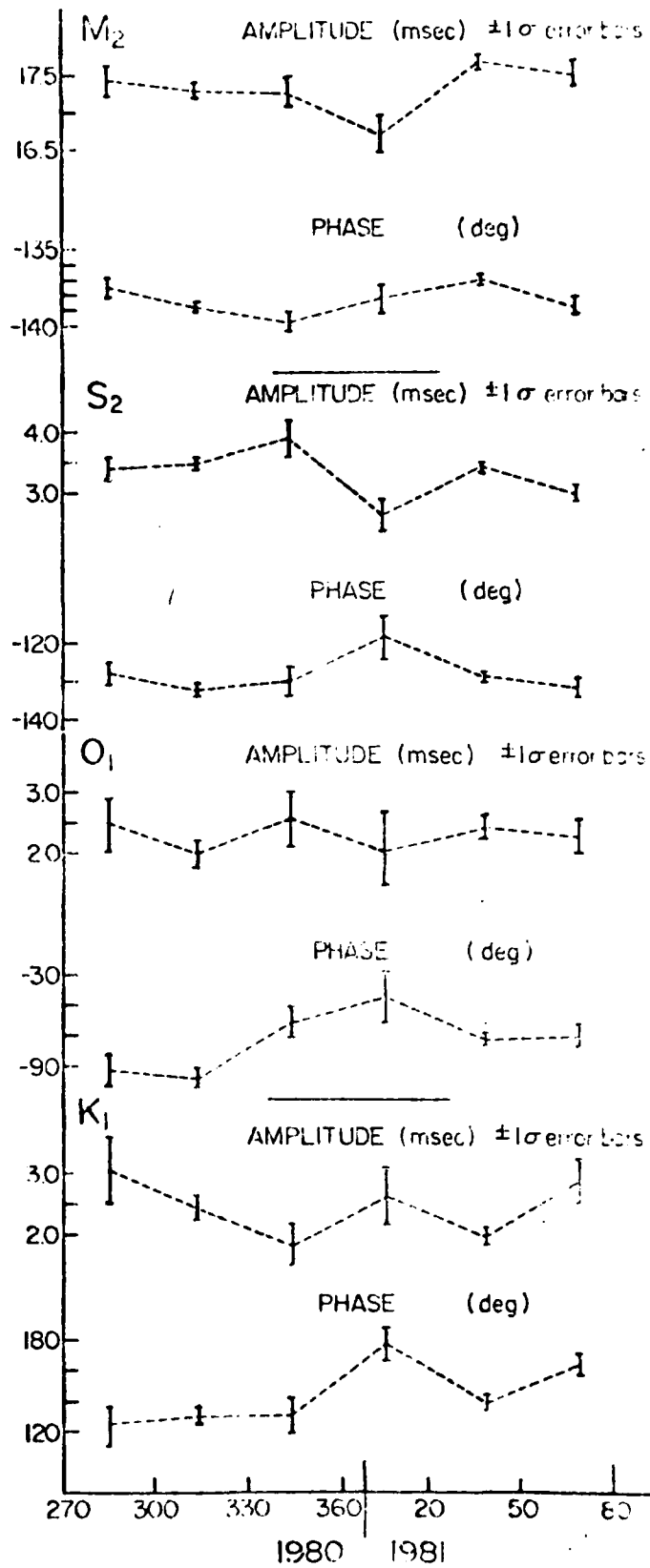


Figure 30

Charlevoix M<sub>2</sub> Observed West Tilt Phasor Plot  
 Gbp 105, Borehole 1

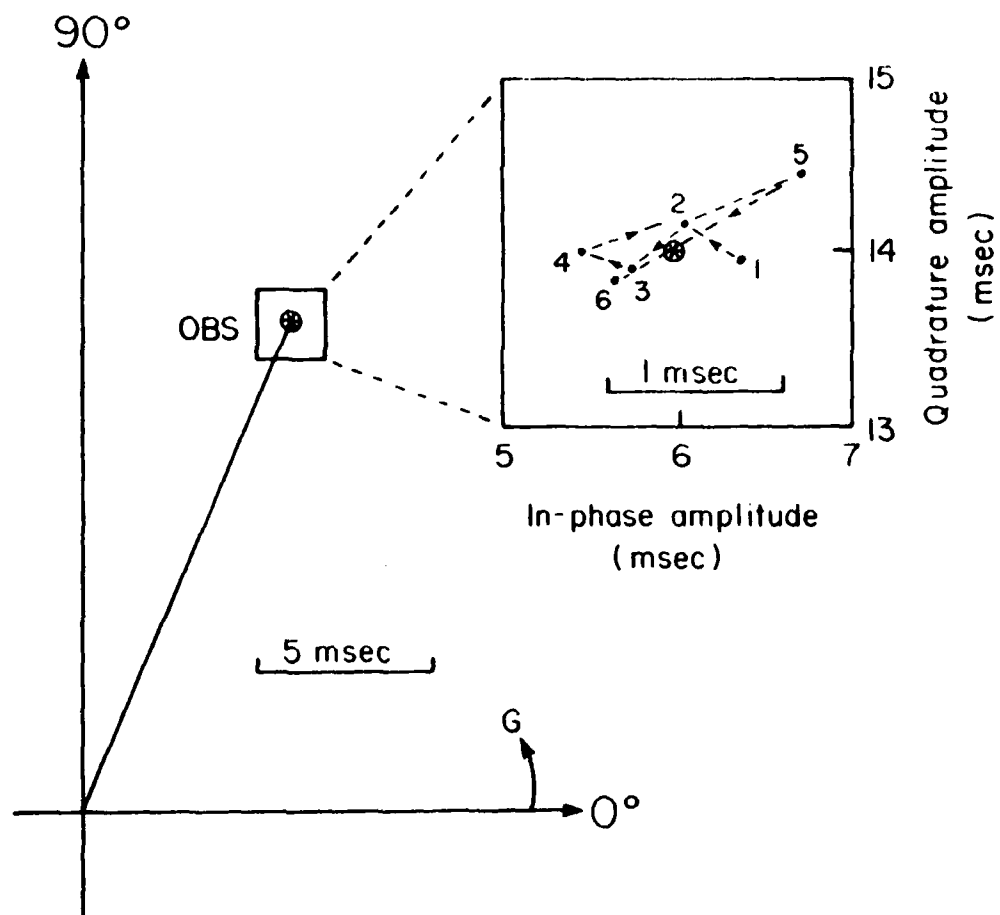


Figure 31

Charlevoix  $M_2$  Observed South Tilt Phasor Plot  
Gbp 105, Borehole 1

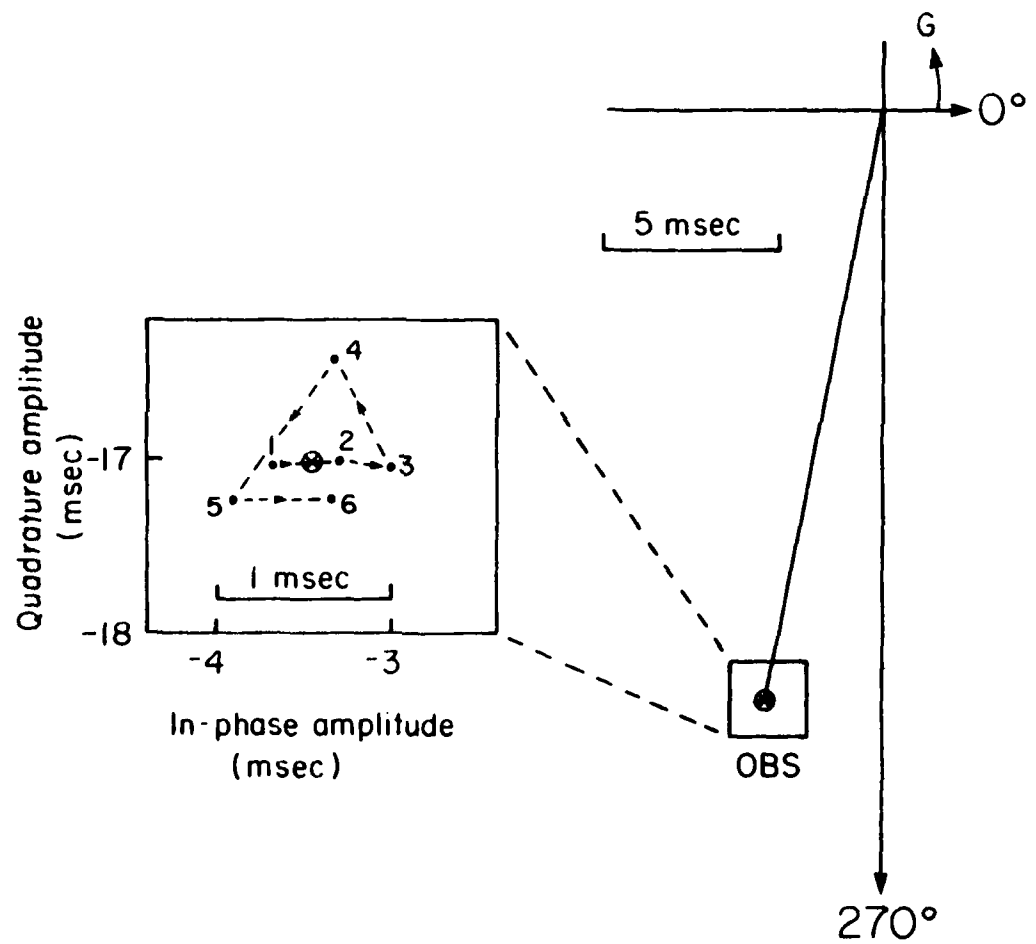


Figure 32

### Borehole M<sub>2</sub> Amplitude Variations

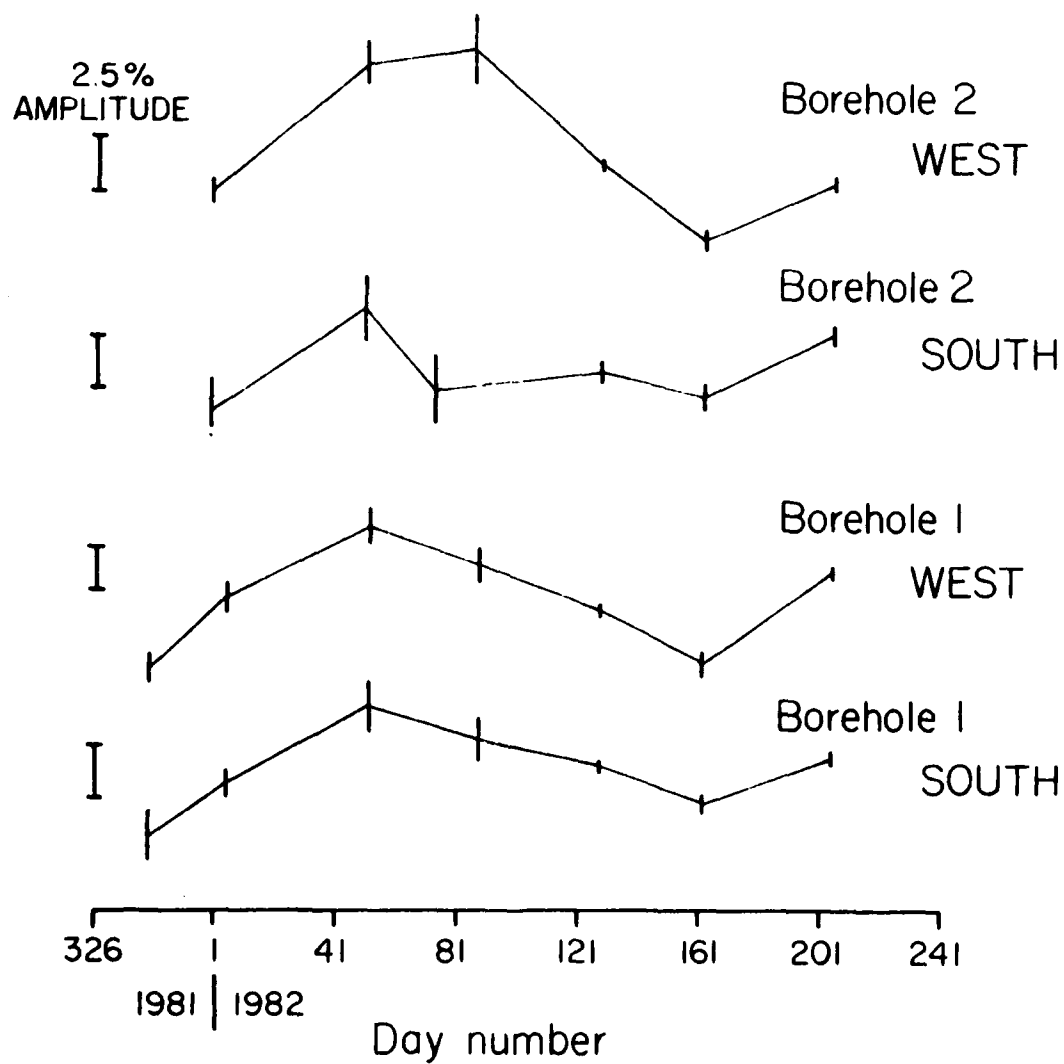


Figure 33  
101

### Borehole M<sub>2</sub> Phase Variations

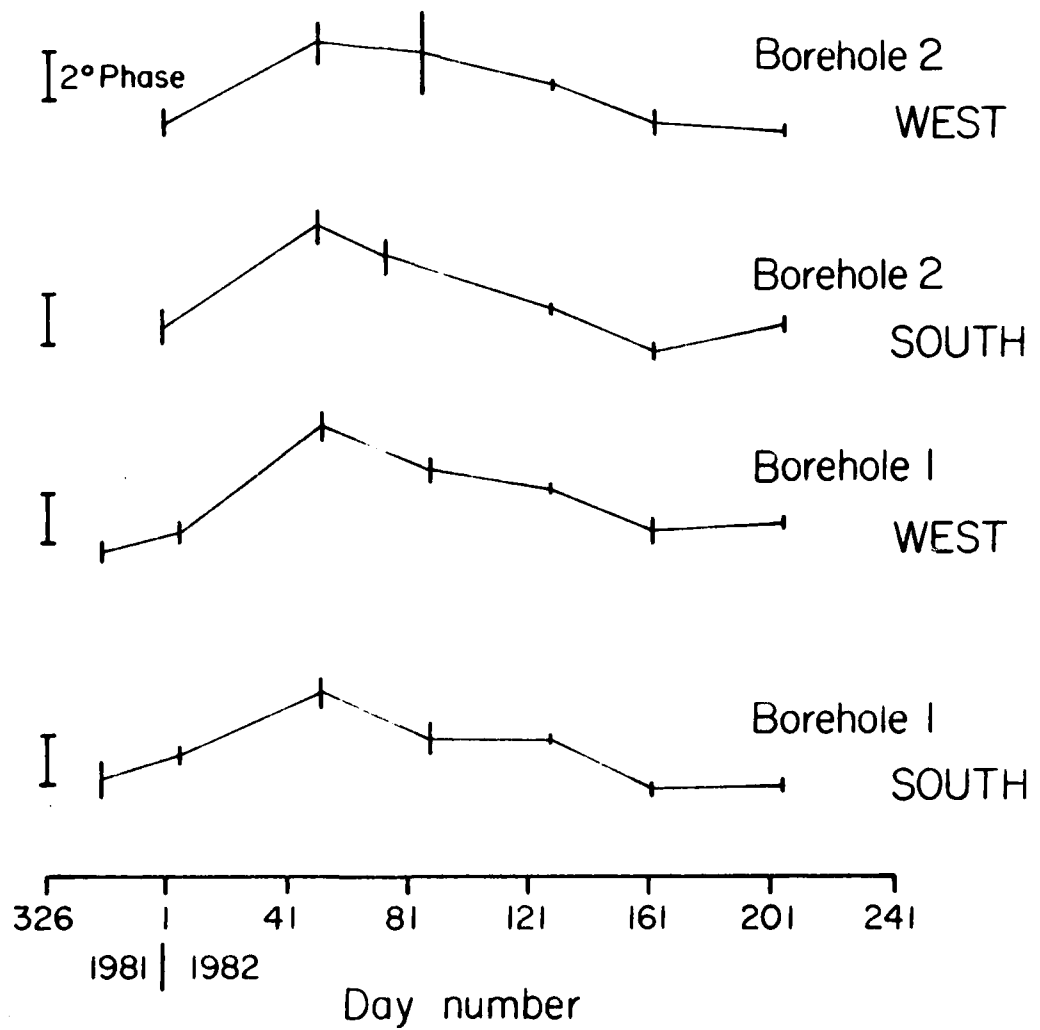


Figure 34

Charlevoix M<sub>2</sub> Observed West Tilt Phasor Plot  
 Gbp 106, Borehole 2

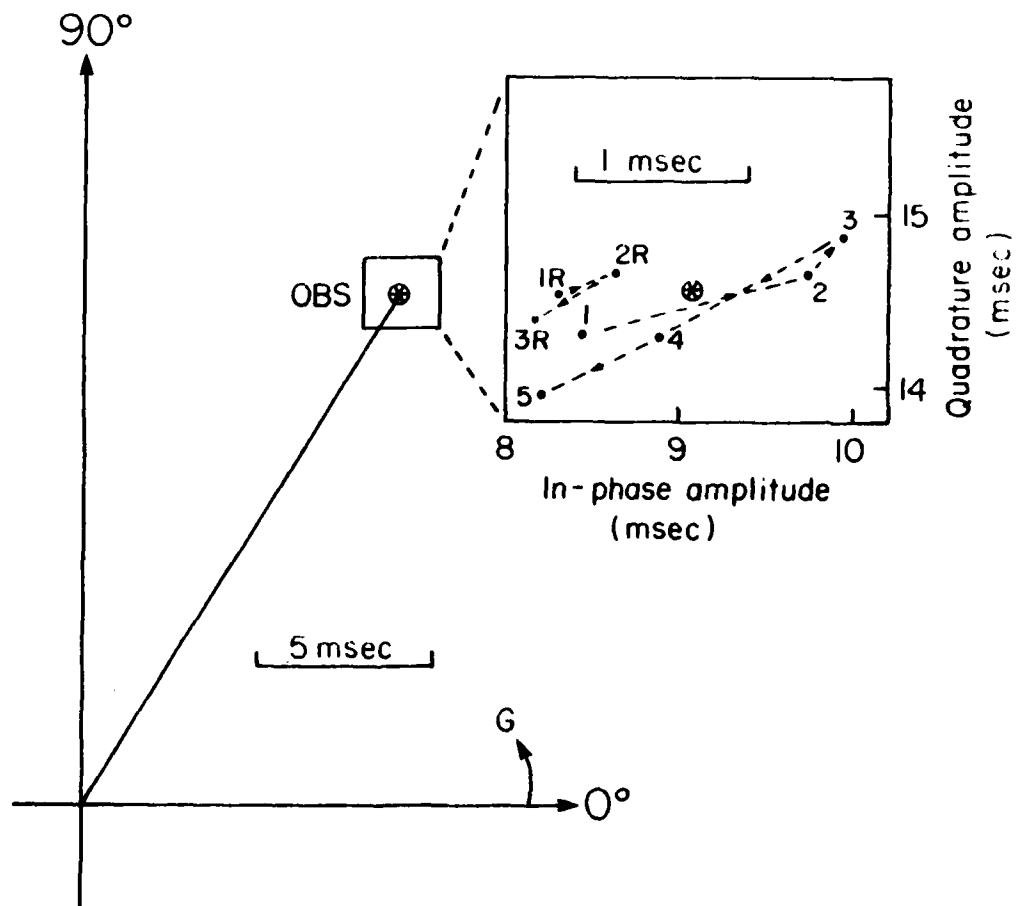


Figure 35

Charlevoix  $M_2$  Observed South Tilt Phasor Plot  
 Gbp 106, Borehole 2

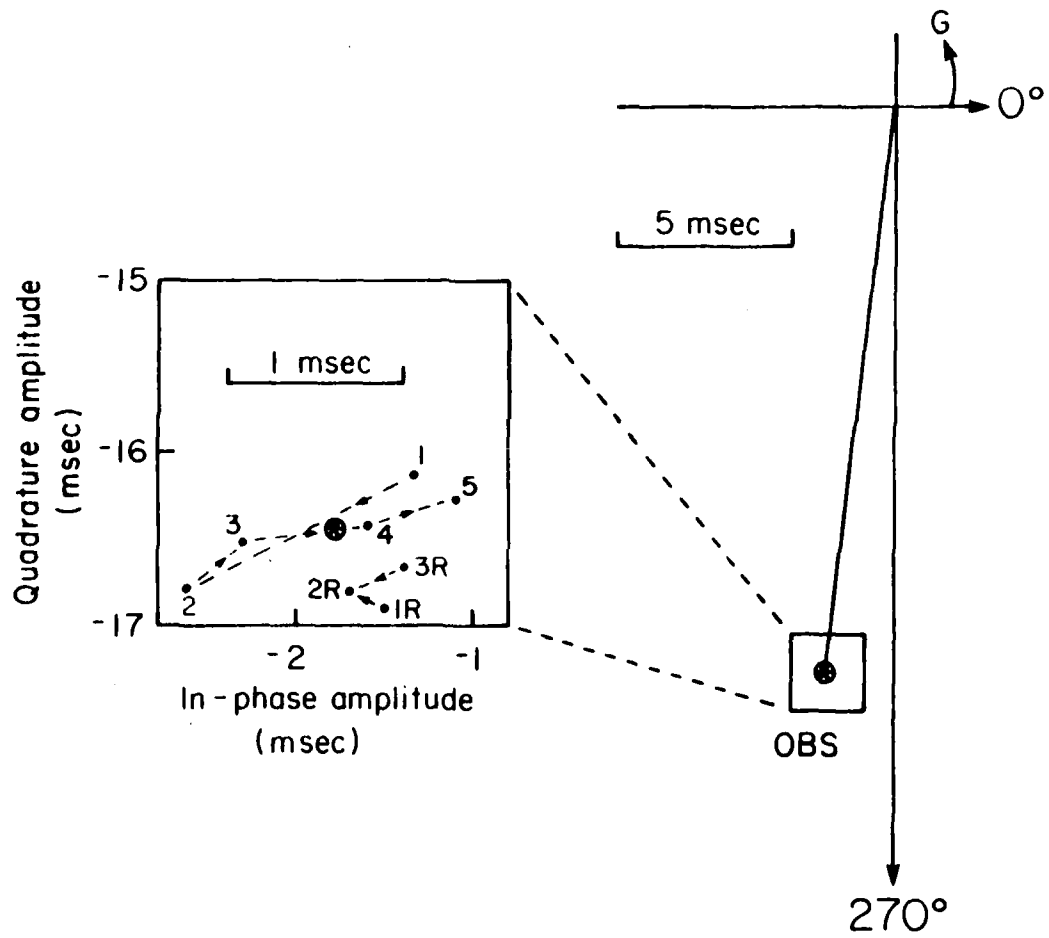


Figure 36

Charlevoix M<sub>2</sub> Observed West Tilt Phasor Plot  
Gbp 107, Borehole 1

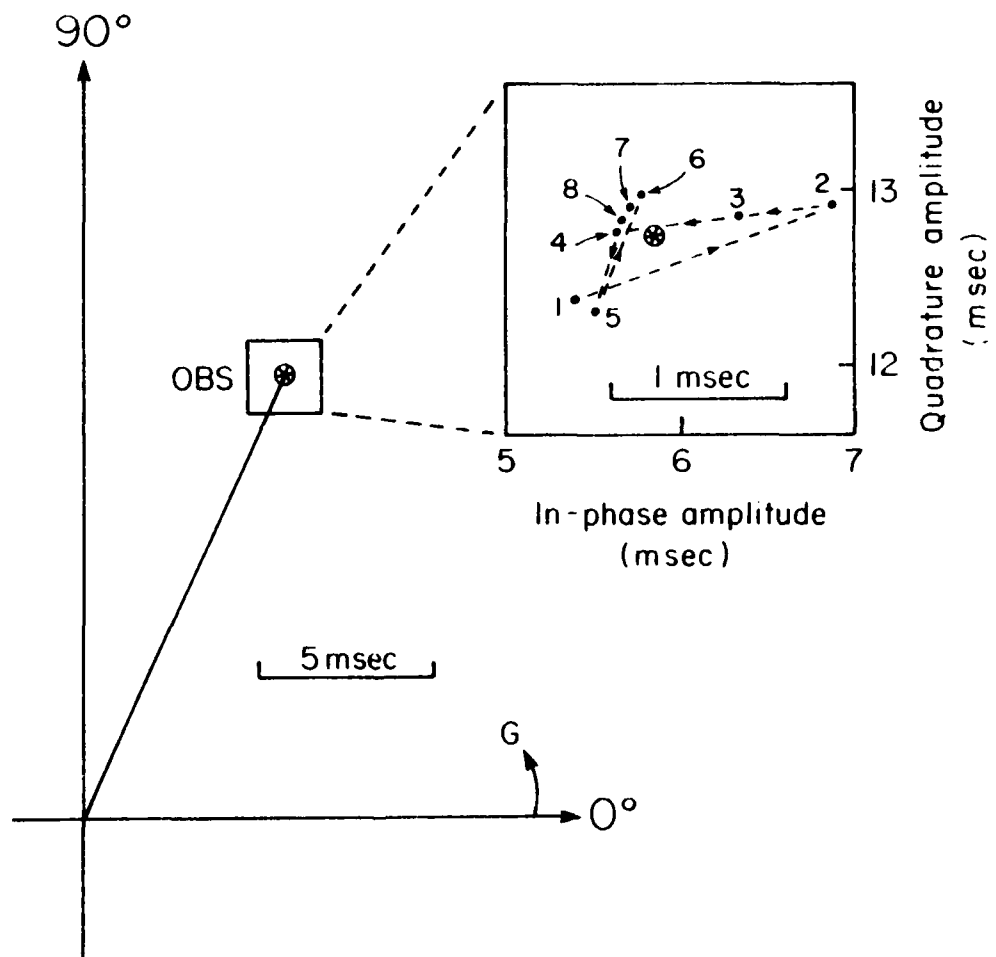


Figure 37

Charlevoix M<sub>2</sub> Observed South Tilt Phasor Plot  
Gbp 107, Borehole 1

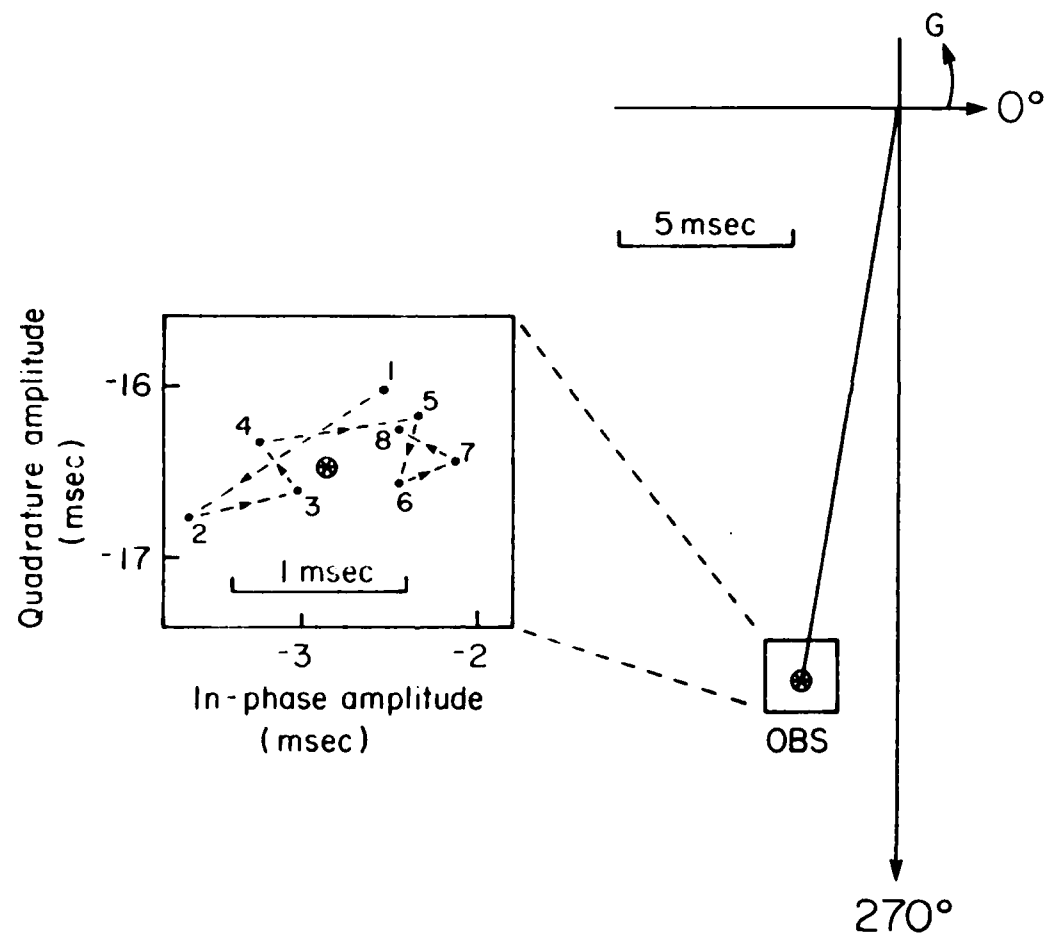


Figure 38

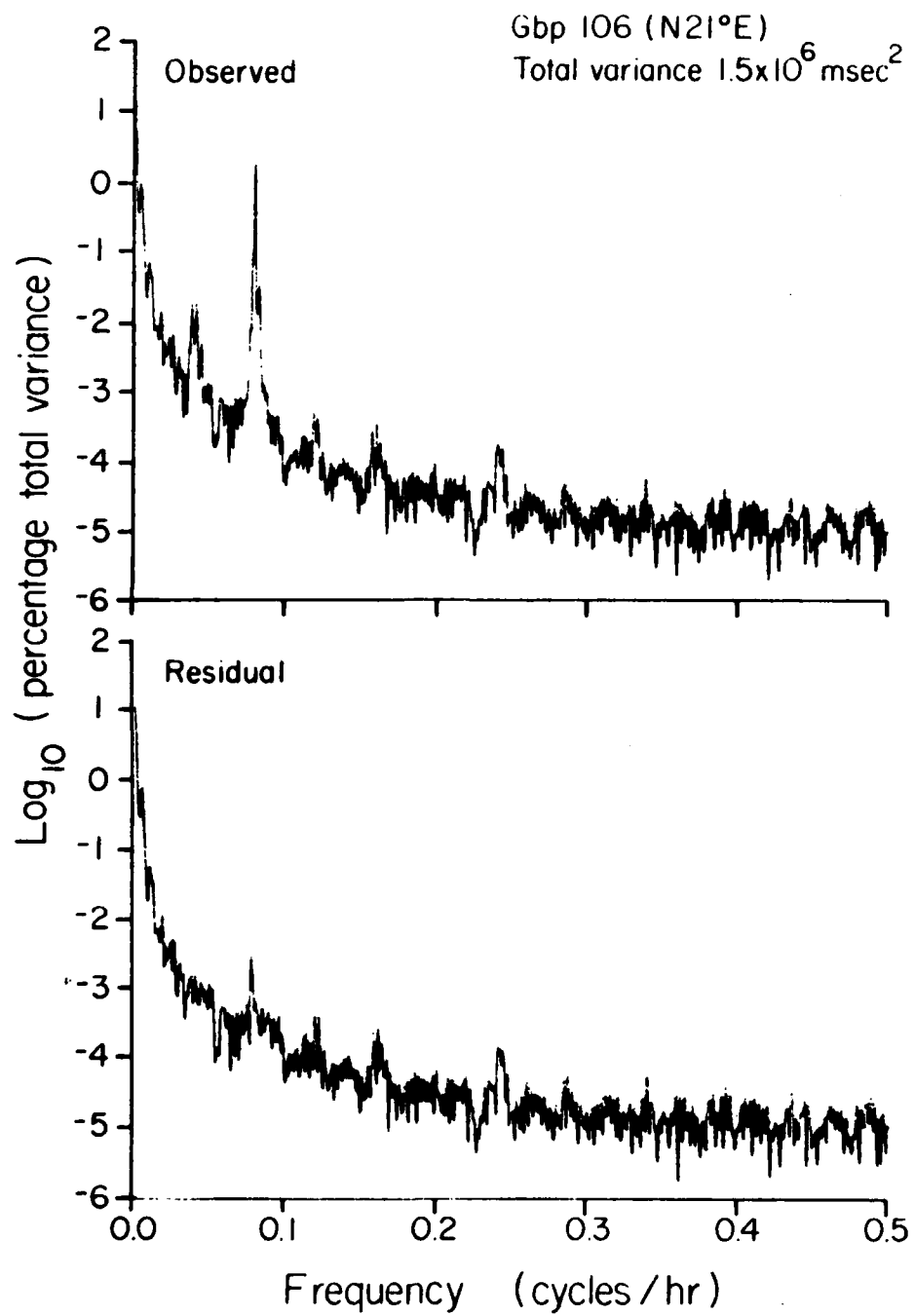


Figure 39

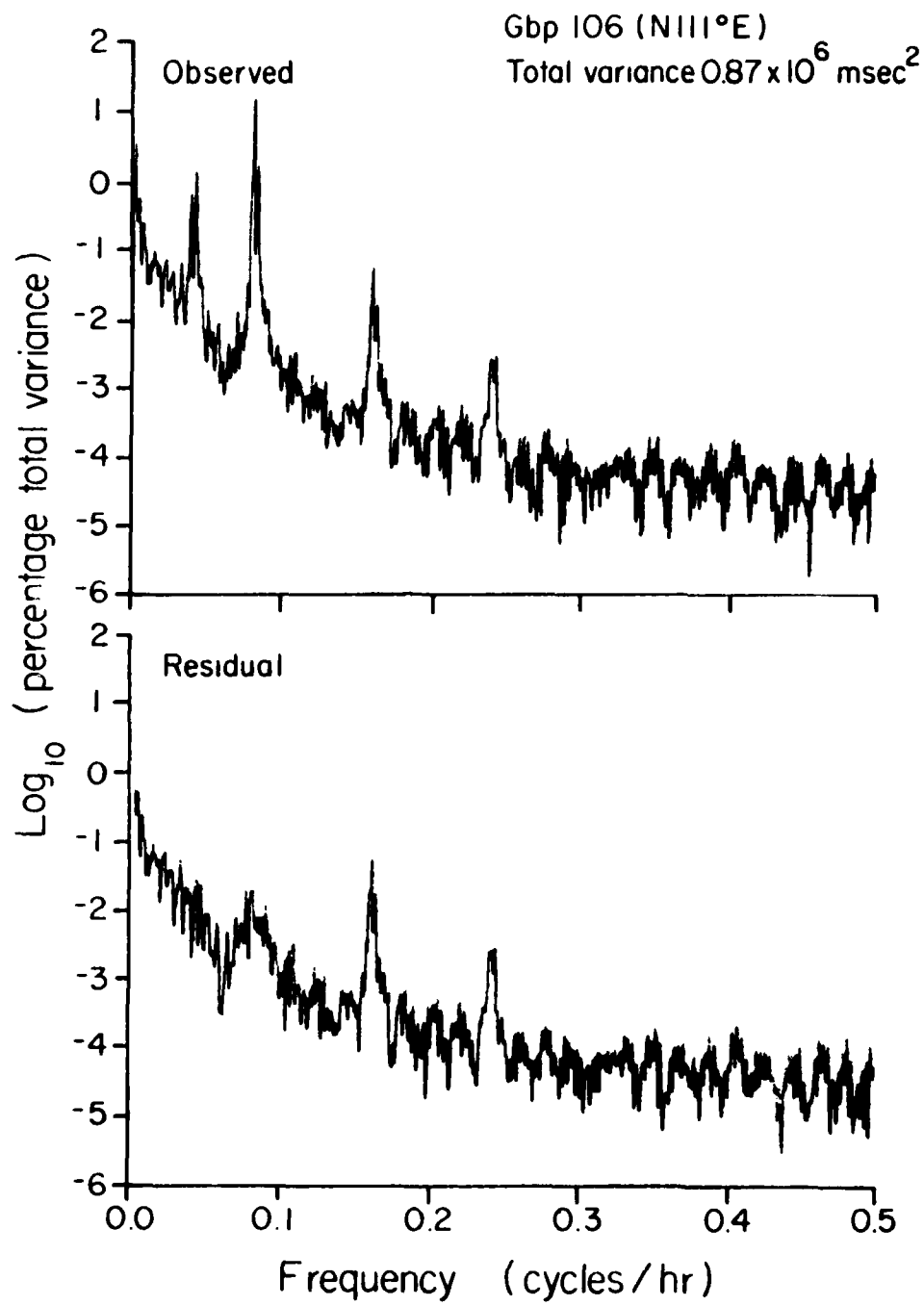


Figure 40

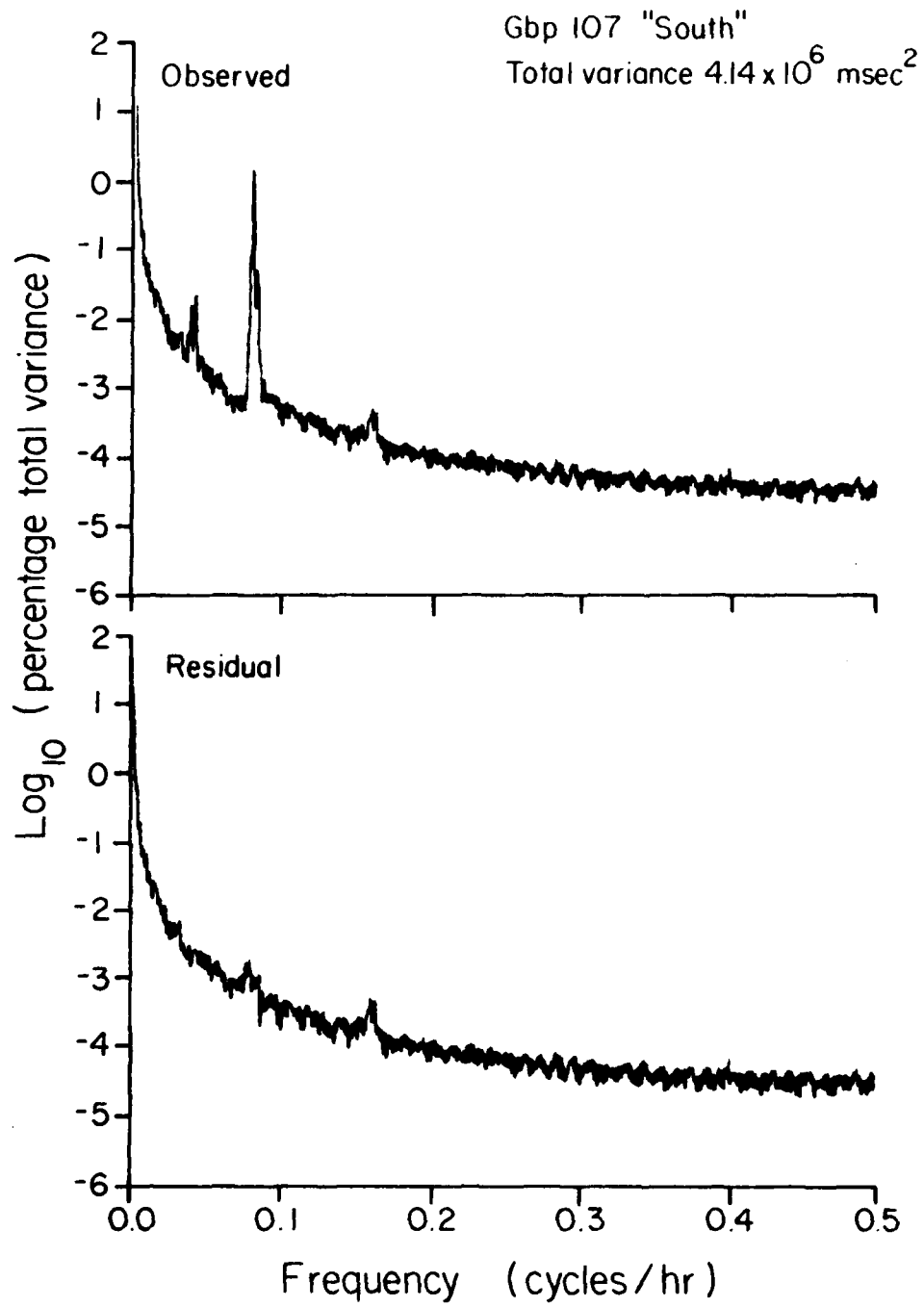


Figure 41

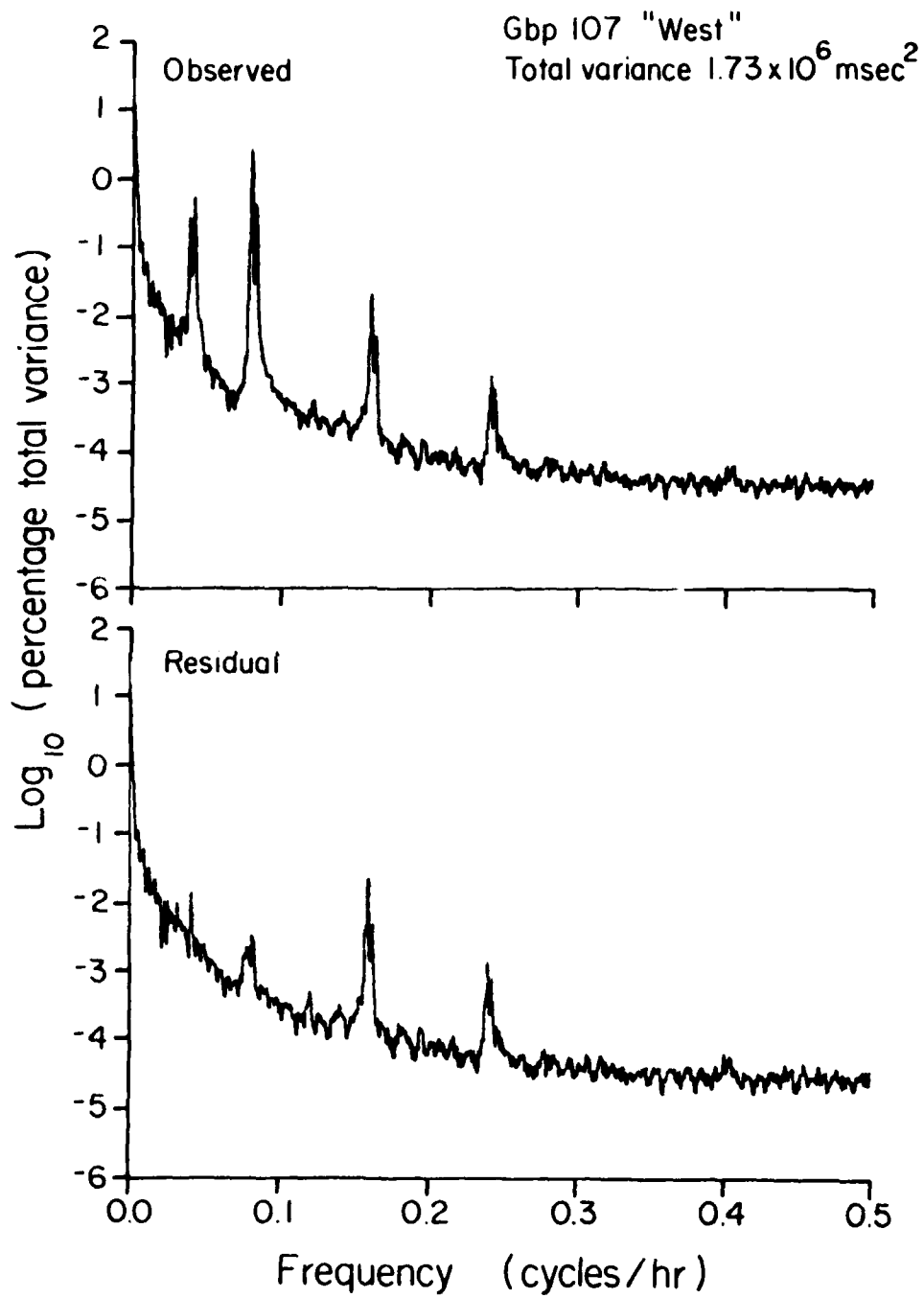


Figure 42

Charlevoix Observed  $M_2$  West Tilt Phasor Plot  
ANAC Tiltmeters

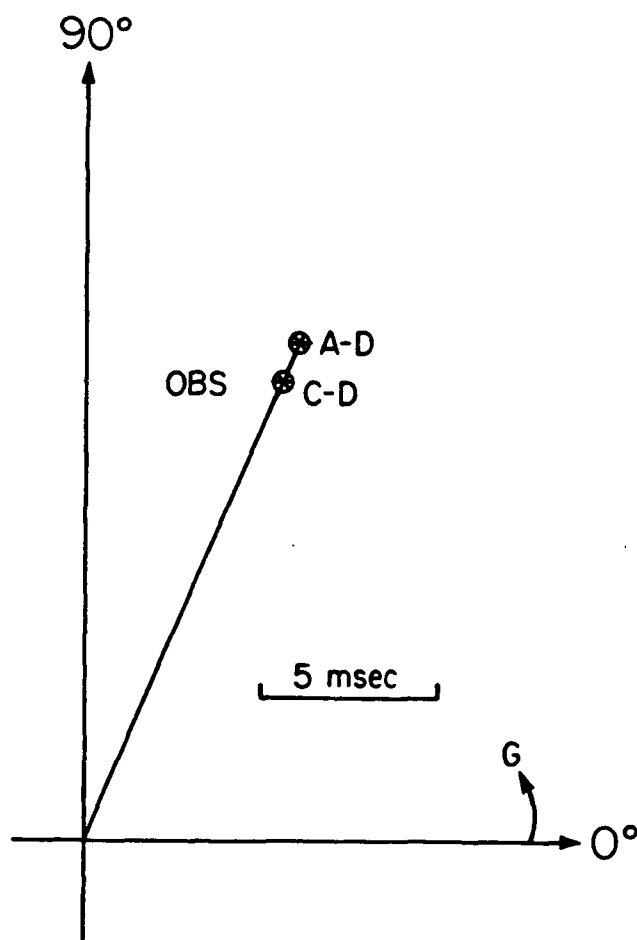


Figure 43

Charlevoix Observed  $M_2$  South Tilt Phasor Plot  
ANAC Tiltmeters

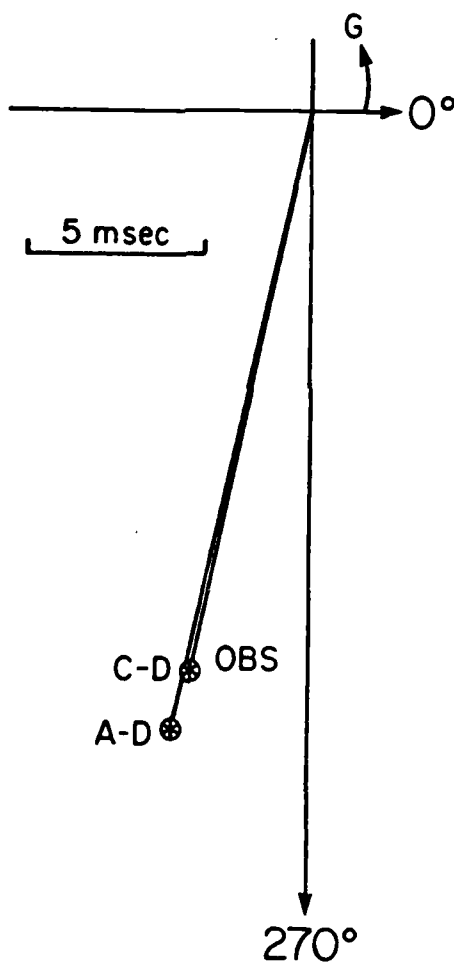


Figure 44

Charlevoix Observed  $O_1$  West Tilt Phasor Plot  
ANAC Tiltmeters

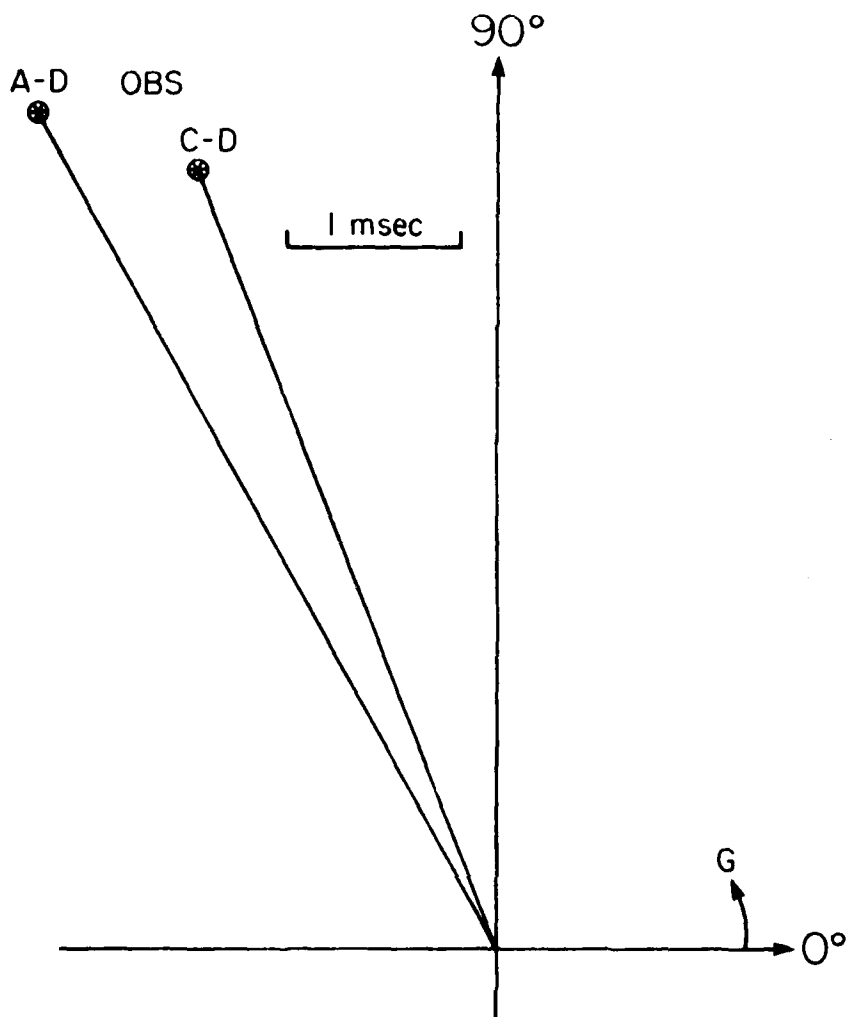


Figure 45

Charlevoix Observed  $O_1$  South Tilt Phasor Plot  
ANAC Tiltmeters

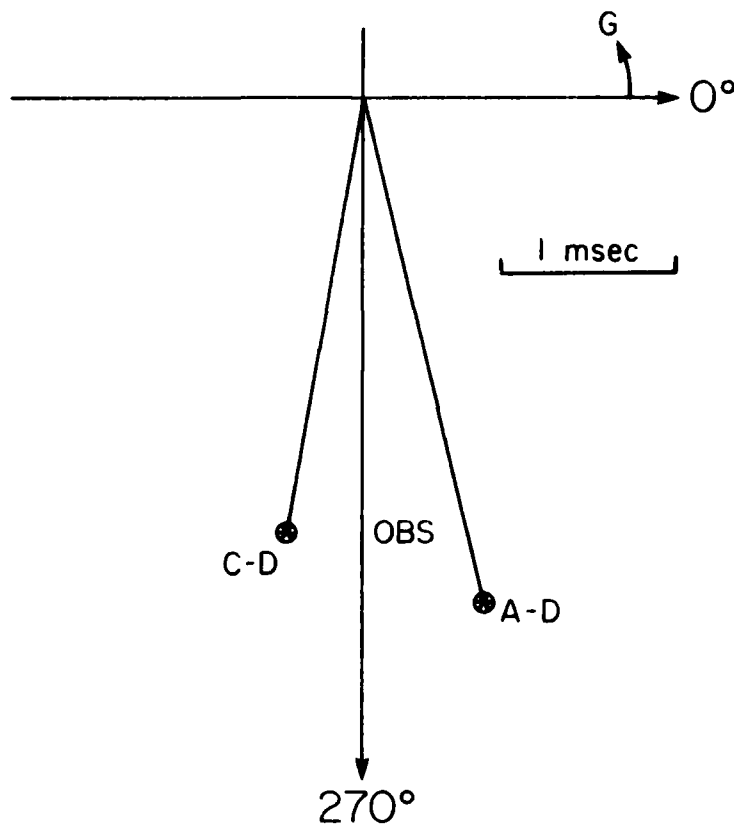


Figure 46

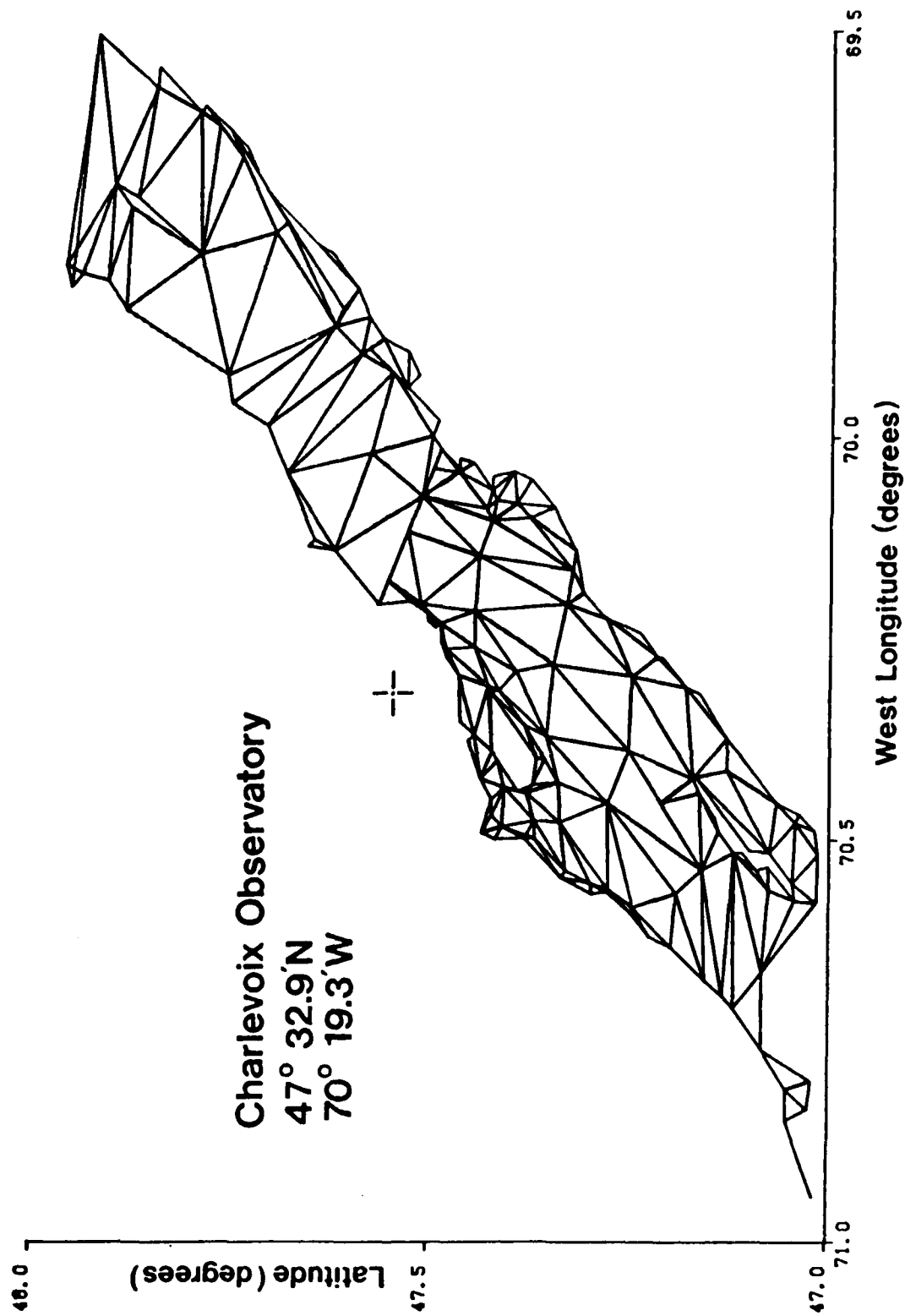


Figure 47

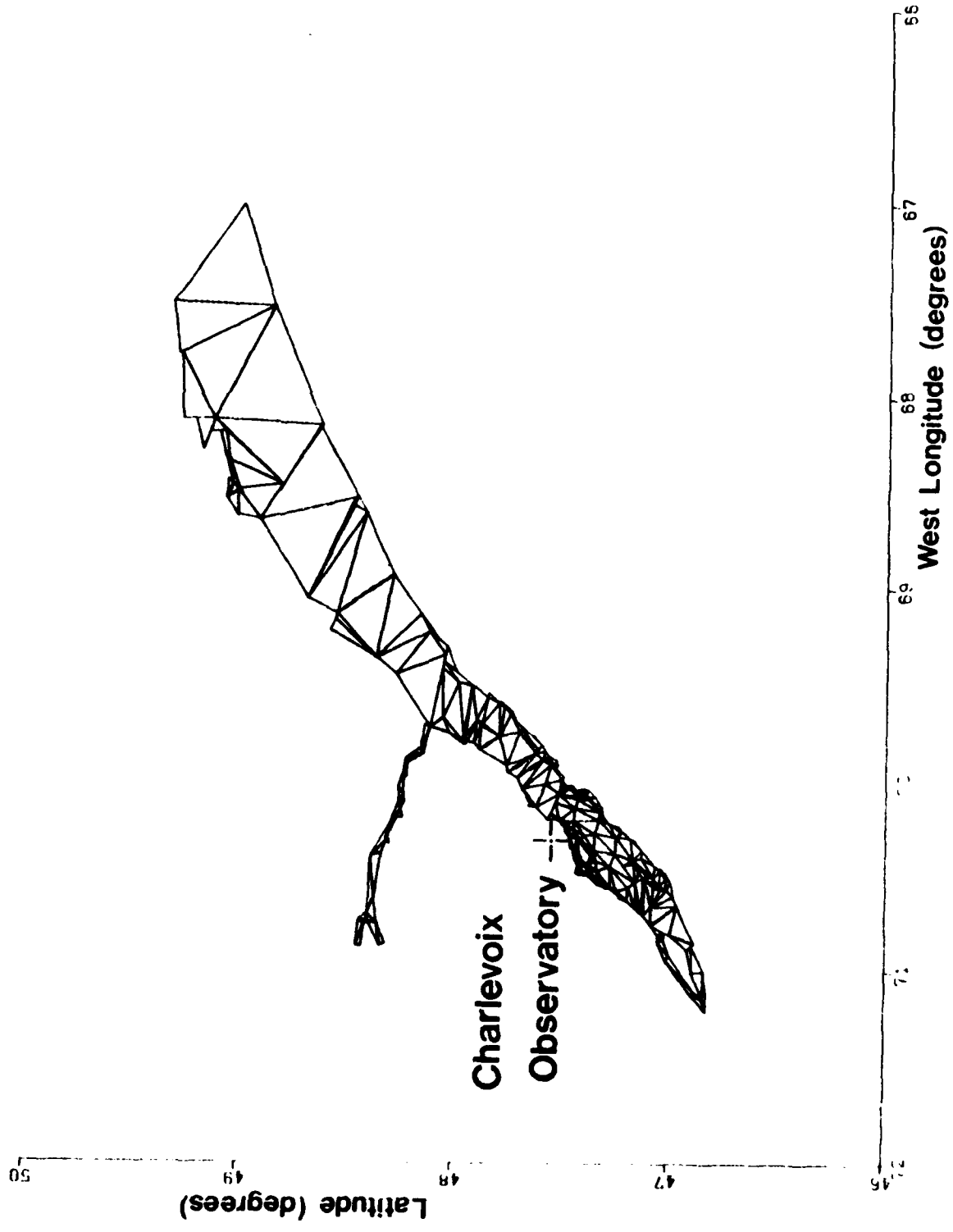


Figure 48



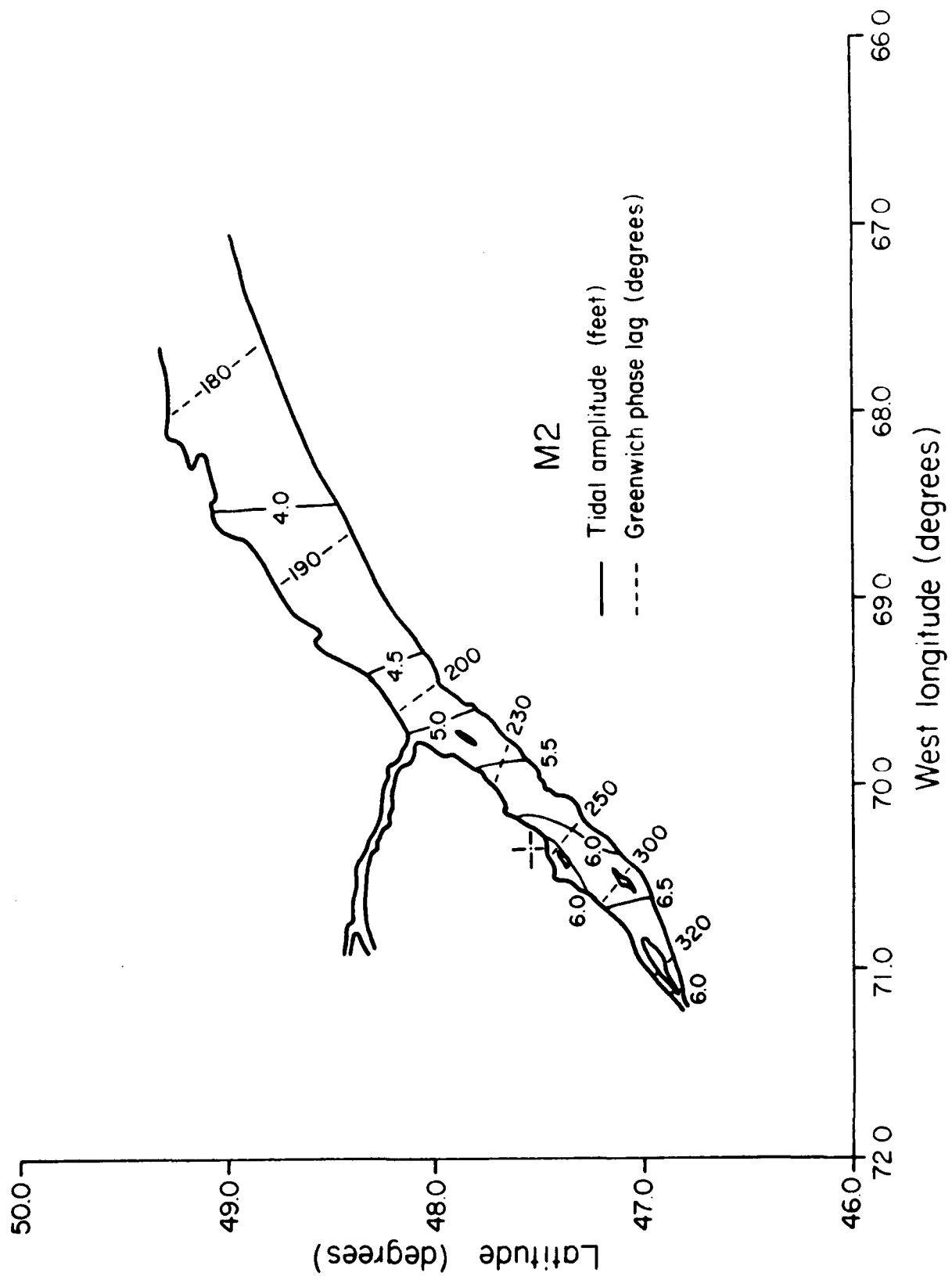


Figure 49b

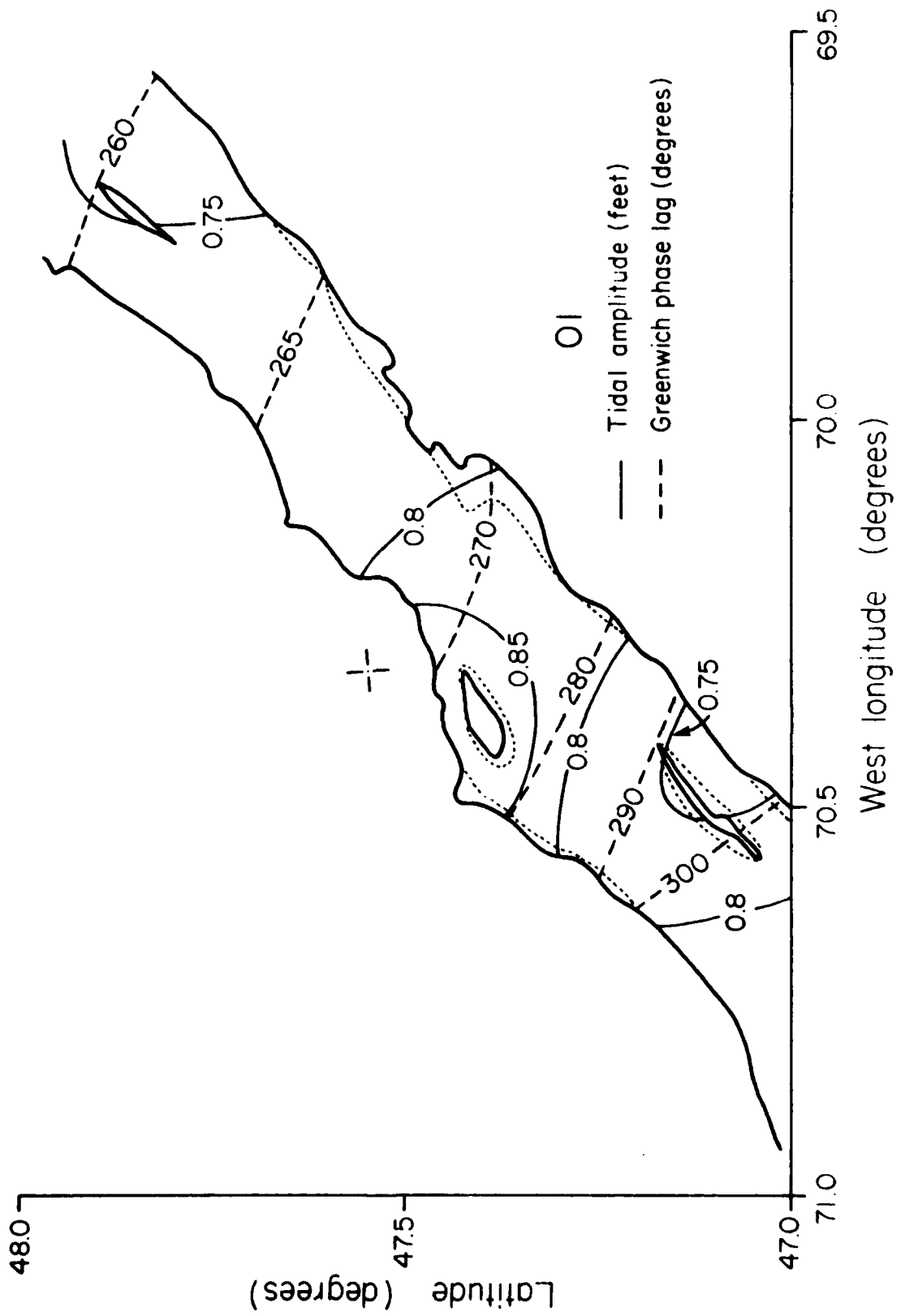


Figure 50a

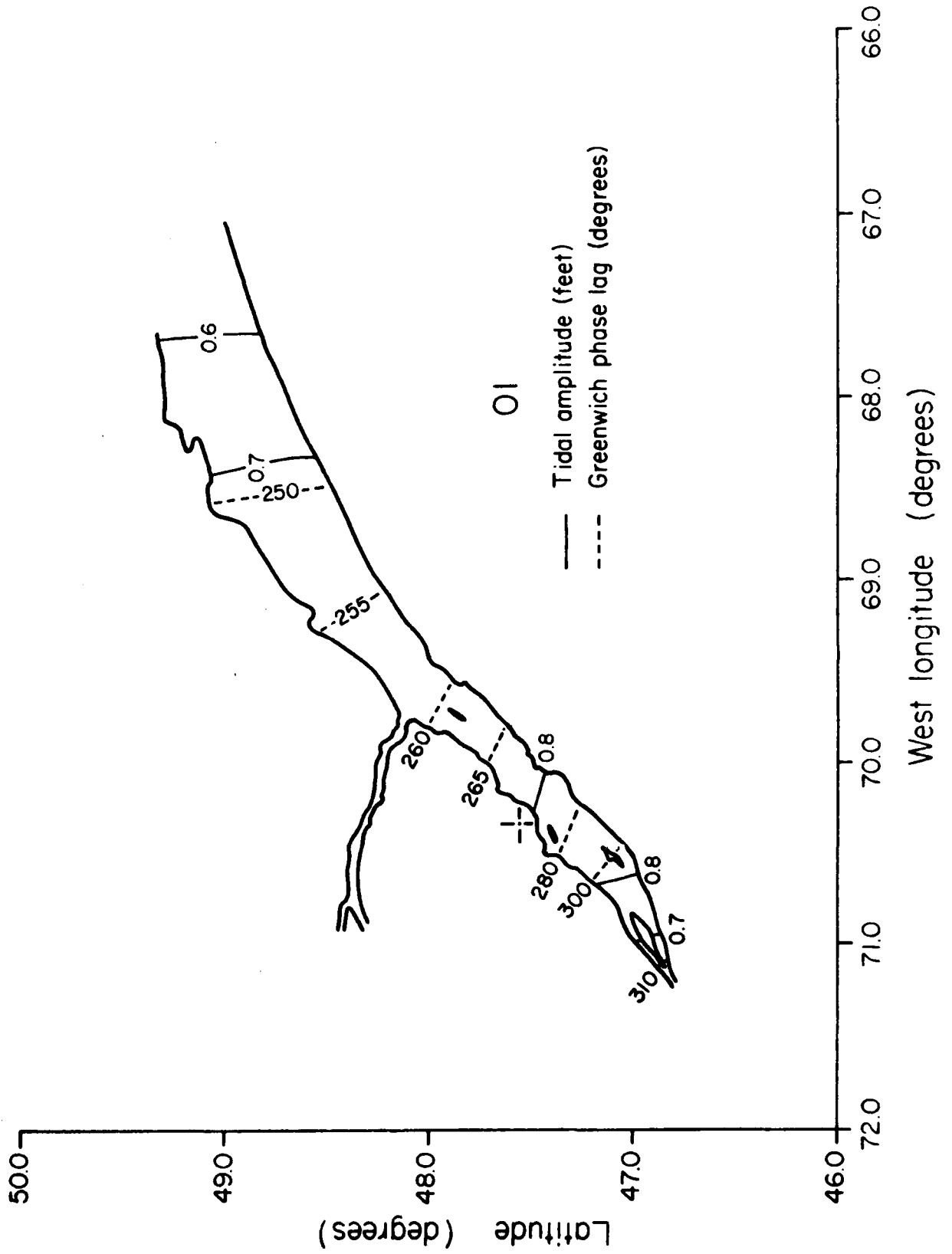


Figure 50b

Charlevoix M<sub>2</sub> West Load Tilt Phasor Plot  
 Gbp 105, Borehole 1

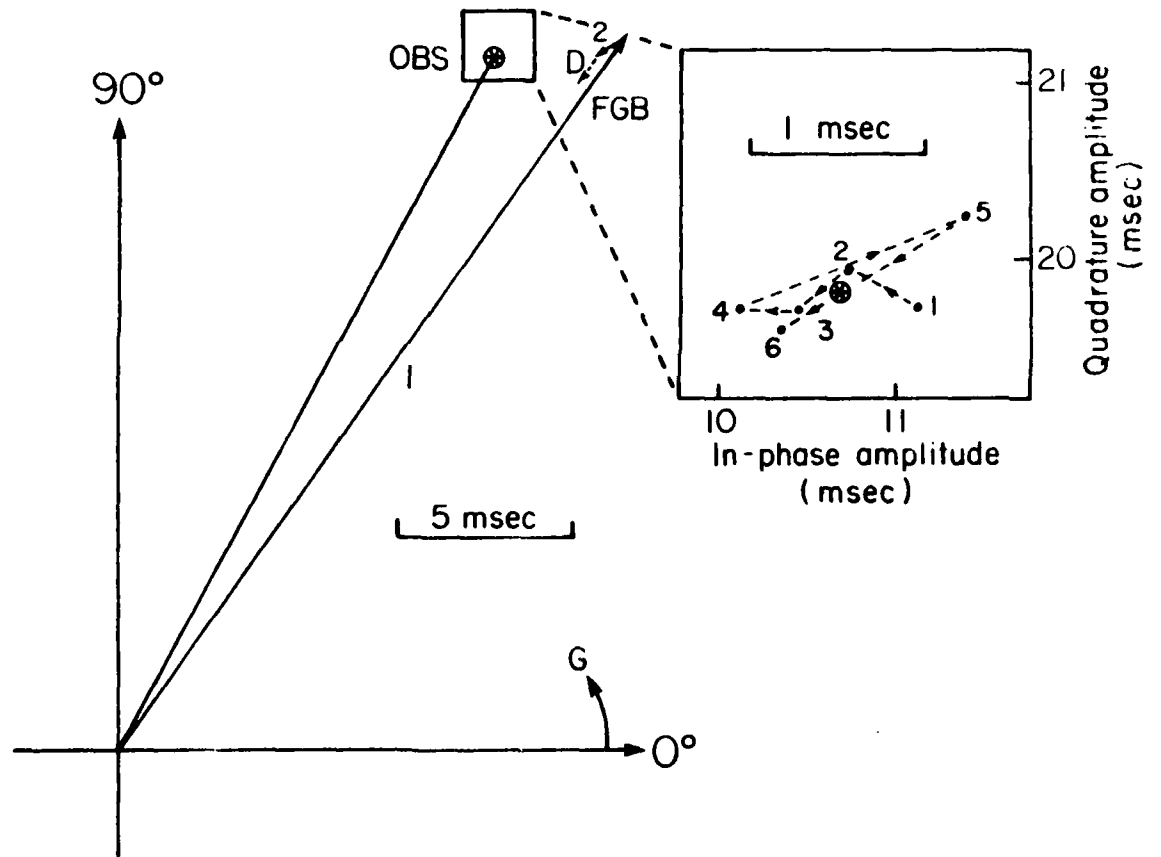


Figure 51

Charlevoix M<sub>2</sub> West Load Tilt Phasor Plot  
Gbp 106, Borehole 2

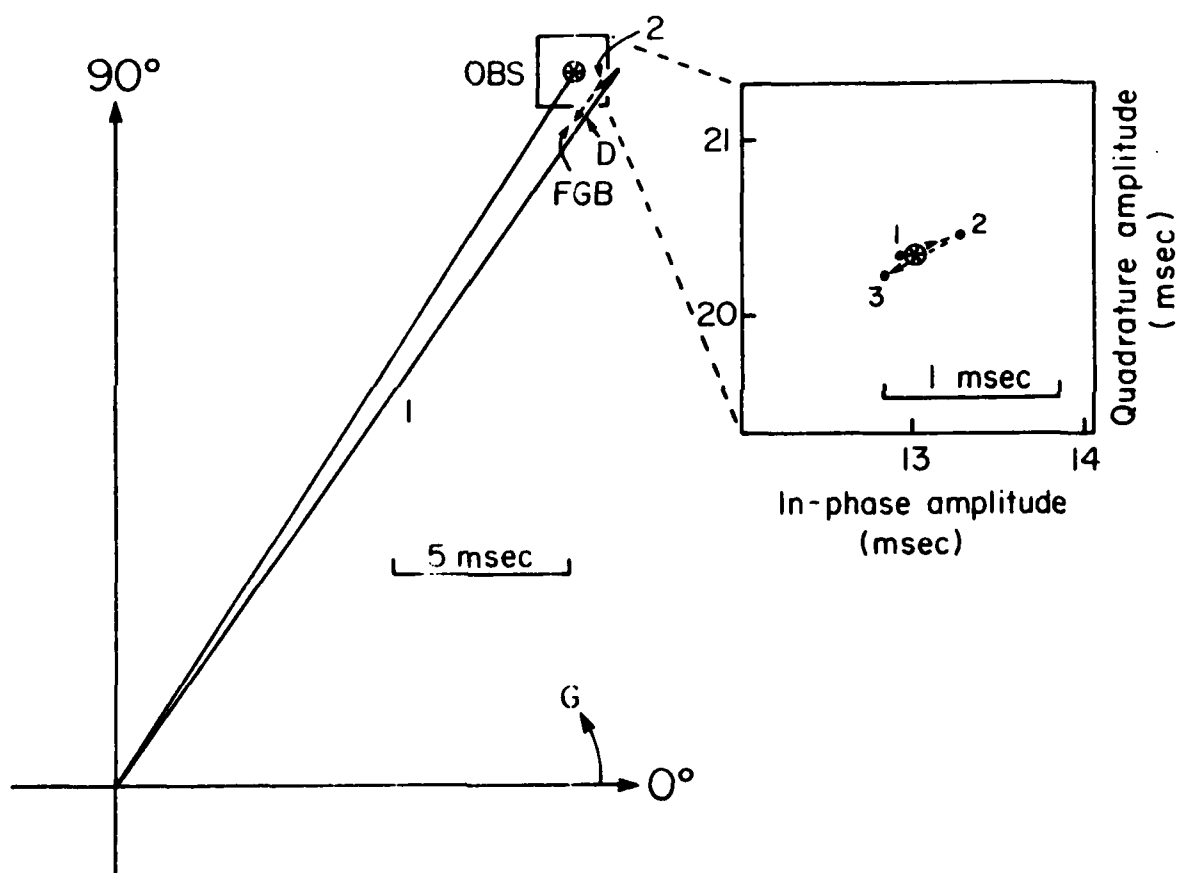


Figure 52

Charlevoix M<sub>2</sub> West Load Tilt Phasor Plot  
 Gbp 107, Borehole 1

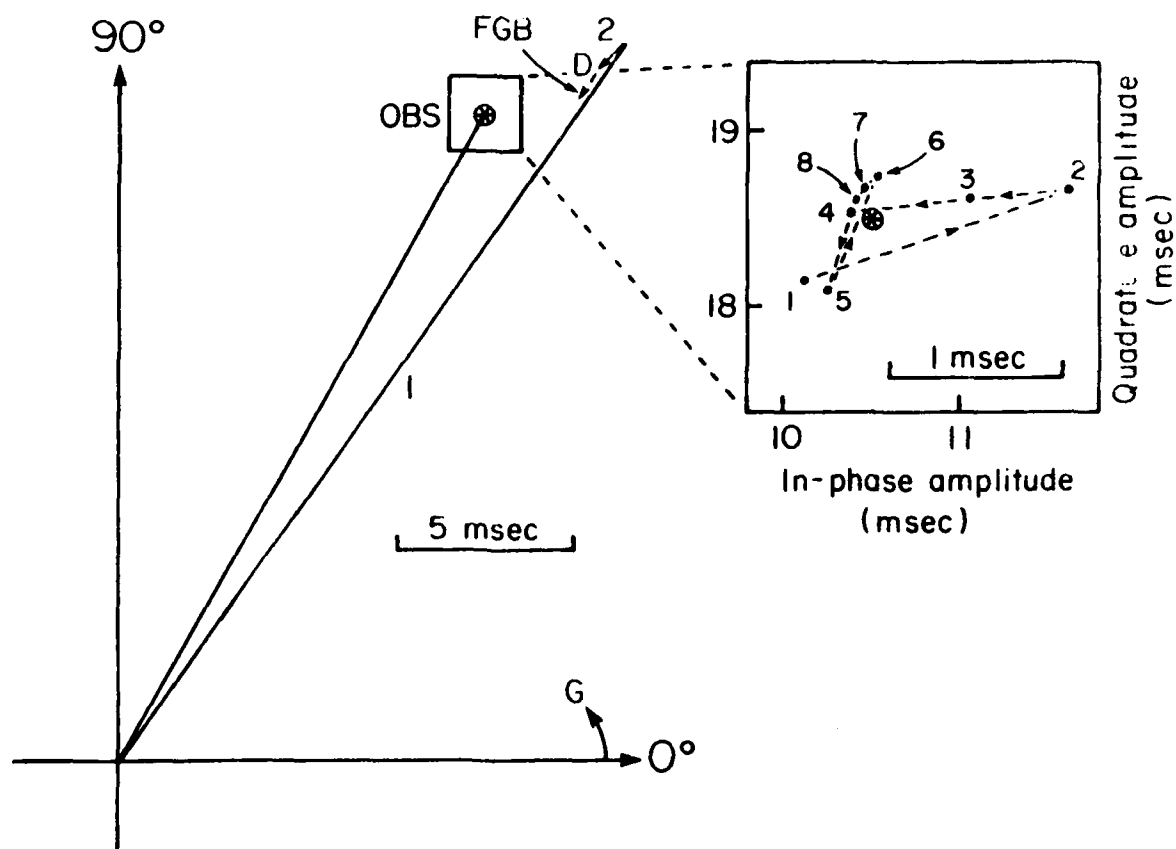


Figure 53

Charlevoix M<sub>2</sub> South Load Tilt Phasor Plot  
 Gbp 105, Borehole 1

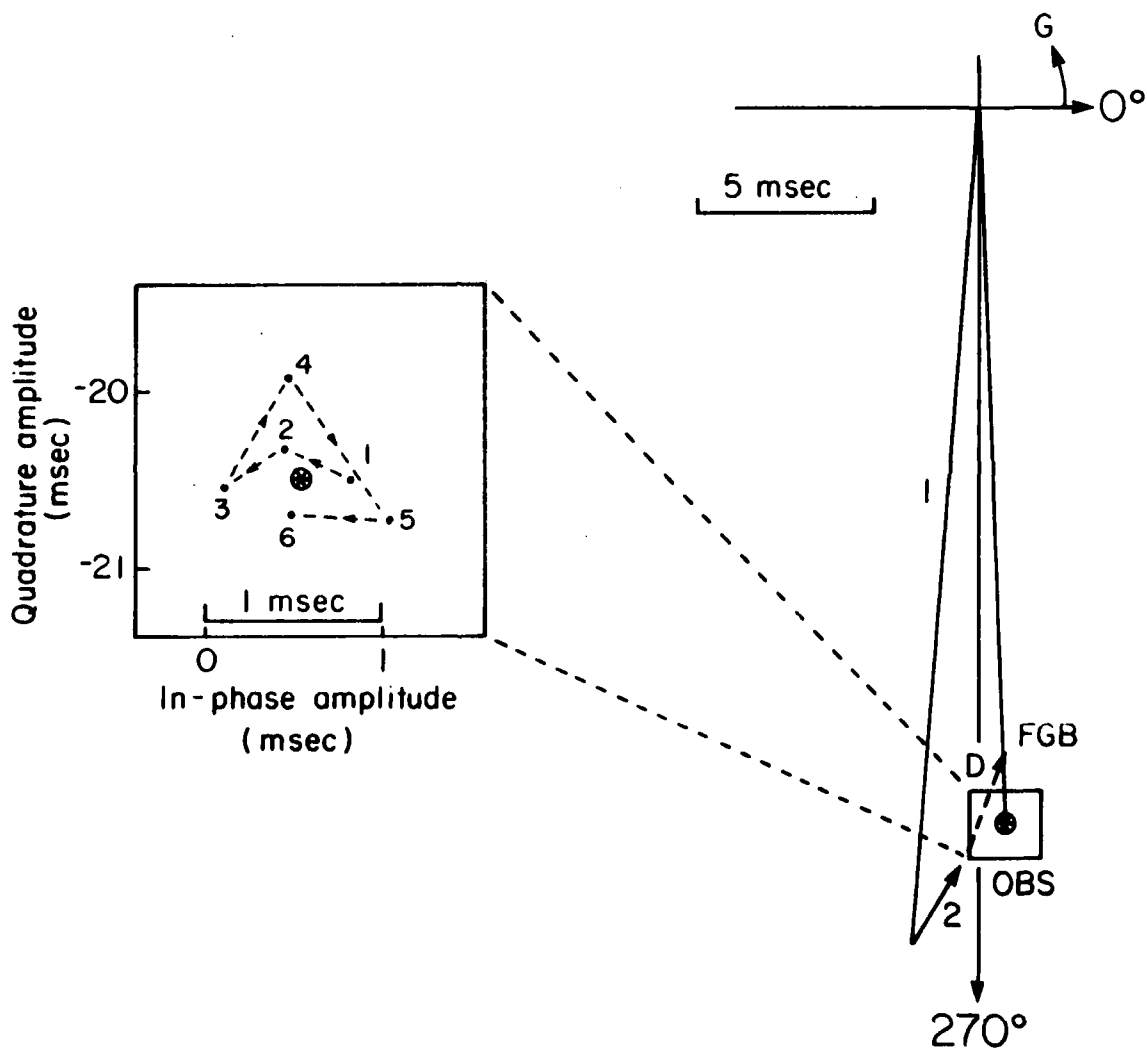


Figure 54

Charlevoix M<sub>2</sub> South Load Tilt Phasor Plot  
Gbp 106, Borehole 2

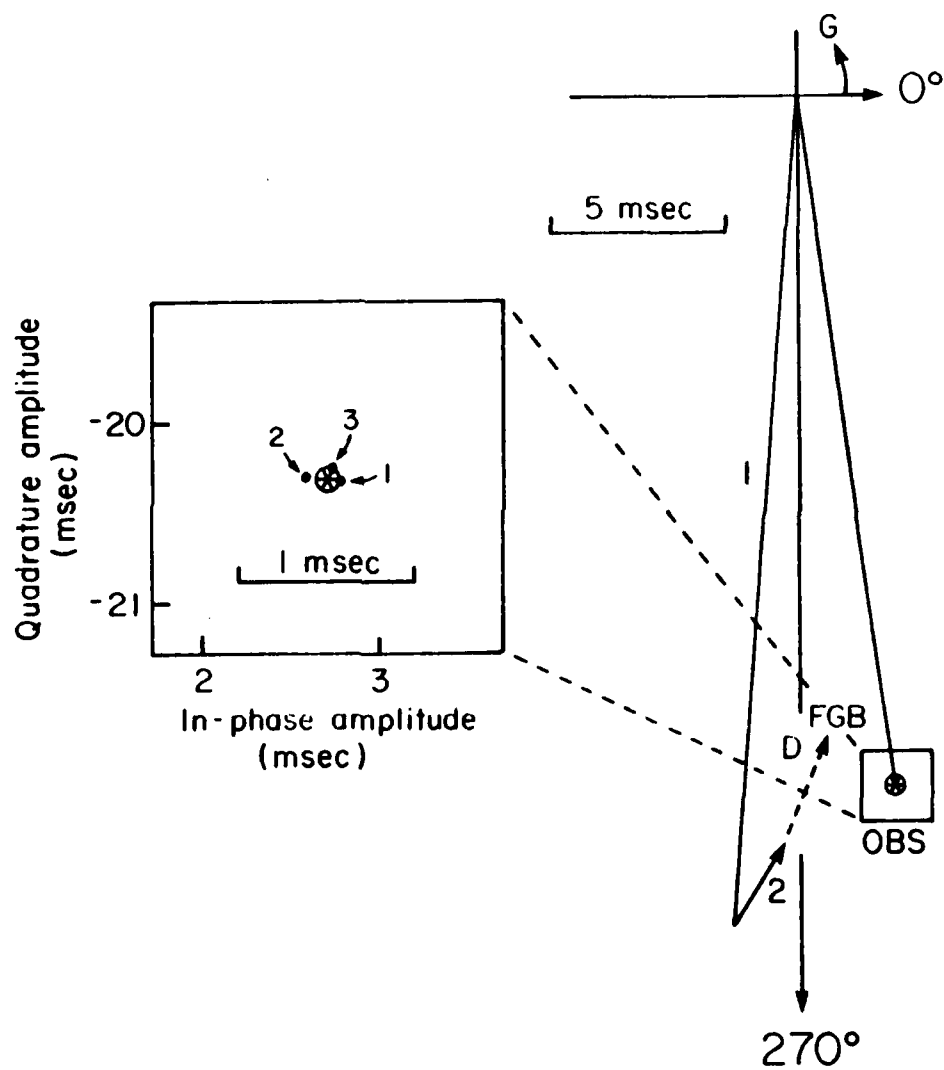


Figure 55 .

Charlevoix M<sub>2</sub> South Load Tilt Phasor Plot  
 Gbp 107, Borehole 1

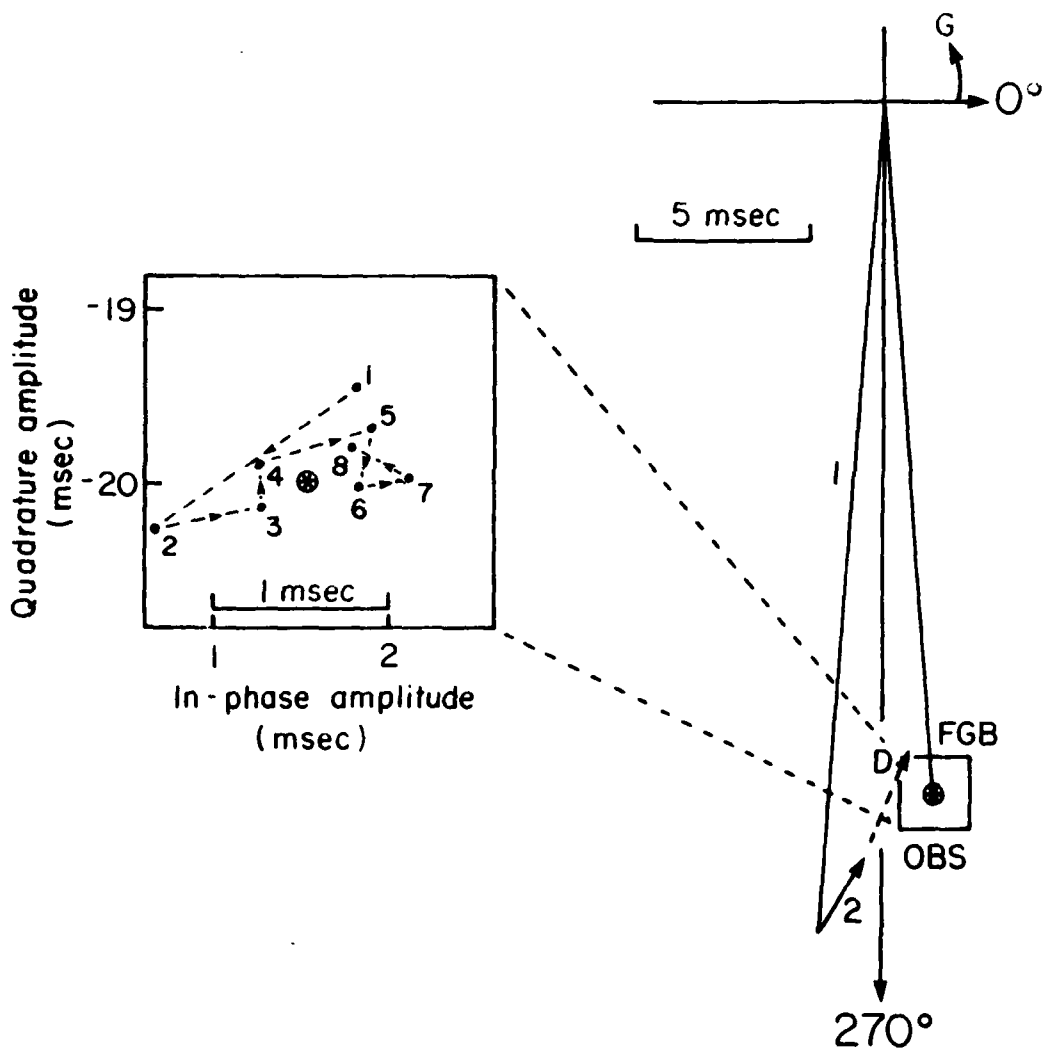


Figure 56

Charlevoix O<sub>1</sub> West Load Tilt Phasor Plot  
Gbp 105, Borehole 1

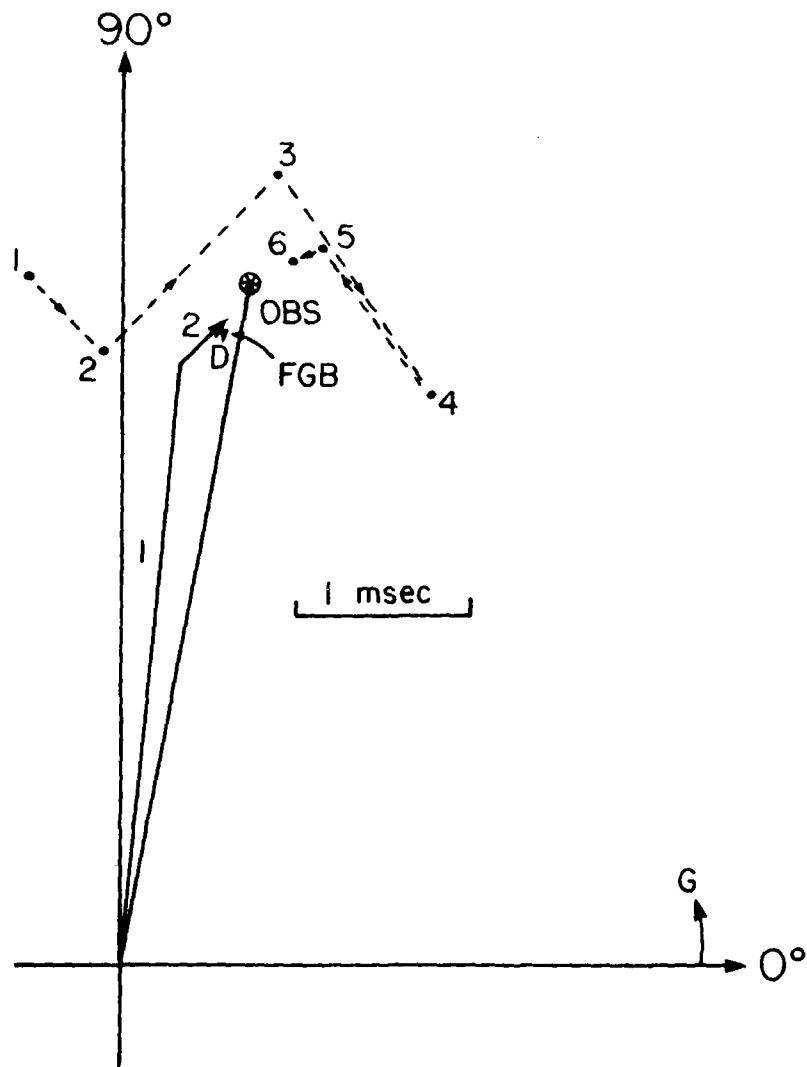


Figure 57

Charlevoix O<sub>1</sub> West Load Tilt Phasor Plot  
Gbp 106, Borehole 2

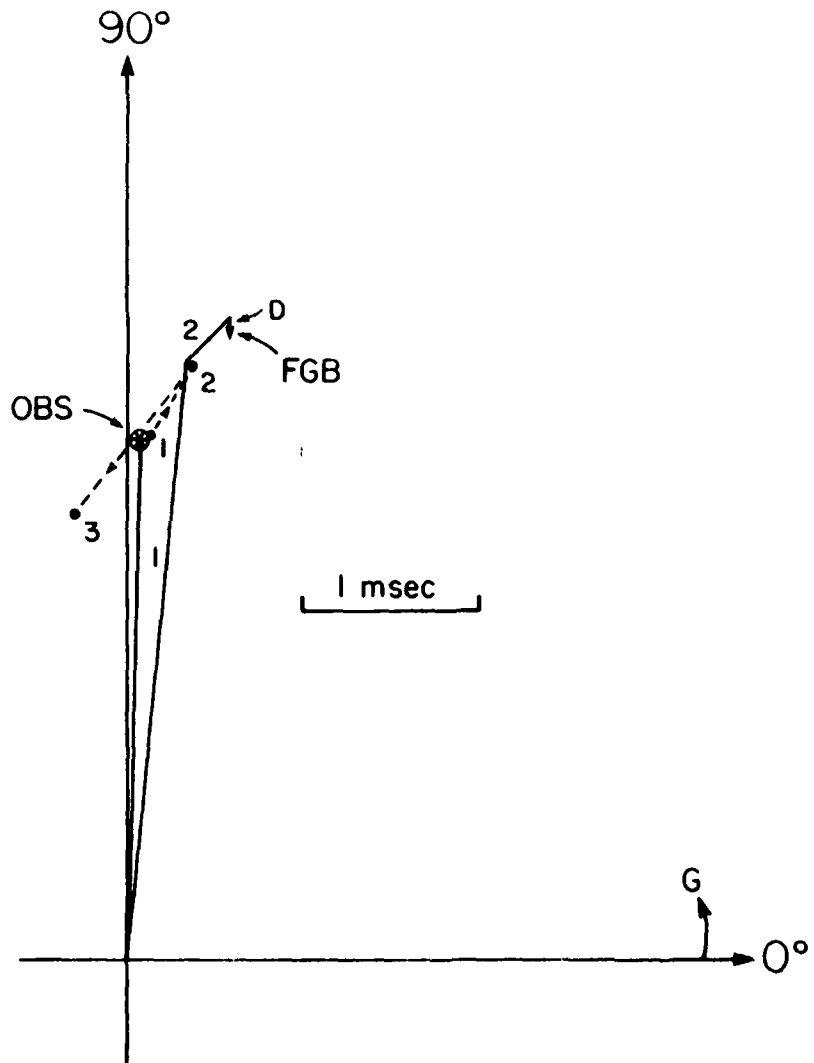


Figure 58

Charlevoix O<sub>1</sub> West Load Tilt Phasor Plot  
Gbp 107, Borehole 1

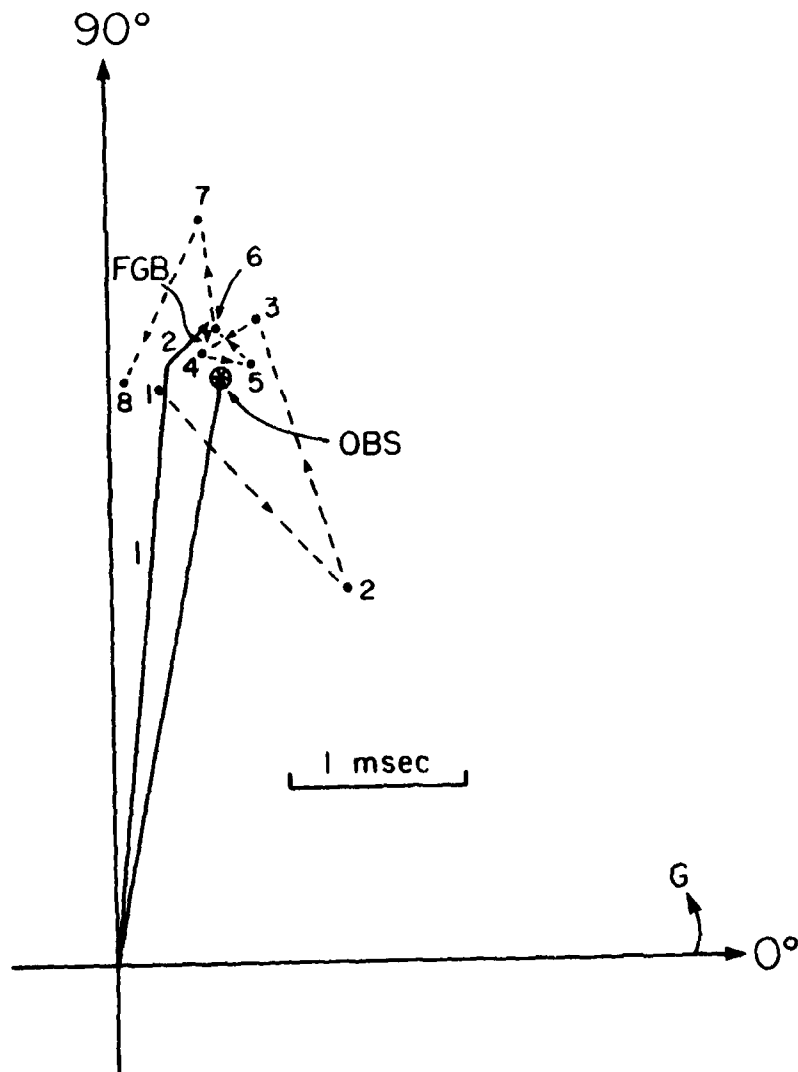


Figure 59

Charlevoix O<sub>1</sub> South Load Tilt Phasor Plot  
Gbp 105, Borehole 1

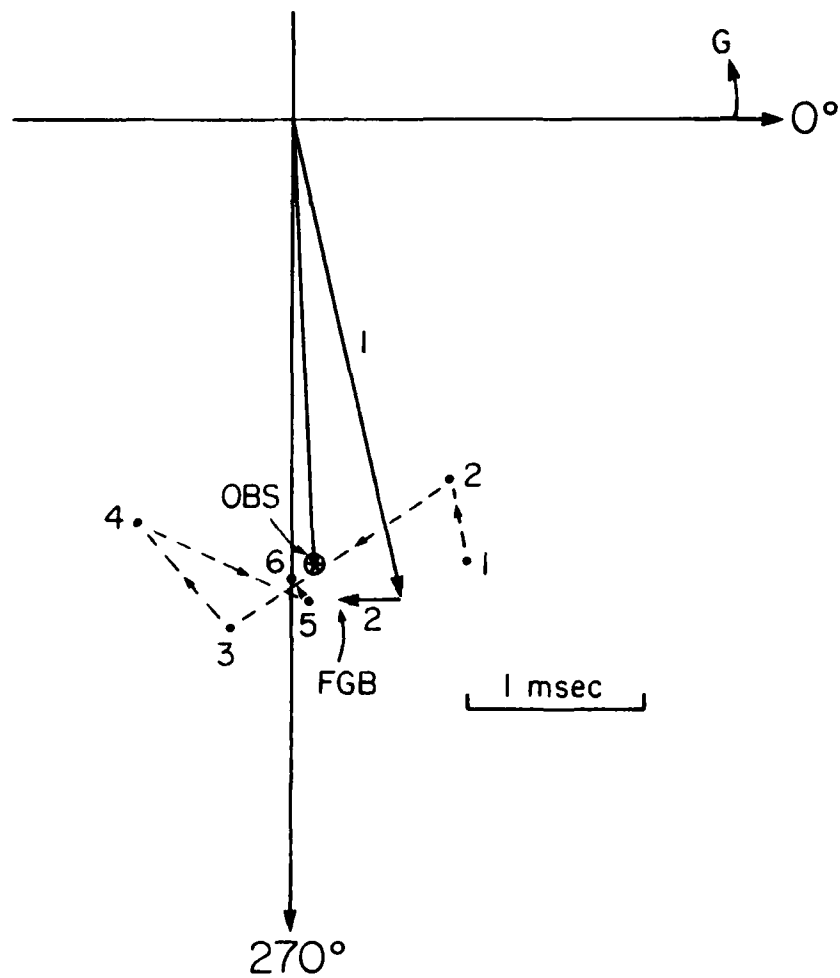


Figure 60



Charlevoix O<sub>1</sub> South Load Tilt Phasor Plot  
Gbp 107, Borehole 1

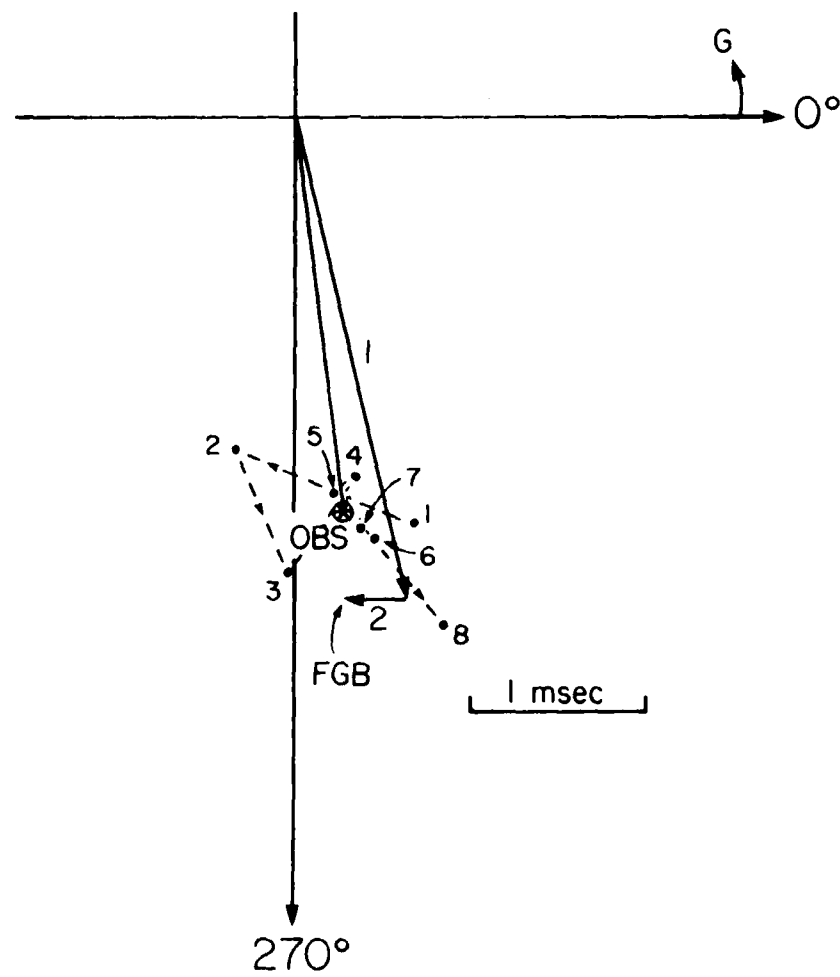


Figure 62

END

FILMED

1977

DINIC